

## UPPER PLATE RESPONSE TO RIDGE SUBDUCTION AND OCEANIC PLATEAU ACCRETION, WASHINGTON CASCADES AND SURROUNDING REGION: IMPLICATIONS FOR PLATE TECTONIC EVOLUTION OF THE PACIFIC NORTHWEST (U.S.A. AND SW CANADA) IN THE PALEOGENE

Tracking no: GS2629R

**Authors:**

Robert Miller (San Jose State University), Paul Umhoefer (Northern Arizona University), Michael Eddy (Purdue University), and Jeffrey Tepper (University of Puget Sound)

**Abstract:**

The interaction between subduction zones and oceanic spreading centers is a common tectonic process, and yet our understanding of how it is manifested in the geologic record is limited to a few well-constrained modern and ancient examples. In the Paleogene, at least one oceanic spreading center interacted with the northwestern margin of North America. Several lines of evidence place this triple-junction near Washington and southern British Columbia in the early-middle Eocene and we summarize a variety of new datasets that permit us to track the plate tectonic setting and geologic evolution of this region from 65 to 40 Ma. The North Cascades segment of the voluminous Coast Mountains continental magmatic arc experienced a magmatic lull between ca. 60-50 Ma interpreted to reflect low-angle subduction to low-angle subduction. During this period of time the Swauk basin began to subside inboard of the paleo-trench in Washington and the Siletzia oceanic plateau began to develop along the Farallon-Kula or Farallon-Resurrection spreading center. Farther east, peraluminous magmatism occurred in the Omineca belt and Idaho batholith. Accretion of Siletzia and ridge-trench interaction occurred between ca. 53-49 Ma, as indicated by: (i) near-trench magmatism from central Vancouver Island to NW Washington; (ii) disruption and inversion of the Swauk basin during a short-lived contractional event; (iii) voluminous magmatism in the Kamloops - Challis belt accompanied by major E-W extension east of the North Cascades in metamorphic core complexes and supra-detachment basins and grabens; and (iv) southwestward migration of magmatism across NE Washington. These events suggest that flat slab subduction from ~60-52 Ma was followed by slab rollback and breakoff during accretion of Siletzia. A dramatic magmatic flare-up was associated with rollback and breakoff between ca. 49.4 Ma and 45 Ma, and included bimodal volcanism near the eastern edge of Siletzia, intrusion of granodioritic to granitic plutons in the crystalline core of the North Cascades, and extensive dike swarms in the North Cascades. Transtension during and shortly before the flare-up led to >300 km of total offset on dextral strike-slip faults, formation of the Chumstick strike-slip basin, and subhorizontal ductile stretching and rapid exhumation of 8-10 kb metamorphic rocks in the North Cascades crystalline core. By ca. 45 Ma, the Farallon - Kula (or Resurrection) - North American triple-junction was likely located in Oregon, subduction of the Kula or Resurrection plate was established outboard of Siletzia, and strike-slip faulting was localized on the north-striking Straight Creek - Fraser River fault. Motion of this structure terminated by 35 Ma. These events culminated in the establishment of the modern Cascadia convergent margin.

1        **UPPER PLATE RESPONSE TO RIDGE SUBDUCTION AND OCEANIC PLATEAU ACCRETION,**

2        **WASHINGTON CASCADES AND SURROUNDING REGION: IMPLICATIONS FOR PLATE TECTONIC**

3        **EVOLUTION OF THE PACIFIC NORTHWEST (U.S.A. AND SW CANADA) IN THE PALEOGENE**

4        **Miller, Robert B.**, Department of Geology, San José State University, One Washington Square,

5        San Jose, CA 95192; **\*Umhoefer, Paul J.**, School of Earth & Sustainability, Northern Arizona

6        University, P.O. Box 4099, Flagstaff, AZ 86011; **Eddy, Michael P.**, Earth, Atmospheric, and

7        Planetary Sciences Department, Purdue University, 550 Stadium Mall Drive, West Lafayette, IN

8        47907; **Tepper, Jeffrey H.**, Geology Department, University of Puget Sound, 1500 N. Warner St,

9        Tacoma, WA 98416-1048

10        \*Deceased

11        **ABSTRACT**

12        The interaction between subduction zones and oceanic spreading centers is a common

13        tectonic process, and yet our understanding of how it is manifested in the geologic record is

14        limited to a few well-constrained modern and ancient examples. In the Paleogene, at least one

15        oceanic spreading center interacted with the northwestern margin of North America. Several

16        lines of evidence place this triple-junction near Washington and southern British Columbia in

17        the early-middle Eocene and we summarize a variety of new datasets that permit us to track

18        the plate tectonic setting and geologic evolution of this region from 65 to 40 Ma. The North

19        Cascades segment of the voluminous Coast Mountains continental magmatic arc experienced a

20        magmatic lull between ca. 60-50 Ma interpreted to reflect low-angle subduction. During this

21        period of time the Swauk basin began to subside inboard of the paleo-trench in Washington

22 and the Siletzia oceanic plateau began to develop along the Farallon-Kula or Farallon-  
23 Resurrection spreading center. Farther east, peraluminous magmatism occurred in the  
24 Omineca belt and Idaho batholith. Accretion of Siletzia and ridge-trench interaction occurred  
25 between ca. 53–49 Ma, as indicated by: (i) near-trench magmatism from central Vancouver  
26 Island to NW Washington; (ii) disruption and inversion of the Swauk basin during a short-lived  
27 contractional event; (iii) voluminous magmatism in the Kamloops – Challis belt accompanied by  
28 major E-W extension east of the North Cascades in metamorphic core complexes and supra-  
29 detachment basins and grabens; and (iv) southwestward migration of magmatism across NE  
30 Washington. These events suggest that flat slab subduction from ~60–52 Ma was followed by  
31 slab rollback and breakoff during accretion of Siletzia. A dramatic magmatic flare-up was  
32 associated with rollback and breakoff between ca. 49.4 Ma and 45 Ma, and included bimodal  
33 volcanism near the eastern edge of Siletzia, intrusion of granodioritic to granitic plutons in the  
34 crystalline core of the North Cascades, and extensive dike swarms in the North Cascades.  
35 Transtension during and shortly before the flare-up led to >300 km of total offset on dextral  
36 strike-slip faults, formation of the Chumstick strike-slip basin, and subhorizontal ductile  
37 stretching and rapid exhumation of 8-10 kb metamorphic rocks in the North Cascades  
38 crystalline core. By ca. 45 Ma, the Farallon – Kula (or Resurrection) – North American triple-  
39 junction was likely located in Oregon, subduction of the Kula or Resurrection plate was  
40 established outboard of Siletzia, and strike-slip faulting was localized on the north-striking  
41 Straight Creek – Fraser River fault. Motion of this structure terminated by 35 Ma. These events  
42 culminated in the establishment of the modern Cascadia convergent margin.  
43

44 **INTRODUCTION**

45 Plate tectonic margins vary from long-lived stable settings to those that change rapidly  
46 from one type of boundary to another over only a few million years. The modern Cascadia  
47 subduction zone, in the Pacific Northwest (U.S.A) and southwest British Columbia (Canada), has  
48 been a convergent plate margin since the mid-Eocene ( $\leq 45$  Ma) (du Bray and John, 2011).  
49 Earlier, the northern Washington Cascades was part of a long-lived continental magmatic arc  
50 that is also manifested as the Coast Mountains batholith and parts of the Idaho batholith (e.g.,  
51 Gehrels et al., 2009). The North Cascades segment of the Coast Mountains arc was active from  
52 about 96–60 Ma, and changed from a contractional-convergent to oblique-convergent regime  
53 during that time (e.g., Brown and Talbot, 1989; Miller et al., 2009, 2016). Between the older  
54 Coast Mountains and Cascadia magmatic arc regimes was an  $\sim 25$  m.y. period, from ca. 65 – 40  
55 Ma, during which the Washington Cascades and the surrounding region experienced many  
56 dynamic changes that can be linked to two major Paleogene tectonic events: spreading ridge –  
57 trench interaction and the formation and accretion of an oceanic plateau.

58 Plate reconstructions suggest that the Farallon – Kula, Farallon – Resurrection, or  
59 Farallon – Orcas spreading ridge(s) interacted with North America near the Pacific Northwest  
60 during the Paleogene (e.g., Atwater, 1970; Wells et al., 1984; Engebretson et al., 1985;  
61 Haeussler et al., 2003; Madsen et al., 2006; Clennett et al., 2020; Fuston and Wu, 2021) (Fig. 1).  
62 Based on ca. 51-49 Ma near-trench magmatism from central Vancouver Island to northwestern  
63 Washington, a ridge is assumed to have intersected North America near these locations at that  
64 time (e.g., Cowan, 2003; Madsen et al., 2006), although how this triple-junction migrated along  
65 the margin prior to 52 Ma is poorly understood. The Siletzia terrane, a basaltic oceanic plateau,

66 formed along this oceanic spreading center and was accreted to the Pacific Northwest ca. 50  
67 Ma (e.g., McCrory and Wilson, 2013; Wells et al., 2014). Farther inland there was a change from  
68 a long-lived thrust belt (e.g., Mudge and Earhart, 1980; Price, 1981) to east-west extension and  
69 widespread magmatism at ca. 55–53 Ma (e.g., Ewing, 1980; Parrish et al., 1988). These and  
70 other changes in the upper plate of the system are the basis for our attempt at a  
71 comprehensive model of the 65 – 40 Ma tectonic evolution of the Washington Cascades and  
72 Pacific Northwest.

73 In this paper, we synthesize data on the ages and types of sedimentary basins (Evans,  
74 1984; Johnson, 1984; Eddy et al., 2016a; Donaghy et al., 2021), age, geochemistry, and spatial  
75 patterns of magmatism (e.g., Breitsprecher et al., 2003; Madsen et al., 2006; Miller et al., 2009),  
76 and deformation styles and exhumation patterns across Vancouver Island to the Washington  
77 Cascades (e.g., Johnston and Acton, 2003; Miller et al., 2016) (Figs. 2, 3). We present this 25  
78 m.y. geologic history in a series of time slices and place the discussion in the context of the  
79 greater region from northern California to southern British Columbia and inland to the Rocky  
80 Mountains (Fig. 2). Integrated within this discussion are a series of new maps that restore slip  
81 on the major Paleocene - Eocene strike-slip faults (Figs. 4-7). Boundaries between time slices  
82 coincide with transitional periods in at least one of the major processes emphasized in the  
83 synthesis (i.e. magmatism, sedimentation, metamorphism, deformation, exhumation). A critical  
84 aspect of this work is the incorporation of new high-precision U-Pb zircon age constraints tied  
85 to detailed field observations (e.g., Eddy et al., 2016a; 2017a; b; Miller et al., 2016, 2022), which  
86 enables the construction of a detailed time line not previously possible. Moreover, the varied  
87 levels of exhumation within the region allow us to study how the changing tectonic setting was

88 manifested at a wide range of Eocene crustal levels. In particular, we explore the upper-plate  
89 events in the Washington Cascades and surrounding region in relation to changing plate  
90 boundaries, especially the formation and accretion of Siletzia (Wells et al., 2014), and the  
91 shifting location of ridge – trench interaction. The study area is described in terms of western,  
92 central, and eastern regions, which roughly correspond to the forearc, arc, and backarc regions  
93 of the North Cascades segment of the Coast Mountains batholith in the Late Cretaceous (Fig. 2).  
94 We utilize these geographic terms because the dynamic tectonic changes described herein  
95 make it difficult to define regions typically associated with a stable subduction zone.

## 96 **PLATE TECTONIC SETTING**

97 There has long been uncertainty about the Late Cretaceous to early Cenozoic plate  
98 configuration in the northeast Pacific basin. There is general agreement that the Kula plate  
99 originated from rifting of the Pacific plate at ~83 Ma and that the northern boundary of the  
100 Farallon plate was a ridge, which intersected the continental margin at a poorly constrained  
101 location (e.g., Atwater, 1970; Wood and Davies, 1982; Engebretson et al., 1985; Stock and  
102 Molnar, 1988; Thorkelson and Taylor, 1989). Subsequent models proposed the potential  
103 existence of a now-subducted Resurrection plate (e.g., Haeussler et al., 2003; Madsen et al.,  
104 2006; Fuston and Wu, 2021) (Fig. 1) or Orcas plate (Clennett et al., 2020). During the interval  
105 from ca. 85 Ma to 60 Ma, the northern Cordillera was an oblique, transpressional convergent  
106 margin (e.g., Engebretson et al., 1985; Doubrovine and Tarduno, 2008), and northward  
107 translation of the Washington Cascades may have been rapid as the southern part of the Insular  
108 superterrane (the Baja BC hypothesis; e.g., Cowan et al., 1997; Umhoefer and Blakey, 2006).  
109 Relative to North America, motion of the Farallon plate was to the NE to ENE, and motion of the

110 Kula (Resurrection or Orcas?) plate was to the N to NNE, and thus more oblique than that of  
111 the Farallon plate. Both oceanic plates were moving rapidly (50 – 150 km/Myr) during this time  
112 (e.g., Engebretson et al., 1985; Doubrovine and Tarduno, 2008; Wright et al., 2015; Fuston and  
113 Wu, 2021).

114 Formation of the Siletzia terrane was a major factor in the Paleogene tectonic evolution  
115 of the Pacific Northwest. This terrane represents a large igneous province that developed  
116 between 56-49 Ma near an oceanic spreading center, and it is probably an early manifestation  
117 of the Yellowstone hotspot (e.g., Gao et al., 2011; McCrory and Wilson, 2013; Wells et al., 2014;  
118 Camp and Wells, 2021). We support previous work that infers the triple junction between the  
119 Farallon – North America – Kula (or Resurrection or Orcas) plates lay along central Vancouver  
120 Island by 55–53 Ma (e.g., Madsen et al., 2006) (Figs. 1, 4). From 52–49 Ma, a triple junction is  
121 interpreted to have interacted with the continental margin along central to southern Vancouver  
122 Island (Fig. 1), as this interval is marked by near-trench magmatism (Groome et al., 2003;  
123 Madsen et al., 2006), geochemically anomalous backarc magmatism (Ewing, 1980;  
124 Breitsprecher et al., 2003; Ickert et al., 2009; Dostal and Jutras, 2021), and disruption of non-  
125 marine basins (Eddy et al., 2016a). The collision of Siletzia, which started by 53 Ma in SW  
126 Oregon (Wells et al., 2014) and by 51 Ma in northern Washington and southernmost Vancouver  
127 Island, led to a major change in plate geometries and profound changes in the upper plate of  
128 the system from 52–48 Ma, which we describe in more detail below. The plate boundary later  
129 shifted outboard (west) of Siletzia, resulting in the new Cascadia subduction system at ca. 45–  
130 40 Ma (e.g., Wells et al., 1984, 2014; Schmandt and Humphreys, 2011; McCrory and Wilson,  
131 2013; Eddy et al., 2017a; Kant et al., 2018).

132

133 **PRE-PALEOGENE GEOLOGIC SETTING**

134 Prior to 65 Ma, the Pacific Northwest was characterized by a typical convergent margin  
135 with a forearc, continental magmatic arc, back-arc basin, and fold-and-thrust belt that  
136 deformed a Paleozoic passive margin sequence (e.g., Burchfiel et al., 1992). The arc and forearc  
137 were originally farther south relative to the inboard rocks by more than 300 km (e.g., Umhoefer  
138 and Blakey, 2006; Wyld et al., 2006), and potentially a much greater distance as discussed  
139 below.

140 In the forearc (western belt of Fig. 2) are Paleozoic and Mesozoic oceanic and island arc  
141 rocks and overlapping Jura-Cretaceous marine clastic rocks, which were deformed in the mid-  
142 Cretaceous Northwest Cascades thrust system (shown as a single Cretaceous unit on Fig. 3)  
143 (Misch, 1966; Brown, 1987; Brandon et al., 1988). Structurally above these rocks are mostly  
144 Jura-Cretaceous rocks of the western mélange belt (Fig. 3), which is interpreted as an  
145 accretionary complex (Tabor, 1994) and contains rocks at least as young as 72 Ma (Dragovich et  
146 al., 2014; Sauer et al., 2017a). The Upper Cretaceous to Paleocene Nanaimo Group (e.g.,  
147 Mustard, 1994), exposed mostly on southern Vancouver Island, is interpreted as a foreland  
148 basin to the Northwest Cascades thrust system (Brandon et al., 1988), and has depositional  
149 ages extending from at least ca. 84 Ma to 63 Ma (e.g., Matthews et al., 2017; Coutts et al.,  
150 2020).

151 The Cretaceous arc in northern Washington and southern British Columbia is  
152 represented by medium- to high-grade metamorphic and plutonic rocks in the crystalline core  
153 of the North Cascades and southern British Columbia (central belt of Fig. 2). The crystalline

154 rocks are subdivided into the Wenatchee and Chelan blocks, which are separated by the high-  
155 angle Eocene Entiat fault and bounded to the west by the Straight Creek-Fraser River fault (Fig.  
156 3). Magmatism in the Wenatchee block occurred from 96–87 Ma, and most biotite Ar/Ar and  
157 K/Ar cooling ages are >60 Ma, whereas magmatism in the Chelan block ranges from 92–45 Ma  
158 and Eocene cooling ages are common (e.g., Walker and Brown, 1991; Matzel, 2004; Miller et  
159 al., 2009, 2016). The Chelan block also records Paleogene ductile deformation and partial  
160 melting in the highest-grade rocks of the Skagit Gneiss Complex (Gordon et al., 2010a).

161 Pre-Cenozoic rocks directly east of the North Cascades in the eastern belt include: the  
162 Mesozoic Methow basin; ca. 160–105 Ma arc plutonic rocks of the Eagle Complex and  
163 Okanogan Range batholith; ca. 105 Ma arc volcanic rocks of the Spences Bridge Group; and arc  
164 volcanic and sedimentary rocks of the Quesnellia terrane (Fig. 3) (e.g., Greig, 1992; Hurlow and  
165 Nelson, 1993). Farther east are plutonic and metamorphic rocks of the Omineca belt, including  
166 multiple metamorphic core complexes, the Idaho batholith, and Cordilleran passive margin  
167 sediments involved in the Rocky Mountain-Sevier fold-and-thrust belt (Fig. 2).

168

## 169 RESTORATION OF STRIKE-SLIP FAULTS

170 Dextral strike-slip faulting occurred in the northern Cordillera in the Late Cretaceous to  
171 Eocene (e.g., Gabrielse, 1985; Wyld et al., 2006), and within our study region displacements of  
172 ~325 km on strike-slip faults active from ca. 60 – 35 Ma are well documented (Table 1). In the  
173 west, the N-S-striking Straight Creek – Fraser River fault separates the North Cascades  
174 crystalline core of the central belt from the outboard Paleozoic and Mesozoic Northwest

175 Cascades system, mélange belts, and Paleogene rocks of the western belt (Fig. 3). The most  
176 recent estimate of dextral offset on this fault is ~150 km (Monger and Brown, 2016). The  
177 Leavenworth and Entiat faults (Fig. 3) involve the Cascades core and have a total displacement  
178 of ~60 km (Eddy et al., 2017b). The Entiat fault separates the Wenatchee and Chelan blocks  
179 within the core (see above) and the NE boundary of the Cascades core is the Ross Lake fault  
180 system (Ross Lake fault, Gabriel Peak tectonic belt, Hozameen fault, and Foggy Dew fault) (Fig.  
181 3), which probably has ~115 km of dextral offset (Umhoefer and Miller, 1996).

182 These known displacements of ~325 km must be considered in tectonic restorations,  
183 particularly before 50 Ma. To summarize, after 50 Ma there is approximately 1) 150 km of  
184 offset between the western belt and Cascades core of the central belt; 2) 60 km of  
185 displacement within the core; 3) 50 km (of total 115 km) of offset between the core and the  
186 eastern belt; and 4) a cumulative offset of ~265 km between the western and eastern belts  
187 after 50 Ma (Table 1). If we assume that the strike-slip offset from 60 to 50 Ma occurred at  
188 rates comparable to those of the ~50–40 Ma interval, the implication is that another  
189 approximately 250–300 km of offset occurred across Washington from 60 to 50 Ma. About 60  
190 km of this slip has been documented on the Ross Lake fault system (Miller and Bowring, 1990)  
191 and Yalakom fault during that time (Umhoefer and Schiarizza, 1996); precise timing and offset  
192 of faults are difficult to document. From this reasoning, at 55 Ma we show Vancouver Island  
193 and the western belt about 450 km south of the eastern belt (Fig. 4). We note that this is likely  
194 a conservative estimate and does not include any distributed dextral ductile displacement or  
195 movement on minor cryptic structures. Paleomagnetic data indicate much larger cumulative  
196 dextral displacements between ~85–55 Ma of 2000 km or more between the easternmost part

197 of the eastern belt and the central and western belts, and ~1000 km between the western part  
198 of the eastern belt and rocks to the west (e.g., Enkin, 2006; Tikoff et al., 2023). From the  
199 paleomagnetic data, major displacements of the outboard rocks ended by 55 Ma (e.g., Cowan  
200 et al., 1997; Tikoff et al., 2023). Thus, uncertainties are much lower for the positions of units in  
201 the region in the 55 Ma and younger reconstructions (Figs. 4-7).

202 Another potential complication is the rotation in the Oregon Coast Ranges and  
203 Cascades, which is probably related to distributed dextral strike slip and Basin and Range  
204 extension (e.g., Beck, 1984; Wells and Heller, 1988; Colgan and Henry 2009; Wells and  
205 McCaffrey, 2013; Wells et al., 2014). Rotation increases westward and decreases from the  
206 Klamath Mountains northward to the Olympic Peninsula. Statistically significant vertical axis  
207 rotation has not occurred after ca. 50 Ma in the Washington Cascades, at least as far south as  
208 the present latitude of Seattle (e.g., Beske et al., 1973; Beck et al., 1982; Fawcett et al., 2003).  
209 In our reconstructions, we utilize the present trends of structures in the north and restore the  
210 Klamath Mountains to northeastern-most California to account for Basin and Range extension  
211 (e.g., Colgan and Henry, 2009) and rotation. The resulting trend and position of Siletzia  
212 (Washington and Oregon Coast Ranges) in our reconstructions (Figs. 4-7) after accretion is  
213 more northerly than in Wells et al. (2014), which suggests that a portion of the rotation in  
214 Siletzia was taken up on more local blocks at a scale of a few tens of km or less.

215

216 **PALEOGENE TECTONIC HISTORY**

217 In this section, we synthesize the Paleogene tectonic evolution across the Pacific  
218 Northwest (Fig. 3), and divide this ~25 Myr history into five intervals. The time slices are  
219 generally considered from west to east. The major events from 60–40 Ma are summarized on  
220 Fig. 8.

221 **65 – 60 Ma**

222 During this interval the plate boundary was one of oblique convergence. This  
223 interpretation is based on the arc-type tonalitic intrusions (Miller and Bowring, 1990; Miller et  
224 al., 2009), transpressional deformation in the North Cascades and southern Coast Mountain  
225 batholith arc (e.g., Brown and Talbot, 1989; Miller and Bowring, 1990), and contractional  
226 deformation (e.g., Brown et al., 1986; Simony and Carr, 2011) in the hinterland (eastern belt).

227 The forearc (western belt) record is sparse and the timing of deformation in this belt is  
228 poorly known (Tabor, 1994; Sauer et al., 2017a). The only known forearc rocks of this age are  
229 the uppermost clastic strata of the Nanaimo Group on Vancouver Island, which have maximum  
230 depositional ages (MDAs) as young as ca. 63 Ma (Coutts et al., 2020). The youngest dated  
231 (MDA) sandstone in the western mélange belt is ca. 72 Ma (Sauer et al., 2017a), and younger  
232 rocks may be present in this belt, as the upper limit for the mélange is only indicated by an  
233 angular unconformity with Eocene strata.

234 The 65 – 60 Ma interval includes the final stage of a magmatic flare-up in the North  
235 Cascades core (Chelan block) that began ca. 78 Ma (Miller et al., 2009), and was directly  
236 preceded by rapid burial and metamorphism of Cretaceous (protolith age) metasedimentary  
237 rocks that comprise the deep-crustal (up to 12 kbar) Swakane Biotite Gneiss (Valley et al., 2003)  
238 and Skagit Gneiss Complex (7 – 10 kbar; Whitney, 1992; Hanson, 2022) (Fig. 3), between ca. 79

239 – 66 Ma and 74 – 65 Ma, respectively (Sauer et al., 2017b, 2018). Tonalitic magmatism is  
240 recorded by the 65 Ma Oval Peak pluton (Fig. 3), which crystallized at 5 – 6 kbar (Miller and  
241 Bowring, 1990), and sheets (now orthogneisses) in the Skagit Gneiss Complex (Miller et al.,  
242 2016). Leucosomes of this age also are recognized in the Complex (Gordon et al., 2010a). K-Ar  
243 and Ar/Ar biotite cooling ages are sparse, but there is no evidence for major rapid cooling or  
244 exhumation of the Cascades core during this interval (Paterson et al., 2004), and no  
245 sedimentary or volcanic rocks of this age have been recognized in the arc. Dated deformation  
246 during this time interval is limited in the arc region where dextral and reverse shear in the  
247 Gabriel Peak tectonic belt of the Ross Lake fault system (Fig. 3) was inferred to be coeval with  
248 emplacement of the Oval Peak pluton (Miller and Bowring, 1990).

249 In the eastern belt, igneous activity was sparse during this interval and volcanic rocks  
250 are absent. In NE Washington, magmatism was limited to a few ca. 64–56 Ma plutons (e.g.,  
251 Stoffel et al., 1991). North of the international border, intrusion of the quartz monzonitic to  
252 granitic, peraluminous Ladybird granite suite into high-grade Shuswap Complex (Fig. 4) initiated  
253 at 62 Ma (Carr, 1992; Hinckley and Carr, 2006). In Idaho, peraluminous magmatism in the  
254 Bitterroot lobe (Fig. 4) of the Idaho batholith began at ca. 66 Ma and peaked at ca. 60 Ma  
255 (Gaschnig et al. (2010). These peraluminous rocks are part of the “Cordilleran anatetic belt” of  
256 Chapman et al. (2021a), and the magmatism is ascribed to partial melting of crustal rocks  
257 (Mueller et al., 1996; Hinckley and Carr, 2006; Gaschnig et al., 2011).

258 Sedimentary rocks of this age are also very rare in NE Washington. Aside from a <30 km<sup>2</sup>  
259 body of Paleocene conglomerate (Pipestone Canyon Formation) directly west of the Pasayten  
260 fault (Fig. 3) (Kriens et al., 1995), no other strata have been recognized between central

261 Washington and the Sevier foreland basins. The scarcity of sedimentary rocks, and the evidence  
262 of crustal melting, are compatible with the existence of a high-standing orogenic plateau in the  
263 hinterland during this interval (Whitney et al., 2004; Bao et al., 2014). Thrusting also occurred  
264 in the eastern belt in the Shuswap Complex and in the Rocky Mountain - Sevier fold and thrust  
265 belt (e.g., Price, 1981).

266 **60 – 52 Ma**

267 This interval is marked by major changes in magmatism and sedimentation throughout  
268 the region. Near-trench intrusions strongly suggest that an oceanic spreading center lay off  
269 central to southern Vancouver Island by 52 - 51 Ma (Fig. 5) (Groome et al., 2003; Madsen et al  
270 2006). Magmatism and sedimentation occurred in the western belt near the spreading ridge,  
271 but igneous activity was nearly absent in the Cascades core and eastern belt, until the onset of  
272 Challis-Kamloops magmatism at ca. 53 Ma (e.g., Ickert et al., 2009). The formation of  
273 metamorphic core complexes and associated basins in the eastern region also started at ca. 56  
274 Ma (e.g., Brown et al., 2012).

275 Basaltic magmatism began in the Siletzia terrane by ca. 55 Ma in the south (southwest  
276 Oregon) and by 53.2 Ma outboard of the Northwest Cascades system and mélange belts in  
277 western Washington and Vancouver Island in the north, where it continued until at least 48 Ma  
278 (Crescent and Metchosin basalts) (Fig. 2) (Wells et al., 2014; Eddy et al., 2017a). Siletzia consists  
279 of thick sequences of basalt that transition from deep-water lava flows of normal mid-oceanic-  
280 ridge basalt (N-MORB) to shallow water and subaerial flows of enriched mid-oceanic-ridge  
281 basalt (E-MORB) and oceanic-island basalt (OIB) (e.g., Wells et al., 2014). Siletzia is comparable  
282 in volume to other large igneous provinces (Trehu et al., 1994; Wells et al., 2014) and this,

283 combined with isotopic evidence, supports its formation over a 'plume-like' mantle source,  
284 thought to be the Yellowstone hot spot (e.g., Pyle et al., 2015; Phillips et al., 2017; Stern and  
285 Dumitru, 2019; Camp and Wells, 2021). In southern Oregon, the submarine basalts were  
286 overlain by deep-water sediments (Umpqua Group) in this time interval (Wells et al., 2014),  
287 while in Washington sedimentation was initiated in the non-marine Chuckanut and Swauk  
288 Formations of the greater Swauk basin (Fig. 3) (Eddy et al., 2016a). This basin developed on  
289 accreted Paleozoic and Mesozoic rocks of the Northwest Cascades thrust system and the  
290 southern end of the Cascades core. A 56.8 Ma tuff from the lower part of the Chuckanut  
291 Formation and a 59.9 Ma maximum depositional age (MDA) near the base of the Swauk  
292 Formation are compatible with sedimentation in the greater Swauk basin starting at 60 – 57 Ma  
293 (Eddy et al., 2016a). The 56.8 Ma tuff, a 53.7 Ma tuff higher in the Chuckanut section  
294 (Breedlovestrout et al., 2013), and a 53.7 Ma tuff with arc affinities (Summit Creek section; Kant  
295 et al., 2018) in the southern Washington Cascades are the only record of volcanism inboard of  
296 Siletzia in the western belt. There is also no well-documented deformation between 60 Ma and  
297 52 Ma, although a local angular unconformity in the middle to lower part of the Swauk  
298 Formation may be a link to the early collision of Siletzia (Doran, 2009).

299 In the North Cascades core a magmatic lull began at ca. 60 Ma (Miller et al., 2009), and  
300 that lull extended into the southern Coast Mountains to the northwest (Cecil et al., 2018). The  
301 transpressional Gabriel Peak belt (Fig. 3) of the Ross Lake fault system continued to be active  
302 between at least 60 – 55(?) Ma, and was cut by the transtensional Foggy Dew fault zone of the  
303 Ross Lake system at ca. 55–53 Ma (Miller and Bowring, 1990). Ductile deformation probably

304 occurred in domains in the Skagit Gneiss Complex, but otherwise, deformation is not well  
305 documented.

306 In northeastern Washington, magmatism is represented only by scattered, small-volume  
307 intrusions until ~53 Ma, while small mafic bodies began intruding the Idaho batholith region at  
308 ca. 58 Ma (Foster and Fanning, 1997; Gaschnig et al., 2010). Peraluminous magmatism  
309 (Ladybird granite suite), metamorphism, and migmatization continued during the 60–52 Ma  
310 time interval in the Shuswap and Okanagan complexes (e.g., Crowley et al., 2001; Kruckenberg  
311 et al., 2008; Gervais et al., 2010; Brown et al., 2012), and peraluminous magmatism persisted in  
312 the Bitterroot lobe of the Idaho batholith until ca. 53 Ma (Gaschnig et al., 2010) and the  
313 Anaconda core complex of Montana until ca. 56 Ma (e.g., Howlett et al., 2021). This magmatism  
314 in Idaho was directly followed by the Challis magmatic event (ca. 53 – 43 Ma; e.g., Janecke and  
315 Snee, 1993; Ickert et al., 2009; Gaschnig et al., 2010), which extended from Oregon to South  
316 Dakota and Washington and into central British Columbia as the Kamloops belt (Figs. 5, 6) (e.g.,  
317 Ewing, 1980; Breitsprecher et al., 2003). Shallow plutons, dikes, and volcanic rocks characterize  
318 this magmatic event with geochemical affinities ranging from arc to within-plate, and some  
319 rocks being almost entirely crustal melts and others only weakly contaminated melts of the  
320 lithospheric mantle (Ewing, 1980; Thorkelson and Taylor, 1989; Lewis and Kiilsgaard, 1991;  
321 Morris et al., 2000; Breitsprecher et al., 2003; Ickert et al., 2009; Dostal and Jutras, 2021). The  
322 alkalinity of magmas increases markedly south of ca. 51.5° N and the width of the belt widens  
323 south of the international border (e.g., Breitsprecher et al., 2003).

324 In the eastern belt, ductile deformation and thrusting continued in the hinterland of the  
325 Rocky Mountain fold and thrust belt for the early part of this interval (e.g., Simony and Carr,

326 2011). A major transition from contraction to extension, which was time transgressive (e.g.,  
327 Parrish et al., 1988; Harlan et al., 1988; Brown et al., 2012), led to the formation of  
328 metamorphic core complexes and associated extensional basins in NE Washington, British  
329 Columbia, Idaho, and Montana (Fig. 4). Core complexes (e.g., Priest River, Okanogan) and  
330 associated basins initiated earlier north of the WNW-striking Lewis and Clark fault zone than to  
331 the south (Anaconda, Bitterroot) (Foster et al., 2007). Sedimentary basin formation initiated  
332 from ca. 56 Ma next to the Okanogan core complex directly east of the North Cascades to ca. 53  
333 Ma adjacent to the Bitterroot and Anaconda core complexes (e.g., Foster et al., 2007; Howlett  
334 et al., 2021), and in NE Washington continued to 48 Ma (Pearson and Obradovich, 1977;  
335 Suydam and Gaylord, 1997). The absence of sedimentary deposits between the Swauk basin in  
336 the west and the foreland basin east of the thrust belt until extension began and basins formed  
337 suggests that the hinterland region continued to be a high orogenic plateau until ca. 55 Ma  
338 (Whitney et al., 2004; Bao et al., 2014).

339 We postulate that the near complete termination of arc-type magmatism in the North  
340 Cascades core and southern Coast Mountains, and paucity of magmatism east of there, records  
341 a change to low-angle subduction of the Farallon plate at ca. 60 Ma. The peraluminous  
342 magmatism in the east probably resulted mainly from concentrated crustal thickening (e.g.,  
343 Gaschnig et al., 2010).

344 In the eastern belt, the shift to shallow, widespread, and diverse magmatism at ca. 53  
345 Ma accompanied by extension points to a major change from the earlier peraluminous  
346 magmatism. This shift marks the onset of Challis activity and is discussed in more detail in the  
347 next section.

348 **52 – 49.5 Ma**

349 A fundamental change in plate boundary stresses occurred between 52 Ma and 49.5  
350 Ma, as Siletzia encountered the subduction zone in southern Oregon. Collision progressed  
351 northward during this time interval from Oregon to Washington and southern Vancouver Island  
352 (Wells et al., 2014). This collision was coincident with major changes in magmatism,  
353 sedimentation, and the strain field in the upper plate. The Siletzia collision also ultimately led to  
354 a westward shift in the location of the plate boundary (e.g., Schmandt and Humphreys, 2011).

355 The Siletzia collision was accompanied from central Vancouver Island to northwest  
356 Washington by near-trench magmatism from ca. 51 – 49 Ma (Madsen et al., 2006), which is  
357 thought to record the location of a subducting spreading ridge and the Kula-Farallon-North  
358 America or Resurrection-Farallon-North America triple junction (Fig. 5) (e.g., Cowan, 2003;  
359 Groome et al., 2003; Haeussler et al., 2003; Madsen et al., 2006) that would have been the  
360 northern boundary of Siletzia (Wells et al., 2014). This inference is also consistent with the 51  
361 Ma age of the ophiolitic Metchosin Complex on southern Vancouver Island (Massey, 1986, Eddy  
362 et al., 2017a). Near-trench magmatic rocks on Vancouver Island include: 51.2 – 50.5 Ma  
363 bimodal, but dominantly dacitic rocks (Flores volcanics) (Irving and Brandon, 1990); 51.2–48.8  
364 Ma, hypabyssal tonalite, trondhjemite, and granodiorite (Clayquot intrusions) (Madsen et al.,  
365 2006); and in the south peraluminous 50.9 – 50.7 Ma intrusions (Walker Creek intrusions)  
366 (Groome et al., 2003). The Leech River Schist on southern Vancouver Island also records high  
367 T/low P metamorphism at ~51 Ma (Fairchild and Cowan, 1982; Groome et al., 2003). In NW  
368 Washington, local peraluminous magmatism occurred as the ca. 49 Ma Mt. Pilchuck stock (Fig.  
369 3) and nearby Bald Mountain pluton (Yeats and Engels, 1971).

370 Farther inboard, but still west of the Cascades core, basaltic to rhyolitic volcanism began  
371 with the eruption of 51.4 Ma lavas and tuffs (Silver Pass member) of the upper Swauk  
372 Formation (Peterson and Tepper, 2021) and 51.3 Ma dacitic to rhyolitic lavas and pyroclastic  
373 rocks (Taneum Formation) which overlie clastic rocks correlative with the Swauk Formation (Fig.  
374 3) (Tabor et al., 1984; Eddy et al., 2016a; Wallenbrock and Tepper, 2017). These units represent  
375 the initiation of a magmatic belt that roughly parallels the leading edge of subducted Siletzia in  
376 the subsurface (Fig. 2) (Wells et al., 2014), and is attributed to tearing of the Farallon slab (Kant  
377 et al., 2018).

378 The approach and collision of Siletzia is also recorded in folding and changes in  
379 paleotopography in the western belt. Sedimentation in the Swauk basin persisted until at least  
380 ca. 50.8 Ma, the youngest MDA from stratigraphically high in the basin (Eddy et al., 2016a;  
381 Senes, 2019), but a drainage reversal from SW- to NE-flowing streams occurred at ca. 51 Ma  
382 (Eddy et al., 2016a) and may record the initial stages of collision of Siletzia at the latitude of the  
383 Swauk basin. A NW-vergent fold-and-thrust belt developed in SW Oregon in response to  
384 collision and involved Siletzia basalts, overlying Umpqua Group, and Klamath basement  
385 terranes. Unconformably overlying marine strata (Tyee Formation) demonstrate that accretion  
386 was completed between 50.5 Ma and 49 Ma at that latitude (Wells et al., 2000, 2014). In the  
387 central Washington Cascades, the Swauk Formation is folded and locally faulted under a short-  
388 lived (<1.5 Myr) angular unconformity with the overlying Teanaway Formation (Foster, 1958).  
389 The Teanaway Formation includes a 49.3 Ma rhyolite near its base (Eddy et al., 2016a) and is  
390 dominated by subaerial basalts, in contrast to the marine strata in SW Oregon. Contractual  
391 structures also attributed to the accretion of Siletzia are folds in the Chuckanut Formation in

392 the northwestern Swauk basin (Misch, 1966; Johnson, 1984), some of the upright folds in the  
393 Skagit Gneiss Complex of the North Cascades core (Miller et al., 2016), and the Cowichan fold-  
394 and-thrust belt on Vancouver Island, which is approximately the same age and has a similar  
395 northwesterly trend as the Chuckanut folds (Fig. 5) (Johnston and Acton, 2003).

396 The magmatic lull continued in the North Cascades core (Miller et al., 2009), although  
397 minor partial melting persisted in the Skagit Gneiss Complex (Gordon et al., 2010a). The deep-  
398 crustal (9-12 kbar) Swakane Gneiss in the crystalline core was probably rapidly exhumed during  
399 this interval, in part during distributed ductile shear and top-to-N to –NNE motion on the  
400 Dinkelman decollement (Fig. 3) (Paterson et al., 2004). Dextral-normal slip and associated  
401 mylonitization continued in the Foggy Dew fault zone, a southern strand of the Ross Lake fault  
402 system, and dextral displacement also occurred on the NW-striking Yalakom fault and other  
403 faults west of the Straight Creek-Fraser River fault (Fig. 5) (Miller and Bowring, 1990; Umhoefer  
404 and Schriazza, 1996).

405 East of the Cascades core, magmatism increased with the emplacement of granitoid  
406 plutons, and dominantly metaluminous tonalites and granodiorites. Although arc-like in  
407 mineralogy, many of these plutons have trace element traits compatible with slab-breakoff  
408 magmas (e.g.,  $\text{Sr/Y} > 10$ ,  $\text{La/YbN} > 10$ ; Whalen and Hildebrand, 2019) and Sr-Nd isotopic  
409 compositions indicative of significant contributions from older crust (Tepper and Eddy, 2017).  
410 The earliest U-Pb date associated with this renewed activity is 52 Ma in central Idaho, and  
411 subsequent plutonism appears to have migrated to the SW across NE Washington (Fig. 6C)  
412 (Tepper, 2016). Metamorphism and deformation continued in the metamorphic core  
413 complexes in southern British Columbia, NE Washington, Idaho, and Montana, as did Challis-

414 Kamloops magmatism and sedimentation in extensional basins where MDAs of locally derived  
415 sediments cluster around 50 Ma in southern British Columbia and northeastern Washington  
416 (e.g., Ewing, 1980; Suydan and Gaylord, 1997; Foster et al., 2007; Brown et al., 2012; Rubino et  
417 al., 2021). In contrast to NE Washington, no pattern of magmatism migration is seen across the  
418 Challis to Absaroka area in Idaho and Wyoming (e.g., Feeley and Cosca, 2003). The thermal  
419 peak in the Shuswap metamorphism was at ca. 53–49 Ma (Crowley et al., 2001).

420 Deformation in the eastern belt was dominated by roughly east-west extension,  
421 although contraction may have continued at deep levels in the Shuswap metamorphic core  
422 complex until ca. 52–49 Ma (Crowley et al., 2001; Gervais et al., 2010; Gervais and Brown,  
423 2011). The peak of extension and exhumation in the Okanogan core complex occurred at 53 –  
424 50 Ma (Brown et al., 2012). Brittle slip of uncertain sense reactivated the high-angle,  $\geq 250$ -km-  
425 long Pasayten fault (Fig. 3) along the eastern boundary of the Methow basin, and ended in  
426 Washington before eruption of ca. 48 Ma volcanic rocks, which overlap the fault (White, 1986).

427 In summary, the transition from a low-angle, transpressional subduction regime to a  
428 dextral transtensional regime was largely complete by the end of this time interval. The  
429 collision of Siletzia explains the deformation in the Swauk basin and along strike to the NW, and  
430 the southwestward migration of magmatism in NE Washington is consistent with rollback of the  
431 northern Farallon slab (Figs. 5, 6C). The slab ruptured west of the Cascades core and is marked  
432 in part by a belt of magmatism that started at the end of this time period and lasted until ca. 48  
433 Ma (Kant et al., 2018) (Fig. 6). Previous explanations for this Challis – Kamloops magmatism  
434 include a decrease in the rate of plate convergence (Constenius, 1996), passage of a slab  
435 window (Thorkelson and Taylor, 1989; Breitsprecher, et al., 2003; Ickert et al., 2009), buckling

436 and “sideways” slab rollback (Humphreys, 1995, 2009), and rollback and breakoff of the  
437 Farallon slab (Tepper, 2016). Slab rollback and breakoff, and slab window evolution are the  
438 most widely cited scenarios (see review by Humphreys and Grunder, 2022).

439 **49.5 – 45 Ma**

440 The short-lived deformation episode resulting from the collision of Siletzia was followed  
441 by profound changes in the tectonic evolution of the Pacific Northwest. A new subduction zone  
442 of the Kula or Resurrection plate beneath North America was established along the west side of  
443 Siletzia during this time interval (Fig. 6) (e.g., Schmandt and Humphreys, 2011). A dextral  
444 transtensional regime dominated, and a new non-marine strike-slip basin formed next to the  
445 Cascades core (Fig. 6). A magmatic flare-up occurred in the Cascades core and in the adjacent  
446 parts of the western belt, and magmatism and extension continued in the eastern belt, but  
447 were more aerially restricted after ca. 48 Ma.

448 In the west, the effects of the collision of Siletzia were waning by this time as  
449 magmatism ended in the southern part of Siletzia at ca. 50-49 Ma (Wells et al., 2014), and in  
450 northern Siletzia at ca. 48 Ma (Eddy et al., 2017a). The collision was followed in the Olympic  
451 Mountains (northern Siletzia) by deposition of turbidites (Blue Mountain unit) that have  
452 maximum depositional ages ranging from 47.8 to 44.7 Ma (Eddy et al., 2017a).

453 To the east of Siletzia, magmatism attributed to slab rollback, tear, and breakoff  
454 continued until ca. 45 Ma, producing compositionally diverse volcanic and plutonic rocks that in  
455 part formed parallel to the edge of Siletzia in the subsurface and are commonly near the  
456 Straight Creek fault and its splays (Fig. 6) (Trehu et al., 1994; Kant et al., 2018). Distinctive traits

457 of these rocks include their bimodal nature, with OIB affinities of the mafic lavas and crustal  
458 signatures of the silicic rocks. On the west side of the Straight Creek fault are basalt and lesser  
459 rhyolite flows interbedded with nonmarine sedimentary rocks in the Naches and Barlow Pass  
460 units (Fig. 3). East of the Straight Creek fault, the prolific Teanaway dike swarm intruded the  
461 deformed rocks of the Swauk basin (Fig. 3) (Tabor et al., 1984; Miller et al., 2022), and is  
462 interpreted to be related to the dominantly basaltic, ca. 49.3 Ma Teanaway Formation. The  
463 mafic rocks are medium-K tholeiitic basalts and basaltic andesites (Clayton, 1973; Peters and  
464 Tepper, 2006; Roepke et al., 2013), which are derived from mantle that is inferred to have been  
465 metasomatized during earlier subduction (Tepper et al., 2008). The NNE (035°) average  
466 orientation of the dikes provides the most robust evidence for initiation of right-lateral strike-  
467 slip on the Straight Creek fault at ~49 Ma (e.g., Miller, et al., 2022).

468 Starting at 49.2 Ma, the Chumstick basin formed between the right-stepping  
469 Leavenworth and Entiat strike-slip faults, directly west of the Chelan block (Evans, 1994; Eddy et  
470 al., 2016a) (Fig. 3). Abundant stratigraphic, paleocurrent, and detrital geochronologic data  
471 suggest that the basin formed during strike-slip faulting (Eddy et al., 2016a; Donaghy et al.,  
472 2021). The main western subbasin formed from 49.2 to ~46.5 Ma, and fault reorganization at  
473 ~46.5 - 44 Ma started inversion of the western subbasin and the formation of a narrow eastern  
474 subbasin next to the Entiat fault (Fig. 3). After this reorganization, strike-slip faulting localized  
475 on the Entiat and Straight Creek faults. The youngest (<45.9 Ma) sediments of the Chumstick  
476 Formation top the Leavenworth fault and probably correlate with the arkosic Roslyn Formation,  
477 which overlies the Teanaway Formation (Evans, 1994; Eddy et al., 2016a) (Fig. 3).

478                   The magmatic lull in the Cascades core ended at ~49.4 Ma, close in time to the eruption  
479                   of Teanaway volcanic rocks south of the Cascades core. The ensuing short-lived (until ca. 45  
480                   Ma) flare-up has the highest magmatic addition rate and the shortest duration of the three  
481                   flare-up events in the North Cascades since the mid-Cretaceous. It began with the ca. 49.6 Ma  
482                   Lost Peak stock, followed by two large (ca. 300 km<sup>2</sup> each) plutons, the Cooper Mountain and  
483                   Golden Horn batholiths, which intruded at 49.3-47.9 Ma and 48.5–47.7 Ma (Eddy et al., 2016b;  
484                   Miller et al., 2016), respectively, across the Ross Lake fault zone and into both the Cascades  
485                   core and the Methow basin (Fig. 3). These plutons and coeval variably deformed 49.4–47.2 Ma  
486                   intrusions (now orthogneisses) in the Skagit Gneiss Complex are commonly granodioritic in  
487                   contrast to the mainly Cretaceous tonalitic intrusions of the two older flare-ups (e.g., Misch,  
488                   1966; Haugerud et al., 1991; Miller et al., 2009). The ca. 49–48 Ma intrusions also range from  
489                   gabbro to granite, and include alkaline granites. Between ~47.9–46.5 Ma, magmatism in the  
490                   core migrated westward from the Ross Lake fault zone. The ~46.5 Ma Duncan Hill pluton and  
491                   45.5 Ma Railroad Creek pluton (Fig. 3) were the last of the large intrusions in the North  
492                   Cascades (Miller et al., 2021), and on the basis of their age and location, they appear to be the  
493                   youngest sizable elements related to slab rollback (Fig. 6C). The youngest magmatic rocks are  
494                   ca. 44.9 Ma lineated granite sheets (Misch, 1968; Haugerud et al., 1991; Wintzer, 2012; Miller  
495                   et al., 2016).  $\epsilon_{\text{Ndi}}$  values for some of the 49.3–45 Ma intrusive rocks are the least radiogenic  
496                   values for North Cascades intrusions, and imply a greater crustal component than in earlier  
497                   flare-ups (Matzel et al., 2008).

498                   Extensive dike intrusion into a  $\geq 600$  km<sup>2</sup> region of the Cascades core and adjacent rocks  
499                   to the east and south began at ca. 49.3 with the Teanaway dikes and at least one other dike

500 swarm, and continued until ca. 45 Ma (Miller et al., 2022). The largest number of dikes intruded  
501 between ca. 49.3–47 Ma. Many of these rhyolitic to basaltic dikes overlap spatially with the 49–  
502 46.5 Ma granodioritic plutons of the core. Some of the dikes have trace element signatures of  
503 arc magmas and some are adakites; they are interpreted to be the product of melting of  
504 eclogitic lower crust in response to intrusion of mantle-derived basalts (Davidson et al., 2015).

505 Metamorphism during this time interval is restricted to domains in the Skagit Gneiss  
506 Complex of the Cascades core where metamorphic monazite growth continued at least locally  
507 until 46 Ma (Gordon et al., 2010a). NW-striking foliation and subhorizontal lineation formed in  
508 the Complex from ca. 49.5–45 Ma (Haugerud et al., 1991; Wintzer, 2012; Miller et al., 2016),  
509 and foliation was deformed into upright gentle to open, generally SE- or NW-plunging folds of  
510 foliation between ca. 49 Ma to 47 Ma (Miller et al., 2016). Motion of the Ross Lake fault zone  
511 ended at ca. 49 Ma, but the Entiat fault was active until at least 46.9 Ma and ended by 44.4 Ma,  
512 and the N-S-trending Straight Creek fault experienced dextral slip from ca. 49 Ma and was  
513 sealed by 35 Ma (Misch, 1966; Tabor et al., 1984; Miller and Bowring, 1990). Excision and top-  
514 to-the north motion continued on the Dinkelman decollement at least until ca. 49–47 Ma  
515 (Matzel, 2004; Paterson et al., 2004). The Eocene dikes also provide information on the strain  
516 field. Their average orientation is ~035°, and the resultant extension direction (305°–125°) is  
517 oblique to the strike (~320°) of the North Cascades orogen and to the stretching lineation  
518 (average trend of 330°–150°) in the Skagit Gneiss Complex (Miller et al., 2022). Overall, these  
519 structures are compatible with the regional dextral transtensional tectonic regime.

520 The 49.5–45 Ma interval was marked by rapid cooling and exhumation of parts of the  
521 Cascades core. The 8–12 kbar Swakane Gneiss was in part exhumed by the Dinkelman

522 decollement and was at the surface in the Chumstick basin by 48.5 Ma (Tabor et al., 1987; Eddy  
523 et al., 2016a). Most of the  $^{40}\text{Ar}/^{39}\text{Ar}$  and K-Ar hornblende, biotite, and muscovite cooling ages in  
524 the 7–10 kbar Skagit Gneiss Complex are ca. 50–44 Ma (Engels et al., 1976; Wernicke and Getty,  
525 1997; Tabor et al., 2003; Gordon et al., 2010b), and thermochronology indicates very rapid  
526 cooling in some areas, with rates of perhaps 100°C/m.y. at ca. 47–45 Ma (Wernicke and Getty,  
527 1997).

528 In the eastern belt, magmatism, sedimentation, and extension all continued during the  
529 early part of this interval, and magmatism and extension were largely waning by the end.  
530 Igneous activity was still migrating southwestward across NE Washington (Fig. 6C). In British  
531 Columbia, the >200 km<sup>2</sup>, granodioritic Needle Peak pluton intruded the Methow basin at ca. 48  
532 Ma (Monger, 1989), and Challis-Kamloops magmatism to the east had largely ended by ca. 47  
533 Ma (Ickert et al., 2009; Dostal and Jutras, 2021).

534 Extension and sedimentation related to the metamorphic core complexes in NE  
535 Washington and British Columbia were on the wane during this interval. Termination of  
536 sedimentation at ~48 in NE Washington was roughly coeval with the end of volcanism (Suydam  
537 and Gaylord, 1997). Mylonitization in the Okanogan Complex ended at ca. 49 Ma with cooling  
538 through 47 Ma (Kruckenberg et al., 2008). The Priest River Complex was rapidly exhumed from  
539 ca. 50–48 Ma (Doughty and Price, 2000; Stevens et al., 2016), but extension and exhumation  
540 continued through this interval in Idaho and Montana in the Bitterroot and Anaconda core  
541 complexes (Foster et al., 2007, 2010; Howlet et al., 2021). The Lewis and Clark fault zone  
542 continued to act as a boundary between the older core complexes to the north and the  
543 younger complexes to the south.

544 **45 - 40 Ma**

545 This interval marks the end of slab foundering and the establishment of a new north-  
546 south subduction zone and arc that became Cascadia. Subduction was occurring beneath much,  
547 if not all, of Oregon and Washington by the end of this period (Fig. 7). Sedimentation occurred  
548 in the western belt, but ended in the Chumstick basin, as did Challis-Kamloops magmatism in  
549 the eastern belt.

550 Arc magmatism began at ca. 45 Ma in southwest Washington where local basaltic  
551 andesites and andesites erupted (du Bray and John, 2011) and by 40 Ma in southwest Oregon  
552 (e.g., Darin et al., 2022). In northwestern Washington, similar volcanic rocks occur in a belt that  
553 lies west of the younger part of the Cascades arc and also includes 45 – 35 Ma granodioritic  
554 intrusions, and abundant 45–40 Ma tuffs occur in the Puget Group (Fig. 3) (Vine, 1969; Tabor et  
555 al., 1993, 2000; Dragovich et al., 2009, 2011, 2013, 2016; MacDonald et al., 2013). Within this  
556 belt the oldest rocks appear to be at the northern end, but there is a lack of precise dates for  
557 units in the south. Local dacite and rhyolite domes (Wenatchee domes) intruded the Chumstick  
558 basin to the east at ca. 44.5 Ma (Gilmour, 2012; Eddy et al., 2017b) and may be the youngest  
559 intrusive rocks related to slab rollback and/or breakoff (White et al., 2021). In SW Washington  
560 and Oregon, the Tillamook magmatic episode occurred from 42 to 34 Ma (Parker et al., 2010;  
561 Chan et al., 2012; Wells et al., 2014). This episode included volcanic rocks (Tillamook Volcanics,  
562 Yachats basalt, and Grays River Volcanics) in NW Oregon and SW Washington, which are  
563 interpreted by some workers to be related to the Yellowstone hotspot, and were synchronous  
564 with margin-parallel extension (e.g., Wells et al., 2014; Camp and Wells, 2021).

565 Sedimentation in the western belt includes both deep and shallow marine deposits on  
566 the Olympic Peninsula (Einarsen, 1987; Babcock et al., 1994). Inboard, in the Puget Sound  
567 region, the deltaic to shallow marine middle(?) to late Eocene Puget Group (Fig. 3; Vine, 1969;  
568 Buckovic, 1979; Johnson and O'Connor, 1994) was deposited on Siletzia on the west and the  
569 older rocks of the western North Cascades on the east. The Puget Sound basin likely formed in  
570 the forearc to the early Cascadia arc.

571 Sedimentation ended in the Chumstick basin, but continued in the overlying, ca. 44–42  
572 Ma arkosic Deadhorse Canyon unit and the Roslyn Formation (Evans, 1994; Eddy et al., 2016a).  
573 (Fig. 3). The latter, which rests on the Teanaway Formation south of the Cascades core, may be  
574 the easternmost part of the regional depositional system that included the Puget Group.

575 Magmatism ceased in the Cascades core at ca. 44.9 Ma and ductile deformation in the  
576 Skagit Gneiss Complex had also ended at ca. 45 Ma (Miller et al., 2016). Dextral strike slip ended  
577 between 46.9 Ma and 44.5 Ma on the Entiat fault (Evans, 1994; Eddy et al., 2016a) and  
578 continued to a later time on the Straight Creek fault, which is intruded by a 34 Ma pluton (e.g.,  
579 Tabor et al., 2003).

580 East of the Cascades core, Challis magmatism terminated at ca. 43 Ma (Gaschnig et al.,  
581 2010). Extension and cooling of the Bitterroot and Anaconda core complexes continued until ca.  
582 39 Ma, as did sedimentation (Foster et al., 2010; Howlett et al., 2021). Motion on the Lewis and  
583 Clark fault zone presumably ended as well.

584

585 **DISCUSSION**

586           We emphasized in the introduction that the Pacific Northwest in the Paleogene is an  
587           excellent place to examine a variety of processes resulting from ridge-trench interaction and  
588           oceanic plateau collision. In the following, we explore the upper-plate response shortly before,  
589           during, and after the Farallon- Kula or Farallon-Resurrection ridge encountered the trench  
590           bordering North America near Vancouver Island, and the consequences of the collision of  
591           Siletzia.

592           **Relation of the 60 – 50 Ma Magmatic Lull to Slab Dynamics**

593           It is likely that the end of long-lived arc magmatism in the Cascades core at ca. 60 Ma  
594           and the overall low volume of magmatism from ca. 60–50 Ma eastward to the Idaho batholith  
595           resulted from flat-slab subduction. Moreover, magmatism in the Idaho batholith during this  
596           interval probably resulted from crustal thickening and not subduction-related processes  
597           (Gaschnig et al., 2010). The shallowing of the slab may be attributable to the rapid subduction  
598           of young buoyant lithosphere, as also proposed by others for the greater region (e.g.,  
599           Thorkelson and Taylor, 1989; Haeussler et al., 2003). Strong suction in the mantle wedge may  
600           have played a role, as proposed for the Laramide belt (Humphreys, 2009; O'Driscoll et al.,  
601           2009). Note that the Laramide belt in northern Wyoming was directly east of Siletzia at 55 Ma  
602           in our reconstruction (Fig. 4).

603           The northern boundary of the flat slab is inferred to be northeast of central Vancouver  
604           Island (Fig. 4) where there is a transition in pluton ages within the Coast Mountains batholith.  
605           The southern Coast Mountains have a 60 – 50 Ma magmatic lull much like the Cascades core of  
606           this study, whereas to the north, a high magma addition event attributed to arc magmatism

607 occurred from 61–48 Ma (Cecil et al., 2018). A projection of the triple junction off central  
608 Vancouver Island through the boundary in the Coast Mountains to the NE may run to the  
609 northern edge of the Shuswap Complex at this time, which potentially explains the location of  
610 the belt of major extension along the eastern edge of the flat slab from British Columbia to  
611 southern Idaho and western Montana. Alternatively, the flat slab may have underlain the  
612 region of the magmatic lull, but just south of most of the Shuswap to Okanogan extensional  
613 belt (Fig. 4), in which case the latter would be kinematically tied to the Tintina fault – Rocky  
614 Mountain trench (Price and Carmichael, 1986) and magmatism would occur in a slab window  
615 (e.g., Breitsprecher et al., 2003). Seismic tomography and reconstructions of plate motions in  
616 the NE Pacific also suggest a major boundary inboard from Vancouver Island (Fuston and Wu,  
617 2021). Plate motion models indicate rapid northward rates of either the Kula or Resurrection  
618 plates from ca. 65–50 Ma that were highly oblique to the North American plate boundary  
619 (Engebretson et al. 1985; Matthews et al., 2016), and this may have produced a large slab  
620 window under western Canada (Fuston and Wu, 2021; cf. Madsen et al., 2006) north of the  
621 proposed flat slab.

622 The magmatic lull and flat slab extended to the south of the crystalline core of the North  
623 Cascades, which on the basis of known strike-slip faults (Wyld et al., 2006; this study) was at the  
624 latitude of current central Oregon to the Oregon – Washington border at ca. 60–50 Ma. Post-50  
625 Ma volcanic and sedimentary strata obscure relations to the south and east of the Wenatchee  
626 block; in our reconstruction at 55 Ma (Fig. 4), and projecting faulting back to 60 Ma, the North  
627 Cascades would have lain near the NW edge of the Klamath – Blue Mountains terranes and the

628 flat slab beneath the Pacific Northwest would be continuous with the well-established Laramide  
629 flat slab to the south (see Tikoff et al. [2023] for an alternative hypothesis).

630

631 **Consequences of Collision of Siletzia**

632 The inferred position of the intersection of the Farallon – Resurrection/Kula ridge with  
633 the trench is complicated by the eruption of Siletzia basalts and the construction of an oceanic  
634 plateau above a hot spot mantle plume (e.g., Wells et al., 2014). In the region of the  
635 Washington Cascades, major changes occurred in the upper plate of the system due to collision  
636 of this oceanic plateau.

637 Notable aspects of Siletzia collision are the short duration of the associated  
638 deformation, its profound inboard influence, and the subsequent change in plate boundary  
639 stresses along the newly established North America margin. The most important structural  
640 response was the brief shortening that migrated from southwest Oregon to central Washington  
641 and Vancouver Island during the 51 – 49 Ma interval (Fig. 5) (Wells et al., 2014). In the Swauk  
642 basin, folding and formation of an angular unconformity is tightly bracketed between ~50.8 Ma  
643 and 49.3 Ma (Eddy et al., 2016a). The reversal of drainage in the Swauk basin at ~51 Ma is  
644 probably one of the first signs of Siletzia collision at that latitude (Eddy et al., 2016a). Younger  
645 upright folding continued until ca. 48 Ma at deeper crustal levels in the Skagit Gneiss Complex  
646 of the Chelan block of the Cascades core ~175 km inboard of Siletzia (Miller et al., 2016).  
647 Folding only bracketed between ca. 65 Ma and 48 Ma (Kriens et al., 1995) in the Methow basin  
648 farther to the northeast may have been induced by collision. In contrast, in the eastern belt,

649  $\geq 235$  km inboard of Siletzia, extension in most of the core complexes continued unabated.

650 Peak metamorphism of the voluminous Shuswap Complex and several other core complexes at

651  $\sim 53\text{--}49$  Ma was roughly coincident with the proposed flat slab and Siletzia collision. One

652 explanation for the widespread eastern extension and timing of magmatism and

653 metamorphism may be the rollback of the flat slab, which we propose was underway in

654 Washington by ca. 52 Ma (Figs. 5, 6C).

655 In the western belt, sedimentation continued in the early stages of collision after the

656 drainage reversal in the Swauk basin at 51 Ma, but presumably ended during folding and

657 certainly before the Swauk-Teanaway unconformity and eruption of Teanaway volcanic rocks at

658 49.3 Ma. Note that the youngest Swauk Formation strata are in lake and fluvial facies in the far

659 eastern end of the Swauk basin near the Leavenworth fault (Tabor et al., 1982; Senes, 2019),

660 and their position may be related to an eastward migration of late basin subsidence related to

661 the collision. In the eastern belt, sedimentation continued in the supra-detachment extensional

662 basins and grabens until ca. 48 Ma, just after this slab is inferred to have rolled back to the SW.

663 The collision of Siletzia with the continental margin influenced magmatism much farther

664 eastward than it influenced deformation and sedimentation. We attribute this to the shut off of

665 northeastward flat subduction caused by the collision-related plate reorganization (e.g.,

666 Schmandt and Humphreys, 2011). Magmatism migrated to the southwest across NE

667 Washington and reached the Golden Horn batholith at the northeast margin of the Cascades

668 core at ca. 48.3 Ma (Figs. 3, 6C). This migration has been interpreted to result from slab rollback

669 (Tepper, 2016) and breakoff, as the Farallon plate detached and formed the subvertical “slab

670 curtain" currently imaged seismically beneath Idaho and eastern Washington (Schmandt and  
671 Humphreys, 2011).

672

673 **What Drove the 49.3 Ma to 45.5 Ma Magmatic Flare-up?**

674 Plutons in the North Cascades crystalline core and dike swarms across the study area  
675 record a major magmatic flare-up at 49.3–45.5 Ma (Miller et al., 2009), shortly after Siletzia  
676 collision. This flare-up is concentrated in the Chelan block of the core, but also includes plutons  
677 that intruded the Methow basin directly east and northward of the core for ca. 70 km into  
678 Canada (e.g., Needle Peak pluton), volcanic rocks on the west and south sides of the core, and  
679 voluminous dike swarms (Figs. 3, 6) (e.g., Tabor et al., 1984; Eddy et al., 2016b; Miller et al.,  
680 2016, 2022). The Eocene flare-up is marked by the highest magmatic addition rate and shortest  
681 duration of any of the magmatic events in the North Cascades.

682 The factors that control initiation and termination of magmatic 'flare-ups', such as the  
683 Eocene event, are controversial (e.g., Chapman et al., 2021b). Isotopic data from intrusions  
684 emplaced during flare-ups in some arcs imply increased crustal melting and have led to the  
685 orogenic cycle hypothesis in which flare-ups are driven by melting of fertile backarc crustal  
686 material thrust into the deep levels of an arc or underlying mantle (e.g., Ducea and Barton,  
687 2007; DeCelles et al., 2009). Others have argued that voluminous melting results dominantly  
688 from processes external to the arc, including slab break-off and ridge subduction, and largely  
689 involves mantle-derived melts (e.g., Decker et al., 2017; Schwartz et al., 2017; Ardila et al.,  
690 2019), which in turn can drive an increase of partial melting of the crust.

691 The Eocene Cascades core plutons have been considered the latest pulse of arc  
692 magmatism in the North Cascades by earlier workers (e.g., Matzel et al., 2008; Miller et al.,  
693 2009), and magmatism to the east in the Challis-Kamloops belt has been interpreted to occur  
694 within a slab window (e.g., Thorkelson and Taylor, 1989; Breitsprecher et al., 2003). In our view,  
695 the flare-up is related to the Farallon slab rollback and breakoff. At ~49.5 Ma, the southwest-  
696 migrating rollback magmatism had reached the northeast margin of the Cascades core (Tepper,  
697 2016) and the edge of a large slab window may have lain nearby to the north (Fig. 6). The  
698 accretion of Siletzia and termination of subduction led the slab to break off, as shown in part by  
699 the belt of bimodal volcanic rocks lacking an arc signature near the Straight Creek fault (Figs. 3,  
700 6, 9) (Kant et al., 2018). The Eocene age Cascades core plutons have a wider isotopic range than  
701 earlier plutons (Matzel et al., 2008), but their geochemistry does not permit distinguishing  
702 between an arc or slab break-off origin as the crustal component of melt during break-off  
703 would be mafic lower crust of the Late Cretaceous arc. Dextral strike-slip, slab rollback, and  
704 breakoff were concentrated in and near the Cascades core, and we infer that the slab was  
705 ripped apart leading to upwelling of asthenospheric mantle and decompression melting (Fig. 9).

706 A speculative additional interpretation is that the breakoff-related magmatism  
707 continued to the southeast beneath the Columbia River Basalt Group in the Pasco basin to the  
708 Clarno Formation of NE Oregon (Figs. 2, 6). The Pasco basin is on strike with the Eocene  
709 Chumstick basin and seismic velocities suggest that beneath the Miocene basalt is a thick,  
710 asymmetric sedimentary basin of probable Eocene age and an associated mafic underplate  
711 (Catchings and Mooney, 1988; Gao et al., 2011). These mafic rocks may be similar to the  
712 Teanaway Basalt of the flare-up. The Clarno Formation is not well dated, but available ages

713 suggest that the volcanic rocks erupted starting at ca. 53–50 Ma (Bestland et al., 2002). Note  
714 that in our reconstruction for 48 Ma the Clarno area is about 100 km SE of the North Cascades  
715 flare-up and the western breakoff belt west of the Straight Creek fault would have been about  
716 40–50 km closer to the Clarno at 50 Ma. If the Siletzia terrane lay on a small microplate within  
717 the shrinking northern Farallon plate as we show (Fig. 6), then the southeast edge of the slab  
718 that rolled back and broke off may have been near the Clarno volcanics (cf. Humphreys, 2009).

719

720 **Upper Plate Deformation After Siletzia Collision**

721 The ca. 49–45 Ma structural record west of the Fraser River-Straight Creek fault is  
722 largely restricted to high-angle NW-striking faults and associated local folds, whereas in the  
723 central and eastern belts a wide array of structures can be used to evaluate deformation.  
724 Eocene dikes, dextral strike-slip faults, basins, and ductile structures in the Cascades are broadly  
725 coeval with dikes, faults bounding non-marine basins, and ductile fabrics in metamorphic core  
726 complexes in NE Washington and southern British Columbia (Fig. 6) (e.g., Ewing, 1980; Parrish  
727 et al., 1988; Eddy et al., 2016a; Miller et al., 2016). Dikes in the eastern belt are not well dated,  
728 but most K-Ar dates from volcanic rocks in NE Washington range between 51–48 Ma (Pearson  
729 and Obradovich, 1977), and thus overlap temporally with the older (49.3–47.5 Ma) dikes in the  
730 Cascades and the magmatic flare-up. Dikes intruding the Kettle metamorphic core complex,  
731 ~140 km east of the North Cascades, strike ~012°–022° (McCarley Holder et al., 1990; their Fig  
732 1). These dikes are subparallel to the normal faults that separate the Kettle and Okanogan core  
733 complexes from Eocene grabens (Keller, Republic, and Toroda), which strike 008–020°. Farther  
734 east, ENE-WSW (~075°–255°) brittle slip occurred on the Newport fault, which is the upper

735 boundary of the Priest River Complex (Harms and Price, 1992), and east and south of the Lewis  
736 and Clark fault zone, slip on the Bitterroot and Anaconda detachments is top-to-the-east-  
737 southeast (~100–110°) (Kalakay et al., 2003; Foster et al., 2007). Brittle extension directions  
738 from the dikes and faults bounding the grabens suggest that they are oblique (ca. 15°–50°  
739 counter clockwise) to those of the voluminous N–NE-striking (average of 035°), ~49.3–47.5 Ma  
740 dikes in the Cascades.

741 A major difference between faults in the eastern belt and those in the western and  
742 central belts is that the eastern faults are apparently purely dip slip, whereas faults (Ross Lake,  
743 Entiat, Leavenworth, Straight Creek) in the central and western belts are dextral strike slip, and  
744 most have a subordinate component of normal slip. Dextral slip does occur to the east on the  
745 Lewis and Clark fault zone (Figs. 2, 6), but this structure strikes ~E-W and transfers slip between  
746 the Anaconda, Bitterroot, and Priest River core complexes (e.g., Foster, et al., 2007). The  
747 combination of dextral strike-slip faults and dike swarms of the Cascades core region is most  
748 compatible with a N-S dextral shear and related WNW – ESE extension.

749 Eocene ductile stretching in mylonites in core complexes ranges from ~105–285° in the  
750 Bitterroot and Anaconda complexes in Montana (Foster et al. 2007), to 074-254° in the Priest  
751 River Complex (Harms and Price, 1992; Doughty and Price, 1999) near the Washington – Idaho  
752 border, to E-W in the Kettle Complex (Rhodes and Cheney (1981), to W-NW – E-SE (~295-115°)  
753 in the Okanogan Complex (Kruckenberg, 2008; Brown et al., 2012) ~ 40 km east of the Cascades  
754 core. Broadly coeval, subhorizontal Eocene ductile stretching in the North Cascades is ~330 -  
755 150° in the Skagit Gneiss Complex to close to N-S in the Swakane Gneiss. Thus, ductile extension  
756 directions rotate progressively clockwise by ~75° from east to west. The sense of rotation is the

757 same, but the magnitude of rotation is greater, then that of the upper-crustal structures.  
758           Rotation of extension directions fits with the progressively greater influence of dextral  
759   shear closer to the plate margin in response to the plate reorganization at ~49.5 Ma after  
760   Siletzia collision. Extension and transtension led to orogenic collapse in the core complexes  
761   (e.g., Price and Carmichael, 1986; Parrish et al., 1988; Vanderhaege and Teyssier, 2001),  
762   whereas strike slip occurred to the west on the faults bounding and cutting the North Cascades  
763   core.

764

#### 765 **Eocene Global Plate Reorganization**

766           The dramatic tectonic transitions in the Pacific Northwest region at ca. 52–49 Ma  
767   coincide with a fundamental plate reorganization in the Pacific Basin and a global change in  
768   plate vectors at ~53–47 Ma (e.g., Whittaker et al., 2007; O'Connor et al., 2013; Seton et al.,  
769   2015). This plate reorganization in the Pacific may have been driven by subduction of the  
770   Izanagi-Pacific ridge at ca. 60–46 Ma (Wu and Wu, 2019), with the ensuing initiation of  
771   subduction in the Tonga-Kermadec and Izu-Bonin-Mariana system occurring at ca. 53–50 Ma  
772   (Sharp and Clague, 2006; Whittaker et al., 2007a; Tarduno et al., 2009). The ~50 Ma bend in the  
773   Hawaiian –Emperor seamount chain also coincides with a change in Pacific plate motion and  
774   Australian-Antarctic plate reorganization at that time (Sharp and Clague, 2006; Whittaker et al.,  
775   2007). It has been suggested that Pacific – Kula plate spreading also changed at ca. 53.3 Ma to  
776   43.8 Ma (Lonsdale, 1988), and that Kula – North America relative motion became more  
777   northerly and faster at 57 Ma (Doubrovine and Tarduno, 2008). Other major global events  
778   roughly coeval with the fundamental changes in the Pacific Northwest region include initiation

779 of the Aleutian arc and the dramatic slowing of Greater India at ca. 50 Ma resulting from  
780 collision with Asia (e.g., Copley et al., 2010; van Hinsbergen et al., 2011).

781 It appears that the significant changes in the tectonics of the Pacific Northwest at 52 –  
782 49 Ma are the consequence of both a global plate reorganization and the regional collision of  
783 the ridge-centered Siletzia oceanic plateau. The global plate changes resulted in faster and  
784 perhaps more northerly relative plate motion in the Pacific Northwest, which in turn resulted in  
785 the formation of the new N-S- striking strike-slip Straight Creek – Fraser River fault. However,  
786 most of the complex changes summarized here are the result of the profound changes due to  
787 the Siletzia collision and westward stepping of the subduction zone, and triple-junction  
788 migration during the 60 – 40 Ma interval.

789

## 790 **ACKNOWLEDGEMENTS**

791 This research was supported by National Science Foundation grants EAR-1119358 and  
792 EAR-1945352 to R.B. Miller, EAR-1945260 to M.P. Eddy, EAR-1119252 to J.H. Tepper, EAR-  
793 1119063 to P.J. Umhoefer, and EAR-1118883 to S. Bowring. Our late colleague and friend Paul  
794 Umhoefer was a driving force for much of this synthesis and particularly the fault  
795 reconstructions. The late Sam Bowring also played an important role in the research presented  
796 here. M.S. and B.S thesis students at Northern Arizona University, San Jose State University, and  
797 the University of Puget Sound contributed to our research project and include Katie Bryant, Erin  
798 Donaghy, Melissa Gunderson, Lisa Kant, Jen Pence, and Francesca Senes. We thank Stacia

799 Gordon, Margi Rusmore, and Noah McLean for helpful discussions. We thank Gene Humphreys  
800 and Derek Thorkelson for their thorough and very helpful reviews of the manuscript.

801

802 **References Cited**

803 Ardila, A.M.M., Paterson, S.R., Memeti, V, Parada, M.A., and Molina, P.G., 2019, Mantle driven  
804 Cretaceous flare-ups in Cordilleran arcs: *Lithos*, v. 326-327, p. 19-27.

805 Atwater, T., 1970, Implications of plate tectonics for the Cenozoic tectonic evolution of western  
806 North America: *Geological Society of America Bulletin*, v. 81, p. 3513–3536.

807 Babcock, R.S., Suczek, C.A., and Engebretson, D.C., 1994, The Crescent “Terrane,” Olympic  
808 Peninsula and Southern Vancouver Island: *Washington Division of Geology and Earth*  
809 *Resources Bulletin* 80, p. 141–157.

810 Bao, X., Eaton, D.W., and Guest, B., 2014, Plateau uplift in western Canada caused by  
811 lithospheric delamination along a craton edge: *Nature Geoscience*, v. 7, p. 830–833.

812 Beck, M.E., 1984, Has the Washington-Oregon coast range moved northward?: *Geology*, v. 12,  
813 p. 737–740.

814 Beck, M.E., Burmester, R.F., and Schoonover, R., 1982, Tertiary paleomagnetism of the North  
815 Cascade Range, Washington: *Geophysical Research Letters*, v. 9, p. 515-518.

816 Beske, S.J., Beck, M.E., and Noson, L., 1973, Paleomagnetism of the Miocene Grotto and  
817 Snoqualmie batholiths, central Cascades, Washington: *Journal of Geophysical Research*, v.  
818 78, p. 2601-2608.

819 Bestland, E.A., Hammond, P.E., Blackwell, D.L.S., Kays, M.A., Retallack, G.J., and Stimac, J., 2002,  
820       Geologic framework of the Clarno unit, John Day Fossil Beds National Monument,  
821       central Oregon: Oregon Department of Geology and Mineral Industries, Open-file  
822       Report, 0-02-03, 39 p.

823 Bradley, D.C., Kusky, T.M., Haeussler, P.J., Goldfarb, R.J., Miller, M.L., Dumoulin, J.A., Nelson,  
824       S.W., and Karl, S.M., 2003, Geologic signature of early Tertiary ridge subduction in  
825       Alaska, *in* Sisson, V.B., Roeske, S.M., and Pavlis, T.L., eds., Geology of a Transpressional  
826       Orogen Developed During Ridge-trench InteractionAlong the North Pacific Margin:  
827       Geological Society of America Special Paper 371, p. 19–49, <https://doi.org/10.1130/0-8137-2371-X.19>.

829 Brandon, M.T., Cowan, D.S., and Vance, J.A., 1988, The Late Cretaceous San Juan thrust system,  
830       San Juan Islands, Washington: Geological Society of America Special Paper, v. 221, 81 p.

831 Breedlovestrout, R.L., Evraets, B.J., and Parrish, J.T., 2013, New Paleogene paleoclimate analysis  
832       of western Washington using physiognomic characteristics from fossil leaves:  
833       Palaeogeography, Palaeoclimatology, Palaeoecology, v. 392, p. 22–40, doi: 10.1016/j  
834       .palaeo.2013.08.013 .

835 Breitsprecher, K., Thorkelson, D.J., Groome, W.G., and Dostal, J., 2003, Geochemical  
836       confirmation of the Kula-Farallon slab window beneath the Pacific Northwest in Eocene  
837       time: Geology, v. 31, p. 351-354.

838 Brown, E.H., 1987, Structural geology and accretionary history of the Northwest Cascades  
839       system, Washington and British Columbia: Geological Society of America Bulletin, v. 99, p.

840 201–214.

841 Brown, E.H., and Talbot, J.L., 1989, Orogen-parallel extension in the North Cascades crystalline

842 core, Washington: *Tectonics*, v. 8, p. 1105–1114, doi: 10.1029/TC008i006p01105.

843 Brown, R.L., Journeay, J.M., Lane, L.S., Murphy, D.C., and Rees, C.J., 1986, Obduction,

844 backfolding and piggyback thrusting in the metamorphic hinterland of the southeastern

845 Canadian Cordillera: *Journal of Structural Geology*, v. 8, p. 255–268.

846 Brown, S.R., Gibson, H.D., Andrews, G.D.M., Thorkelson, D.J., Marshall, D.M., Vervoort, J.D., and

847 Rayner, N., 2012, New constraints on Eocene extension within the Canadian Cordillera

848 and identification of Phanerozoic protoliths for footwall gneisses of the Okanagan Valley

849 shear zone: *Lithosphere*, v. 4, p. 353–377.

850 Buckovic, W.A., 1979, The Eocene deltaic system of west-central Washington, in Armentrout, J.,

851 Cole, M.R., and Terbest, H., eds., *Cenozoic Paleogeography of the Western United States*:

852 Society of Economic Paleontologists and Mineralogists Pacific Section, Pacific Coast

853 Paleogeography Symposium 3, p. 147–163.

854 Burchfiel, B.C., Cowan, D.S., and Davis, G.A., 1992, Tectonic overview of the Cordilleran orogen

855 in the western United States, in Burchfiel, B.C., Lipman, P.W., and Zoback, M., eds., *The*

856 *Cordilleran Orogen: Coterminous U.S. in the Western United States*: Boulder, Colorado,

857 Geological Society of America, *The Geology of North America*, v. G-3, p. 407–479.

858 Camp, V.E., and Wells, R.E., 2021, The case for a long-lived and robust Yellowstone hot spot:

859 GSA Today, v. 31, <https://doi.org/10.1130/GSATG477A.1>.

860 Carr, S.D., 1992, Tectonic setting and U-Pb geochronology of the Early Tertiary Ladybird  
861 Leucogranite Suite, Thor-Odin - Pinnacles Area, Southern Omineca Belt, British Columbia:  
862 Tectonics, v. 11, p. 258-278.

863 Catchings, R.D., and Mooney, W.D., 1988, Crustal structure of the Columbia Plateau: Evidence  
864 for continental rifting: Journal of Geophysical Research, v. 93, p. 459-474.

865 Cecil, M.R., Rusmore, M.E., Gehrels, G.E., Woodsworth, G.J., Stowell, H.H., Yokelson, I.N.,  
866 Chisom, C., Trautman, M., and Homan, E., 2018, Along-strike variation in the magmatic  
867 tempo of the Coast Mountains batholith, British Columbia, and implications for processes  
868 controlling episodicity in arcs: Geochemistry, Geophysics, Geosystems, v. 19, p. 4274–  
869 4289. <https://doi.org/10.1029/2018GC007874> 2018.

870 Chan, C.F., Tepper, J.H., and Nelson, B.K., 2012, Petrology of the Grays River volcanics,  
871 southwest Washington: Plume-influenced slab window magmatism in the Cascadia  
872 forearc: Geological Society of America Bulletin, v. 124, p. 1324-1338.

873 Chapman, J.B., 2021a, Runyon, S.E., Shields, J.E., Lawler, B.L., Pridmore, C.J., Scoggin, S.H.,  
874 Swaim, N.T., Trzinski, A.E., Wiley, H.N., Barth, A.P., and Haxel, G.B., 2021a, The North  
875 American Cordilleran anatetic belt: Earth Science Reviews, v. 215,  
876 <https://doi.org/10.1016/j.earscirev.2021.103576>.

877 Chapman, J.B., Shields, J.E., Ducea, M.N., Paterson, S.R., Attia, S., and Ardill, K.E., 2021b, The  
878 causes of continental arc flare ups and drivers of episodic magmatic activity in Cordilleran  
879 orogenic systems: Lithos, v. 398-399, doi.org/10.1016/j.lithos.2021.106307.

880 Clayton, D.N., 1973, Volcanic history of the Teanaway Basalt, east-central Cascade Mountains,  
881 Washington [M.S. thesis]: Seattle, Washington, University of Washington, 55 p.

882 Clennett, E.J., Sigloch, K., Mihalynuk, M.G., Seton, M., Henderson, M.A., Hosseini, K.,  
883 Mohammadzaheri, A., Johnston, S.T., and Müller, R.D., 2020, A quantitative tomotectonic  
884 plate reconstruction of western North America and the eastern Pacific Basin:  
885 Geochemistry, Geophysics, Geosystems, e2020GC009117,  
886 <https://doi.org/10.1029/2020GC009117>.

887 Colgan, J.P., and Henry, C.D., 2009, Rapid middle Miocene collapse of the Mesozoic orogenic  
888 plateau in north-central Nevada: International Geology Review, v. 51, p. 920-961.

889 Constenius, K.N., 1996, Late Paleogene extensional collapse of the Cordilleran foreland fold  
890 and thrust belt: Geological Society of America Bulletin, v. 108, p. 20–39.

891 Copley, A., Avouac, J.P., and Royer, J-Y., 2010, The India-Asia collision and the Cenozoic  
892 slowdown of the Indian plate; implications for the forces: Journal of Geophysical  
893 Research, v.115, B03410, doi:10.1029/2009JB006634.

894 Coutts, D.S., Matthews, W.A., Englert, R.G., Brooks, M.D., Boivin, M-P, and Hubbard, S.M., 2020,  
895 Along-strike variations in sediment provenance within the Nanaimo basin reveal  
896 mechanisms of forearc basin sediment influx events: Lithosphere, v. 12, p. 180–197.

897 Cowan, D.S., 2003, Revisiting the Baranof–Leech River hypothesis for early Tertiary coastwise  
898 transport of the Chugach–Prince William terrane: Earth and Planetary Science Letters, v.  
899 213, p. 463-475.

900 Cowan, D.S., Brandon, M.T., and Garver, J.I., 1997, Geologic tests for hypotheses for large  
901 coastwise displacements – A critique illustrated by the Baja British Columbia  
902 controversy: *American Journal of Science*, v. 279, p. 117-173.

903 Crowley, J.L., Brown, R.L., and Parrish, R.R., 2001, Diachronous deformation and a strain  
904 gradient beneath the Selkirk allochthon, northern Monashee complex, southeastern  
905 Canadian Cordillera: *Journal of Structural Geology*, v. 23, p. 1103-1121.

906 Darin, M., Armentrout, J.M., and Dorsey, R.J., 2022, Oligocene onset of uplift and inversion of  
907 the Cascadia forearc basin, southern Oregon Coast Range, USA: *Geology*, v. 50, p. 603–  
908 609.

909 Davidson, P., Tepper, J.H., and Nelson, B.K., 2015, Petrology of Eocene dikes near Lake Chelan,  
910 WA; evidence of mantle and crustal melting during the Challis event: *American  
911 Geophysical Union Fall Meeting*, Abstract V23B-B312.

912 DeCelles, P.G., Ducea, M.N., Kapp, P., and Zandt, G., 2009, Cyclicity in Cordilleran orogenic  
913 systems: *Nature Geoscience*, v. 2, p. 251–257.

914 Decker, M., Schwartz, J.J., Stowell, H.H., Klepeis, K.A., Tulloch, A.J., Kitajima, K., Valley, J.W., and  
915 Kylander-Clark, A.R.C., 2017, Slab-triggered arc flare-up in the Cretaceous Median  
916 Batholith and the growth of lower arc crust, Fiordland, New Zealand: *Journal of  
917 Petrology*, v. 58, p. 1145–1172.

918 Donaghy, E.E., Umhoefer, P.J., Eddy, M.P., Miller, R.B., and LaCasse, T., 2021, Stratigraphy,  
919 age, and provenance of the Eocene Chumstick Basin, Washington Cascades; implications

920 for paleogeography and regional tectonics: Geological Society of America Bulletin, v.  
921 133, p. 2418-2438. <https://doi.org/10.1130/B35738.1>.

922 Doran, B.A., 2009, Structure of the Swauk Formation and Teanaway dike swarm, Washington  
923 Cascades [M.S. thesis]: San Jose, California, San Jose State University, 97 p.

924 Dostal, J.D., and Jutras, P., 2021, Tectonic and petrogenetic settings of the Eocene Challis-  
925 Kamloops volcanic belt of western Canada and the northwestern United States:  
926 International Geology Review; doi.org/10.1080/00206814.2021.1992800.

927 Doubrovine, P.V., and Tarduno, J.A., 2008, A revised kinematic model for the relative motion  
928 between Pacific oceanic plates and North America since the Late Cretaceous: Journal of  
929 Geophysical Research, v. 113, B12101, doi.org/10.1029/2008JB005585.

930 Doughty, P.T., and Price, R.A., 1999, Tectonic evolution of the Priest River complex, northern  
931 Idaho and Washington- A reappraisal of the Newport fault with new insights on  
932 metamorphic core complex formation: Tectonics, v. 18, p. 375-393.

933 Doughty, P.T., and Price, R.A., 2000, Geology of the Purcell Trench rift valley and Sandpoint  
934 Conglomerate: Eocene en echelon normal faulting and synrift sedimentation along the  
935 eastern flank of the Priest River metamorphic complex, northern Idaho: Geological Society  
936 of America Bulletin, v. 112, p. 1356-1374.

937 Dragovich, J.D., Littke, H.A., Anderson, M.L., Hartog, R., Wessel, G.R., DuFrane, S.A. Walsh, J.,  
938 MacDonald, J.H., Jr., Mangano, J.F., and Cakir, R., 2009, Geologic map of the Snoqualmie  
939 7.5-minute quadrangle, King County, Washington: Washington Division of Geology and  
940 Earth Resources Geologic Map GM-75, 2 sheets, scale 1:24,000.

941 Dragovich, J.D., Anderson, M.L., Mahan, S.A., Koger, C.J., Saltonstall, J.H., MacDonald, J.H., Jr.,  
942 Wessel, G.R., Stoker, B.A., Bethel, J.P., Labadie, J.E., Cakir, R., Bowman, J.D., and DuFrane,  
943 S.A., 2011, Geologic map of the Monroe 7.5-minute quadrangle, King and Snohomish  
944 Counties, Washington: Washington Division of Geology and Earth Resources Open File  
945 Report 2011-1, 1 sheet, scale 1:24,000, with 24 p. text.  
946 [[http://www.dnr.wa.gov/publications/ger\\_ofr2011-1\\_geol\\_map\\_mon-roe\\_24k.zip](http://www.dnr.wa.gov/publications/ger_ofr2011-1_geol_map_mon-roe_24k.zip)]  
947 Dragovich, J.D., Mahan, S.A., Anderson, M.L., MacDonald, J.H., Jr., Cakir, R., Stoker, B.A., Koger,  
948 C.J., Bethel, J.P., DuFrane, S.A., Smith, D.T., and Villeneuve, N.M., 2013, Geologic map of  
949 the Sultan 7.5-minute quadrangle, King and Snohomish Counties, Washington:  
950 Washington Division of Geology and Earth Resources Map Series 2013-01, 1 sheet, scale  
951 1:24,000, 52 p. text.  
952 [http://www.dnr.wa.gov/publications/ger\\_ms201301\\_geol\\_map\\_sultan\\_24k.zip](http://www.dnr.wa.gov/publications/ger_ms201301_geol_map_sultan_24k.zip).  
953 Dragovich, J.D., Frattali, C.L., Anderson, M.L., Mahan, S.A., MacDonald, J.H., Jr., Stoker, B.A.,  
954 Smith, D.T., Koger, C.J., Cakir, R., Dufrane, S.A., and Sauer, K.B., 2014, Geologic map of the  
955 Lake Chaplain 7.5-minute quadrangle, Snohomish County, Washington: Washington  
956 Division of Geology and Earth Resources Map Series 2014-01, 1 sheet, scale 1:24,000, 51  
957 p. text.  
958 Dragovich, J.D., Mavor, S.P., Anderson, M.L., Mahan, S.A., MacDonald, J.H., Jr., Tepper, J.H.,  
959 Smith, D.T., Stoker, B.A., Koger, C.J., Cakir, R., DuFrane, S.A., Scott, S.P., and Justman,  
960 B.P., 2016, Geologic map of the Granite Falls 7.5-minute quadrangle, Snohomish County,

961 Washington: Washington Division of Geology and Earth Resources Map Series 2016-01,  
962 1 sheet, scale 1:24,000, 63 p. text.

963 du Bray, E.A., and John, D.A., 2011, Petrologic, tectonic, and metallogenic evolution of the  
964 Ancestral Cascades magmatic arc, Washington, Oregon, and northern California:  
965 *Geosphere*, v. 7, p. 1102-1133.

966 Ducea, M.N., and Barton, M.D., 2007, Igniting flare-up events in Cordilleran arcs: *Geology*, v. 35,  
967 p. 1047-1050.

968 Eddy, M.P., Bowring, S.A., Umhoefer, P.J., Miller, R.B., McLean, N.M., and Donaghy, E.E., 2016a,  
969 High-resolution temporal and stratigraphic record of microplate accretion and ridge-  
970 trench interaction preserved in non-marine sedimentary basins in central and western  
971 Washington: *Geological Society of America Bulletin*, v. 128, p. 425-441.

972 Eddy, M.P., Bowring, S.A., Miller, R.B., and Tepper, J.H., 2016b, Rapid assembly and  
973 crystallization of a fossil large-volume silicic magma chamber: *Geology*, v. 44, p. 341-344.

974 Eddy, M.P., Clark, K.P., and Polenz, M., 2017a, Age and volcanic stratigraphy of the Eocene  
975 Siletzia oceanic plateau in Washington and on Vancouver Island: *Lithosphere*, v. 9, p. 652-  
976 664.

977 Eddy, M.P., Umhoefer, P.J., Miller, R.B., Donaghy, E.E., Gundersen, M., and Senes, F.I., 2017b,  
978 Sedimentary, volcanic, and structural processes during triple-junction migration: Insights  
979 from the Paleogene record in central Washington, *in* Haugerud, R.A., and Kelsey, H.M.,  
980 eds., From the Puget Lowland to East of the Cascade Range: *Geologic Excursions in the*

981 Pacific Northwest: Geological Society of America Field Guide 49, p. 143–173,  
982 doi:10.1130/2017.0049(07).

983 Einarsen, J.M., 1987, The petrography and tectonic significance of the Blue Mountain unit,  
984 Olympic Peninsula, Washington (M.S. thesis): Bellingham, Washington, Western  
985 Washington University, 175 p.

986 Engebretson, D.C., Cox, A., and Gordon, R.G., 1985, Relative motions between oceanic and  
987 continental plates in the Pacific basin: Geological Society of America Special Paper 206,  
988 59 p.

989 Engels, J.C., Tabor, R.W., Miller, F.K., and Obradovich, J.D., 1976, Summary of K-Ar, Rb-Sr, U-Pb,  
990 and fission track ages of rocks from Washington State prior to 1975 (exclusive of Columbia  
991 Plateau Basalts): U.S. Geological Survey Miscellaneous Field Studies Map MF-710.

992 Enkin, R.J., 2006, Paleomagnetism and the case for Baja British Columbia, *in* Haggart, J.W., Enkin  
993 R.J., and Monger, J.W.H., eds., Paleogeography of the North American Cordillera: Evidence  
994 For and Against Large-Scale Displacements: Geological Association of Canada Special  
995 Paper 46, p. 233–254.

996 Evans, J.E., 1994, Depositional history of the Eocene Chumstick Formation: Implications of  
997 tectonic partitioning for the history of the Leavenworth and Entiat-Eagle Creek fault  
998 systems, Washington: Tectonics, v. 13, p. 1425–1444.

999 Ewing, T., 1980, Paleogene tectonic evolution of the Pacific Northwest: Journal of Geology, v.  
1000 88, p. 619–638.

1001 Fawcett, T.C., Burmester, R.F., Housen, B.A., and Iriondo, A., 2003, Tectonic implications of  
1002 magnetic fabrics and remanence in the Cooper Mountain pluton, North Cascade  
1003 Mountains, Washington: Canadian Journal of Earth Sciences, v. 40, p. 1335-1356.

1004 Fairchild, L.H., and Cowan, D.S., 1982, Structure, petrology, and tectonic history of the Leech  
1005 River complex northwest of Victoria, Vancouver Island: Canadian Journal of Earth  
1006 Sciences, v. 19, p. 1817-1835.

1007 Feeley, T.C., and Cosca, M.A., 2003, Time vs. composition trends of magmatism at Sunlight  
1008 volcano, Absaroka volcanic province, Wyoming: Geological Society of America Bulletin, v.  
1009 115, p. 714-728.

1010 Foster, D.A., and Fanning, C.M., 1997, Geochronology of the northern Idaho batholith and the  
1011 Bitterroot metamorphic core complex: Magmatism preceding and contemporaneous with  
1012 extension: Geological Society of America Bulletin, v. 109, p. 379–394.

1013 Foster, D.A., Doughty, P.T., and Kalakay, T.J., 2007, Kinematics and timing of exhumation of  
1014 metamorphic core complexes along the Lewis and Clark fault zone, northern Rocky  
1015 Mountains, USA, *in* Sisson, V.B., Roeske, S.M., and Palvis, T.L., eds., Geology of a  
1016 Transpressional Orogen Developed During Ridge-trench Interaction along the North  
1017 Pacific Margin: Geological Society of America Special Paper 371, p. 205-229.

1018 Foster, D.A., Grice, W.C., Jr., and Kalakay, T.J., 2010, Extension of the Anaconda metamorphic  
1019 core complex:  $40\text{Ar}/39\text{Ar}$  thermochronology and implications for Eocene tectonics of  
1020 the northern Rocky Mountains and the Boulder batholith: Lithosphere, v. 2, p. 232-246.

1021 Foster, R.J., 1958, The Teanaway dike swarm of Central Washington: American Journal of  
1022 Science, v. 256, p. 644-653.

1023 Fuston, S., and Wu, J., 2021, Raising the Resurrection plate from an unfolded-slab plate tectonic  
1024 reconstruction of northwestern North America since early Cenozoic time: Geological  
1025 Society of America Bulletin, v. 133, p. 1128-1140.

1026 Gabrielse, H., 1985, Major dextral transcurrent displacements along the Northern Rocky  
1027 Mountain Trench and related lineaments in north-central British Columbia: Geological  
1028 Society of America Bulletin, v. 96, p. 1-14.

1029 Gao, H., Humphreys, E.D., Yao, H., and van der Hilst, R.D., 2011, Crust and lithosphere structure  
1030 of the northwestern U.S. with ambient noise tomography: Terrane accretion and Cascade  
1031 arc development: Earth and Planetary Science Letters, v. 304, p. 202-211.

1032 Gaschnig, R.M., Vervoort, J.D., Lewis, R.S., and McClelland, W.C., 2010, Migrating magmatism in  
1033 the northern US Cordillera: in situ U-Pb geochronology of the Idaho batholith:  
1034 Contributions to Mineralogy and Petrology, v. 159, p. 863-883.

1035 Gaschnig, R.M., Vervoort, J.D., Lewis, R.S., and Tikoff, B., 2011, Isotopic evolution of the Idaho  
1036 batholith and Challis Intrusive Province, northern US Cordillera: Journal of Petrology, v.  
1037 52, p. 2397-2429.

1038 Gehrels, G., Rusmore, M., Woodsworth, G., Crawford, M., Andronicos, C., Hollister, L., Patchett,  
1039 J., Ducea, M., Butler, R., Klepeis, K., Davidson, C., Friedman, R., Haggart, J., Mahoney, B.,  
1040 Crawford, W., Pearson, D., and Girardi, J., 2009, U-Th-Pb geochronology of the Coast

1041 Mountains batholith in north-coastal British Columbia: Constraints on age and tectonic  
1042 evolution: *Geological Society of America Bulletin*, v. 121, p. 1341-1361, doi:  
1043 10.1130/B26404.1.

1044 Gervais, F., and Brown, R.L., 2011, Testing modes of exhumation in collisional orogens:  
1045 Synconvergent channel flow in the southeastern Canadian Cordillera: *Lithosphere*, v. 3, p.  
1046 55–75.

1047 Gervais, F., Brown, R.L., and Crowley, J.L., 2010, Tectonic implications for a Cordilleran orogenic  
1048 base in the Frenchman Cap dome, southeastern Canadian Cordillera: *Journal of Structural  
1049 Geology*, v. 34, p. 941-959.

1050 Gilmour, L.A., 2012, U/Pb ages of Eocene and younger rocks on the eastern flank of the central  
1051 Cascade Range, Washington, USA (M.S. thesis): Seattle, Washington, University of  
1052 Washington, 48 p.

1053 Gordon, S.M., Bowring, S.A., Whitney, D.L., Miller, R.B., and McLean, N., 2010a, Timescales of  
1054 metamorphism, deformation, and crustal melting in a continental arc, North Cascades,  
1055 USA: *Geological Society of America Bulletin*, v. 122, p. 1308–1330.

1056 Gordon, S.M., Whitney, D.L., Miller, R.B., McLean, N., and Seaton, N.C.A., 2010b,  
1057 Metamorphism and deformation at different structural levels in a strike-slip fault zone,  
1058 Ross Lake fault, North Cascades, USA: *Journal of Metamorphic Geology*, v. 28, p. 117–136.

1059 Greig, C.J., 1992, Jurassic and Cretaceous plutonic and structural styles of the Eagle Plutonic  
1060 Complex, southwestern British Columbia, and their regional significance: Canadian Journal  
1061 of Earth Sciences, v. 29, p. 793-811.

1062 Groome, W.G., Thorkelson, D.J., Friedman, R.M., Mortensen, J.M., Massey, N.W.D., Marshall,  
1063 D.D., and Layer, P.W., 2003, Magmatic and tectonic history of the Leech River Complex,  
1064 Vancouver Island, British Columbia: Evidence for ridge-trench intersection and accretion  
1065 of the Crescent Terrane, *in* Sisson, V.B., Roeske, S.M., and Pavlis, T.L., eds., Geology of a  
1066 Transpressional Orogen Developed During Ridge-trench Interaction along the North  
1067 Pacific Margin: Geological Society of America Special Paper 371, p. 327–353.

1068 Haeussler, P.J., Bradley, D.C., Wells, R.E., and Miller, M.L., 2003, Life and death of the  
1069 Resurrection plate: Evidence for its existence and subduction in the northeastern Pacific  
1070 in Paleocene–Eocene time: Geological Society of America Bulletin, v. 115, p. 867-880.

1071 Hanson, A.E.H., Gordon, S.M., Ashley, K.T., Miller, R.B., and Langdon-Lassagne, E., 2022, Multiple  
1072 sediment incorporation events in a continental magmatic arc: insight from the  
1073 metasedimentary rocks of the northern North Cascades, Washington: Geosphere, v. 18,  
1074 <https://doi.org/10.1130/GES02425.1>.

1075 Harlan, S.S., Geissman, J.W.M., Lageson, D.R., and Snee, W.W., 1988, Paleomagnetic and  
1076 isotopic dating of thrust-belt deformation along the eastern edge of the Helena salient,  
1077 northern Crazy Mountains Basin, Montana: Geological Society of America Bulletin, v. 100,  
1078 p. 492-499.

1079 Harms, T.A., and Price, R.A., 1992, The Newport fault: Eocene listric normal faulting,  
1080 mylonitization, and crustal extension in northeast Washington and northwest Idaho:  
1081 Geological Society of America Bulletin, v. 104, p. 745-761.

1082 Haugerud, R.A., and Tabor, R.W., 2009, Geologic map of the North Cascade Range,  
1083 Washington: U.S. Geological Survey Scientific Investigations Map 2940, 2 sheets, scale  
1084 1:200,000; 2 pamphlets, 29 p. and 23 p.

1085 Haugerud, R.A., van der Heyden, P., Tabor, R.W., Stacey, J.S., and Zartman, R.E., 1991, Late  
1086 Cretaceous and early Tertiary plutonism and deformation in the Skagit Gneiss Complex,  
1087 North Cascade Range, Washington and British Columbia: Geological Society of America  
1088 Bulletin, v. 103, p. 1297-1307.

1089 Hinckley, A.M., and Carr, S.D., 2006, The S-type Ladybird leucogranite suite of southeastern  
1090 British Columbia: Geochemical and isotopic evidence for a genetic link with migmatite  
1091 formation in the North American basement gneisses of the Monashee complex: Lithos,  
1092 doi.org/10.1016/j.lithos.2006.03.003.

1093 Howlett, C.J., Reynolds, A.N., and Laskowski, A.K., 2021, Magmatism and extension in the  
1094 Anaconda metamorphic core complex of western Montana and relation to regional  
1095 tectonics: Tectonics, v. 40, p. 1-31, doi:10.1029/2020TC006431.

1096 Humphreys, E.D., 1995, Post-Laramide removal of the Farallon slab, western United States:  
1097 Geology, v. 23, p. 987-990.

1098 Humphreys, E.D., 2009, Relation of flat subduction to magmatism and deformation in the  
1099 western United States, *in* Kay, S.M., Ramos, V.A., and Dickinson, W.R., eds., Backbone of  
1100 the Americas: Shallow Subduction, Plateau Uplift, and Ridge and Terrane Collision:  
1101 Geological Society of America Memoir 204, p. 85–98, doi: 10.1130/2009.1204(04).

1102 Humphreys, E.D., and Grunder, A.L., 2022, Tectonic controls on the origin and segmentation of  
1103 the Cascade arc, USA: *Bulletin of Volcanology*, 84:102, <https://doi.org/10.1007/s00445-022-01611-2>.

1105 Hurlow, H.A., and Nelson, B.K., 1993, U-Pb zircon and monazite ages for the Okanogan Range  
1106 batholith, Washington: Implications for the magmatic and tectonic evolution of the  
1107 southern Canadian and northern United States Cordillera: *Geological Society of America  
1108 Bulletin*, v. 105, p. 231–240.

1109 Ickert, R.B., Thorkelson, D.J., Marshall, D.D., and Ullrich, T.D., 2009, Eocene adakitic volcanism  
1110 in southern British Columbia: Remelting of arc basalt above a slab window:  
1111 *Tectonophysics*, v. 464, p. 164-185.

1112 Irving, E., and Brandon, M.T., 1990, Paleomagnetism of the Flores volcanics, Vancouver Island,  
1113 in place by Eocene time: *Canadian Journal of Earth Sciences*, v. 27, p. 811-817.

1114 Janecke, S.U., and Snee, L.W., 1993, Timing and episodicity of middle Eocene volcanism and  
1115 onset of conglomerate deposition, Idaho: *The Journal of Geology*, v. 101, p. 603–621, doi:  
1116 10.1086/648252.

1117 Johnson, S.Y., 1984, Stratigraphy, age, and paleogeography of the Eocene Chuckanut  
1118 Formation, northwest Washington: Canadian Journal of Earth Sciences, v. 21, p. 92-106.

1119 Johnson, S.Y., and O'Connor, J.T., 1994, Stratigraphy, sedimentology, and provenance of the  
1120 Raging River Formation (Early and middle Eocene), King County, Washington: U.S.  
1121 Geological Survey Bulletin 2085-A, p. A-1 – A-33.

1122 Johnston, S.T., and Acton, S., 2003, The Eocene Southern Vancouver Island Orocline — a  
1123 response to seamount accretion and the cause of fold-and-thrust belt and extensional  
1124 basin formation: Tectonophysics, v. 365, p. 165-183.

1125 Kalakay, T.J., Foster, D.A., and Thomas, R.A., 2003, Geometry, kinematics and timing of  
1126 extension in the Anaconda extensional terrane, western Montana: Northwest Geology, v.  
1127 32, p. 42–72.

1128 Kant, L.B., Tepper, J.H., and Nelson, B.K., 2018, Eocene Basalt of Summit Creek: Slab breakoff  
1129 magmatism in the central Washington Cascades, USA: Lithosphere, v. 10, p. 792-805.

1130 Kriens, B.J., Hawley, D.L., Chapplelear, F.D., Mack, P.D., and Chan, A.F., 1995, Spatial and  
1131 temporal relations between early Tertiary shortening and extension in NW Washington,  
1132 based on geology of the Pipestone Canyon Formation and surrounding rocks: Tectonics, v.  
1133 14, p. 719-735.

1134 Kruckenberg, S.C, Whitney, D.L., Teyssier, C., Fanning, C.M., and Dunlap, W.J., 2008, Paleocene-  
1135 Eocene migmatite crystallization, extension, and exhumation in the hinterland of the

1136 northern Cordillera: Okanogan dome, Washington, USA: Geological Society of America

1137 Bulletin, v. 120, p. 912-929.

1138 Lewis, R.S., and Kiilsgaard, 1991, Eocene plutonic rocks in south central Idaho: Journal of

1139 Geophysical Research: Solid Earth, v. 96, p. 13295-13311.

1140 Lonsdale, P., 1988, Paleogene history of the Kula plate: Offshore evidence and onshore

1141 implications: Geological Society of America Bulletin, v. 100, p. 733-754.

1142 MacDonald, J.H., Jr., Dragovich, J.D., Littke, H.A., Anderson, M., and Dufrane, S.A., 2013, The

1143 Eocene volcanic rocks of Mount Persis: An Eocene continental arc that contains adakitic

1144 magmas: Geological Society of America Abstracts with Programs, v. 45, no. 7, p. 392.

1145 Madsen, J.K., Thorkelson, D.J., Friedman, R.M., and Marshall, D.D., 2006, Cenozoic to Recent

1146 plate configurations in the Pacific Basin: Ridge subduction and slab window magmatism in

1147 western North America: Geosphere, v. 2, p. 11-34.

1148 Massey, N.W.D., 1986, Metchosin Igneous Complex, southern Vancouver Island: Ophiolite

1149 stratigraphy developed in an emergent island setting: Geology, v. 14, p. 602-605.

1150 Matthews, K.J., Maloney, K.T., Zahirovic, S., Williams, S.E., Seton, M., and Müller, R.D., 2016,

1151 Global plate boundary evolution and kinematics since the late Paleozoic: Global and

1152 Planetary Change, v. 146, p. 226-250.

1153 Matthews, W.A., Guest, B., Coutts, D., Bain, H., and Hubbard, S., 2017, Detrital zircons from the

1154 Nanaimo basin, Vancouver Island, British Columbia: An independent test of Late

1155 Cretaceous to Cenozoic northward translation: Tectonics, v. 36, p. 854–876, <https://doi.org/10.1002/2017TC004531>

1156

1157 Matzel, J.E.P., 2004, Rates of tectonic and magmatic processes in the North Cascades

1158 continental magmatic arc [Ph.D. thesis]: Cambridge, Massachusetts, Massachusetts

1159 Institute of Technology, 249 p.

1160 Matzel, J.E.P., Bowring, S.A., and Miller, R.B., 2008, Spatial and temporal variations in Nd

1161 isotopic signatures across the crystalline core of the North Cascades, WA, *in* Shervais, J.,

1162 and Wright, J., eds., Arcs, Ophiolites, and Batholiths: A Tribute to Cliff Hopson: Geological

1163 Society of America Special Paper 438, p. 499–516.

1164 McCarley Holder, G.A., Holder, R.W., and Carlson, D.H., 1990, Middle Eocene dike swarms and

1165 their relation to contemporaneous plutonism, volcanism, core-complex mylonitization,

1166 and graben subsidence, Okanogan Highlands, Washington: Geology, v. 18, p. 1082-1085.

1167 McCrory, P.A., and Wilson, D.S., 2013, A kinematic model for the formation of the Siletz-

1168 Crescent forearc terrane by capture of coherent fragments of the Farallon and

1169 Resurrection plates: Tectonics, v. 32, p. 718-736.

1170 Miller, R.B., and Bowring, S.A., 1990, Structure and chronology of the Oval Peak batholith and

1171 adjacent rocks: Implications for the Ross Lake fault zone, North Cascades, Washington:

1172 Geological Society of America Bulletin, v. 102, p. 1361-1377.

1173 Miller, R.B., and Paterson, S.R., 1999, In defense of magmatic diapirs: Journal of Structural

1174 Geology, v. 21, p. 1161-1173.

1175 Miller, R.B., Paterson, S.R., and Matzel, J.P., 2009, Plutonism at different crustal levels: Insights  
1176 from the ~5-40 km (paleodepth) North Cascades crustal section, Washington, *in* Miller,  
1177 R.B., and Snoker, A.W, eds., Crustal cross sections from the western North America  
1178 Cordillera and elsewhere: Implications for tectonic and petrologic processes: Geological  
1179 Society of America Special Paper 456, p. 125–150.

1180 Miller, R.B., Gordon, S.M., Bowring, S.A., Doran, B.A., McLean, N., Michels, Z., Shea, E.K., and  
1181 Whitney, D.L., 2016, Linking deep and shallow crustal processes during regional  
1182 transtension in an exhumed continental arc, North Cascades, northwestern Cordillera  
1183 (USA): *Geosphere*, v. 12, p. 900-924.

1184 Miller, R.B., Bryant, K.I., Doran, B., Eddy, M.P., Raviola, F.P., Sylva, N., and Umhoefer, P.J., 2022,  
1185 Eocene dike orientations across the Washington Cascades in response to a major strike-  
1186 slip faulting episode and ridge-trench interaction: *Geosphere*, v. 18, no. 2, p. 1–29,  
1187 <https://doi.org/10.1130/GES02387.1>.

1188 Misch, P., 1966, Tectonic evolution of the northern Cascades of Washington State—a west  
1189 Cordilleran case history: Canadian Institute of Mining and Metallurgy, Special Volume 8, p.  
1190 101-148.

1191 Misch, P., 1968, Plagioclase compositions and non-anatectic origin of migmatitic gneisses in  
1192 Northern Cascade Mountains of Washington State: Contributions to Mineralogy and  
1193 Petrology, v. 17, p. 1-70.

1194 Monger, J.W.H., 1989, Geology of the Hope and Ashcroft map areas, British Columbia:  
1195 Geological Survey of Canada Maps 41-1989 and 42-1989.

1196 Monger, J.W.H., and Brown, E.H., 2016, Tectonic evolution of the southern Coast-Cascade  
1197 orogen, *in* Cheney, E.S., ed., The Geology of Washington and Beyond: From Laurentia to  
1198 Cascadia: Seattle, University of Washington Press, p. 101-130.

1199 Morris, G.A., Larson, P.B., and Hooper, P.R., 2000, 'Subduction style' magmatism in a  
1200 nonsubduction setting: The Colville igneous complex, NE Washington State, USA: *Journal  
1201 of Petrology*, v. 41, p. 43–67, <https://doi.org/10.1093/petrology/41.1.43>.

1202 Mudge, M.R., and Earhart, R.L., 1980, The Lewis thrust fault and related structures in the  
1203 Disturbed Belt, northwestern Montana: U.S. Geological Survey Professional Paper 1174,  
1204 18 p.

1205 Mueller, P.A., Heatherington, A.L., D'Arcy, K.A., Wooden, J.L., and Nutman, A.P., 1996,  
1206 Contrasts between Sm-Nd whole-rock and U-Pb zircon systematics in the Tobacco Root  
1207 batholith, Montana: implications for the determination of crustal age provinces:  
1208 *Tectonophysics*, v. 265, p. 169–179.

1209 Mustard, P. S., 1994, The Upper Cretaceous Nanaimo Group, Georgia Basin, *in* Monger, J.W.H.,  
1210 ed., *Geology and Geological Hazards of the Vancouver Region, Southwestern British  
1211 Columbia*: Geological Survey of Canada Bulletin, v. 481, p. 27–95.

1212 O'Connor, J.M, Steinberger, B, Regelous, M., Koppers, A.A.P., Wijbrans, J.R., Haase, K.M.,  
1213 Stoffers, P., Jokat, W., and Garbe-Schönberg, D., 2013, Constraints on past plate and

1214 mantle motion from new ages for the Hawaiian-Emperor Seamount Chain: Geochemistry,  
1215 Geophysics, and Geosystems, v. 14, no. 10, doi:10.1002/ggge.20267.

1216 O'Driscoll, L.J., Humphreys, E., and Saucier, F., 2009, Subduction adjacent to deep continental  
1217 roots: Enhanced negative pressure in the mantle wedge, mountain building and  
1218 continental motion: Tectonophysics, v. 280, p. 61-70.

1219 Parker, D.F., Hodges, F.N., Perry, A., Mitchener, M.E., Barnes, M.A., and Ren, M., 2010,  
1220 Geochemistry and petrology of late Eocene Cascade Head and Yachats Basalt and alkalic  
1221 intrusions of the central Oregon Coast Range, U.S.A.: Journal of Volcanology and  
1222 Geothermal Research, v. 198, p. 311-324.

1223 Parrish, R.R., Carr, S.D., and Parkinson, D.L., 1988, Eocene extensional tectonics and  
1224 geochronology of the southern Omineca Belt, British Columbia and Washington:  
1225 Tectonics, v. 7, p. 181-212

1226 Paterson, S.R., Miller, R.B., Alsleben, H., Whitney, D.L., Valley, P.M., and Hurlow, H., 2004,  
1227 Driving mechanisms for >40 km of exhumation during contraction and extension in a  
1228 continental arc, Cascades core, Washington: Tectonics, v. 23, TC3005, doi:  
1229 10.1029/2002TC001440.

1230 Pearson, R.C., and Obradovich, J.D., 1977, Eocene rocks in northeast Washington: Radiometric  
1231 ages and correlation: U.S. Geological Survey Bulletin 1433, 41 p.

1232 Peters, R.L., and Tepper, J.H., 2006, Petrology of the Teanaway dike swarm, central Cascades,  
1233 Washington: Geological Society of America Abstracts with Programs, v. 38, no. 5, p. 9.

1234 Peterson, P., and Tepper, J.H., 2021, Petrology and tectonic setting of the Silver Pass Volcanics,  
1235 Central Cascades, WA: early evidence of Farallon Slab breakoff: Geological Society of  
1236 America Abstracts with Programs, v. 53, no. 6, doi.org/10.1130/abs/2021AM-368972.

1237 Phillips, B.A., Kerr, A.C., Mullen, E.K., and Weis, D., 2017, Oceanic mafic magmatism in the Siletz  
1238 terrane, NW North America: Fragments of an Eocene oceanic plateau?: *Lithos*, v. 274–  
1239 275, p. 291–303, <https://doi.org/10.1016/j.lithos.2017.01.005>.

1240 Price, R., 1981, The Cordilleran foreland thrust and fold belt in the southern Canadian Rocky  
1241 Mountains, in McClay, K.R., and Price, N.J., eds., *Thrust and Nappe Tectonics*: Geological  
1242 Society, London, Special Publications, v. 9, p. 427-448.

1243 Price, R.A., and Carmichael, D.M., 1986, Geometric test for Late Cretaceous-Paleogene  
1244 intracontinental transform faulting in the Canadian Cordillera: *Geology*, v. 14, p. 468-471.

1245 Pyle D.G., Duncan, R.A., Wells, R.E., Graham, D.W., Hanan, B.B., Harrison, B.K., and Haileab, B.,  
1246 2015, Longevity of YHS volcanism: Isotopic evidence linking the Siletzia LIP (56 Ma) and  
1247 early Columbia River Basalt Group (17 Ma) to mantle sources: *American Geophysical  
1248 Union Fall Meeting*, Abstract V31E-3060.

1249 Rhodes, B.P., and Cheney, E.S., 1981, Low-angle faulting and the origin of Kettle dome, a  
1250 metamorphic core complex in northeastern Washington: *Geology*, v. 9, p. 366-369.

1251 Roepke, E., Tepper, J.H., and Ivener, D., 2013, A petrologic study of the Teanaway Basalt:  
1252 Eocene slab window volcanism in central WA: *American Geophysical Union Fall Meeting*,  
1253 2013, Abstract V31A-2667.

1254 Rubino, E., Leier, A., Cassel, E.J., Archibald, B., Foster-Baril, Z., and Barbeau Jr., D.L., 2021,  
1255 Detrital zircon U–Pb ages and Hf-isotopes from Eocene intermontane basin deposits of  
1256 the southern Canadian Cordillera: *Sedimentary Geology*, v. 422,  
1257 doi.org/10.1016/j.sedgeo.2021.105969.

1258 Sauer, K.B., Gordon, S.M., Miller, R.B., Vervoort, J.D., and Fisher, C.M., 2017a, Evolution of the  
1259 Jura-Cretaceous North American Cordilleran margin: Insights from detrital-zircon U-Pb  
1260 and Hf isotopes of sedimentary units of the North Cascades Range, Washington:  
1261 *Geosphere*, v. 13, no.6, p. 2094-2118, doi. doi.org/10.1130/GES01501.1

1262 Sauer, K.B., Gordon, S.M., Miller, R.B., Vervoort, J.D., and Fisher, C.M., 2017b, Transfer of  
1263 metasupracrustal rocks to midcrustal depths in the North Cascades continental  
1264 magmatic arc, Skagit Gneiss Complex, Washington: *Tectonics*, 10.1002/2017TC004728:

1265 Sauer, K.B., Gordon, S.M., Miller, R.B., Vervoort, J.D., and Fisher, C.M., 2018, Provenance and  
1266 metamorphism of the Swakane Gneiss: implications for incorporation of sediment into  
1267 the deep levels of the North Cascades continental magmatic arc, Washington:  
1268 *Lithosphere*, v. 10, p. 460–477, doi.org/10.1130/L712.1.

1269 Schellart, P., 2020, Control of subduction zone age and size on flat slab subduction: *Frontiers in*  
1270 *Earth Science*, doi.org./10.3389/feart/2020.00026.

1271 Schmandt, B., and Humphreys, E.D., 2011, Seismically imaged relict slab from the 55 Ma Siletzia  
1272 accretion to the northwest United States: *Geology*, v. 39, p. 175–178.

1273 Schwartz, J.J., Klepeis, K.A., Sadorski, J.F., Stowell, H.H., Tulloch, A.J., and Coble, M.A., 2017, The  
1274 tempo of continental arc construction in the Mesozoic Median Batholith, Fiordland, New  
1275 Zealand: *Lithosphere*, v. 9, p. 343-365.

1276 Senes, F.I., 2019, Deformation, sandstone detrital zircon ages, and provenance in and near the  
1277 Eocene Leavenworth fault zone, Washington [M.S. thesis]: San Jose, California, San Jose  
1278 State University, 114 p.

1279 Seton, M., Flament, N., Whittaker, J., Müller, R.D., Gurnis, M., and Bower, D.J., 2015, Ridge  
1280 subduction sparked reorganization of the Pacific plate-mantle system 60–50 million  
1281 years ago: *Geophysical Research Letters*, v. 42, p. 1732–1740,  
1282 doi:10.1002/2015GL063057.

1283 Sharp, W.D., and Clague, D.A., 2006, 50-Ma Initiation of Hawaiian-Emperor bend records major  
1284 change in Pacific plate motion: *Science*, v. 313, p. 1281-1284.

1285 Simony, P.S., and Carr, S.D., 2011, Cretaceous to Eocene evolution of the southeastern  
1286 Canadian Cordillera: Continuity of Rocky Mountain thrust systems with zones of “in-  
1287 sequence” mid-crustal flow: *Journal of Structural Geology*, v. 33, p. 1417-1434.

1288 Stern, R.J., and Dumitru, T.A., 2019, Eocene initiation of the Cascadia subduction zone: A second  
1289 example of plume-induced subduction initiation?: *Geosphere*, v. 15, no. 3, p. 659–681,  
1290 <https://doi.org/10.1130/GES02050.1>.

1291 Stevens, L.M., Baldwin, J.A., Crowley, J.L., Fisher, C.M., and Vervoort, J.D., 2016, Magmatism as  
1292 a response to exhumation of the Priest River complex, northern Idaho: Constraints from  
1293 zircon U–Pb geochronology and Hf isotopes: *Lithos*, v. 262, p. 285–297.

1294 Stock, J., and Molnar, P., 1988, Uncertainties and implications of the Late Cretaceous and  
1295 Tertiary position of North America relative to the Farallon, Kula, and Pacific plates:  
1296 *Tectonics*, v. 7, p. 1339–1384.

1297 Stoffel, K.L., Joseph, N.L., Waggoner, S.Z., Gulick, C.W., Korosec, M.A., and Bunning, B.B., 1991,  
1298 Geologic map of Washington—Northeast quadrant: Washington Division of Geology and  
1299 Earth Resources Geologic Map GM-39, 3 sheets, scale 1:250,000, with 36 p. text.

1300 Suydam, J.D., and Gaylord, D.R., 1997, Toroda Creek half graben, northeast Washington: Late-  
1301 stage sedimentary infilling of a synextensional basin: *Geological Society of America*  
1302 *Bulletin*, v. 109, p. 1333–1348.

1303 Tabor, R.W., 1994, Late Mesozoic and possible early Tertiary accretion in western Washington  
1304 State: The Helena-Haystack mélange and the Darrington-Devils Mountain fault zone:  
1305 *Geological Society of America Bulletin*, v. 106, p. 217–232.

1306 Tabor, R.W., Waitt, R.B., Jr., Frizzell, V.A., Jr., Swanson, D.A., Byerly, G.R., and Bentley, R.D., 1982,  
1307 Geologic map of the Wenatchee quadrangle, Washington: U.S. Geological Survey  
1308 *Miscellaneous Investigations Map*, MI-1311, scale 1:100,000, 1 sheet, 31 p. text.

1309 Tabor, R.W., Frizzell, V.A., Jr., Vance, J.A., and Naeser, C.W., 1984, Ages and stratigraphy of  
1310 lower and middle Tertiary sedimentary and volcanic rocks of the Central Cascades,

1311 Washington: Applications to the tectonic history of the Straight Creek fault: Geological  
1312 Society of America Bulletin, v. 95, p. 26-44.

1313 Tabor, R.W., Frizzell, V.A., Jr., Whetten, J.T., Waitt, R.B., Swanson, D.A., Byerly, G.R., Booth, D.B.,  
1314 Hetherington, M.J., and Zartman, R.E., 1987, Geologic map of the Chelan 30-minute by 60-  
1315 minute quadrangle, Washington: U.S. Geological Survey Geologic Investigation Series, I-  
1316 1661, scale 1:100,000, 1 sheet, 56 p. text.

1317 Tabor, R.W., Frizzell, V.A., Jr., Booth, D.B., Waitt, R.B., Whetten, J.T., and Zartman, R.E., 1993,  
1318 Geologic map of the Skykomish 30- by 60-minute quadrangle: U.S. Geological Survey  
1319 Geologic Investigation Series, I-1663, scale 1:100,000.

1320 Tabor, R.W., Frizzell, V.A., Jr., Booth, D.B., and Waitt, R.B., 2000, Geologic map of the  
1321 Snoqualmie Pass 30x60 minute quadrangle, Washington: U.S. Geological Survey Geologic  
1322 Investigations Map, MI-2538, scale 1:100,000, 1 sheet, 57 p. text.

1323 Tabor, R.W., Haugerud, R.A., Hildreth, W., and Brown, E.H., 2003, Geologic map of the Mount  
1324 Baker 30- by 60-minute quadrangle, Washington: U.S. Geological Survey Geologic  
1325 Investigations Series I-2660, scale 1:100,000.

1326 Tepper, J.H., 2016, Eocene breakoff and rollback of the Farallon slab—An explanation for the  
1327 “Challis event”?: Geological Society of America Abstracts with Programs, v. 48, no. 4,  
1328 paper 327-1, <https://doi.org/10.1130/abs/2016CD-274512>.

1329 Tepper, J.H., and Eddy, M.P., 2017, The cause(s) of widespread Eocene magmatism in the  
1330 Pacific Northwest: insights from geochemistry and geochronology of igneous rocks in

1331 Washington, Geological Society of America Abstracts with Programs. V. 49, no. 6, doi:  
1332 10.1130/abs/2017AM-301043

1333 Tepper, J.H., Clark, K.P., Asmerom, Y., and McIntosh, W.C., 2004, Eocene adakites in the  
1334 Cascadia forearc: Implications for the position of the Kula-Farallon ridge: Geological  
1335 Society of America Abstracts with Programs, v. 36, no. 4, p. 69.

1336 Tepper, J.H., Nelson, B.K., Clark, K., and Barnes, R.P., 2008, Heterogeneity in mantle sources for  
1337 Eocene basalts in Washington: Trace element and Sr-Nd isotopic evidence from the  
1338 Crescent and Teanaway Basalts: American Geophysical Union, Fall Meeting 2008,  
1339 abstract id. V41D-2121.

1340 Thorkelson, D.J., and Taylor, R.P., 1989, Cordilleran slab windows: Geology, v. 17, p. 833-836.

1341 Trehu, A.M., Asudeh, I., Brocher, T.M., Luetgert, J.H., Mooney, W.D., Nabelek, J.L., and  
1342 Nakamura, Y., 1994, Crustal architecture of the Cascadia forearc: Science, v. 266, p. 237–  
1343 243, <https://doi.org/10.1126/science.266.5183.237>.

1344 Tikoff, B., Housen, B.A., Maxson, J.A., Nelson, E.M., Trevino, S., and Shipley, T.F., 2023, Hit-and-  
1345 run model for Cretaceous–Paleogene tectonism along the western margin of Laurentia,  
1346 *in* Whitmeyer, S.J., Williams, M.L., Kellett, D.A., and Tikoff, B., eds., Laurentia: Turning  
1347 Points in the Evolution of a Continent: Geological Society of America Memoir 220, p.  
1348 659-705, doi.org/10.1130/2022.1220(32).

1349 Umhoefer, P.J., and Blakey, R., 2006, Moderate (1600 km) northward translation of Baja British  
1350 Columbia from southern California: An attempt at reconciliation of paleomagnetism and

1351 geology, *in* Haggart, J.W., Enkin, R.J., and Monger, J.W.H., eds., Paleogeography of the  
1352 North American Cordillera: Evidence for and Against Large-scale Displacements:  
1353 Geological Association of Canada, Special Papers, v. 46, p. 307-329.

1354 Umhoefer, P.J., and Miller, R.B., 1996, Mid-Cretaceous thrusting in the southern Coast Belt,  
1355 British Columbia and Washington, after strike-slip fault reconstruction: Tectonics, v. 15,  
1356 p. 545-565.

1357 Umhoefer, P.J., and Schiarizza, P., 1996, Latest Cretaceous to early Tertiary dextral strike-slip  
1358 faulting on the southeastern Yalakom fault system, southeastern Coast Belt, British  
1359 Columbia: Geological Society of America, v. 108, p. 768-785.

1360 Valley, P.M., Whitney, D.L., Paterson, S.R., Miller, R.B., and Alsleben, H., 2003, Metamorphism  
1361 of the deepest exposed arc rocks in the Cretaceous to Paleogene Cascades belt,  
1362 Washington: evidence for large-scale vertical motion in a continental arc: Journal of  
1363 Metamorphic Geology, v. 21, p. 203-220.

1364 Vanderhaege, O., and Teyssier, C., 2001, Crustal-scale rheological transitions during late-  
1365 orogenic collapse: Tectonophysics, v. 335, p. 211-228.

1366 van Hinsbergen, D.J.J., Steinberger, B., Doubrovine, P.V., and Gassmöller, R., 2011, Acceleration  
1367 and deceleration of India - Asia convergence since the Cretaceous: Roles of mantle  
1368 plumes and continental collision: Journal of Geophysical Research, v. 116, B06101,  
1369 doi:10.1029/2010JB008051.

1370     Vine, J.D., 1969, Geology and coal resources of the Cumberland, Hobart, and Maple Valley  
1371           quadrangles, King County, Washington: U.S. Geological Survey Professional Paper 624, 67  
1372           p.

1373     Walker, N.W., and Brown, E.H., 1991, Is the southeast Coast Plutonic Complex the consequence  
1374           of accretion of the Insular superterrane? Evidence from U-Pb zircon geochronometry in  
1375           the northern Washington Cascades: *Geology*, v. 19, p. 714-717.

1376     Wallenbrock, C.J., and Tepper, J.H., 2017, Mid-Eocene arc volcanism in the Central Washington  
1377           Cascades: Petrology of the Taneum Formation and its relation to Farallon plate  
1378           subduction and breakoff: *Geological Society of America Abstracts with Programs*, v. 49,  
1379           no. 6, doi: 10.1130/abs/2017AM-301021.

1380     Wells, R.E., and Heller, P.L., 1988, The relative contribution of accretion, shear, and extension to  
1381           Cenozoic tectonic rotation in the Pacific Northwest: *Geological Society of America  
1382           Bulletin*, v. 100, p. 325–338.

1383     Wells, R.E., and McCaffrey, R., 2013, Steady rotation of the Cascade Arc: *Geology*, v. 41, p.  
1384           1027–1030, doi:10 .1130 /G34514.1.

1385     Wells, R.E., Engebretson, D.C., Snavely, P.D., Jr., and Coe, R.S., 1984, Cenozoic plate motions  
1386           and the volcano-tectonic evolution of western Oregon and Washington: *Tectonics*, v. 3,  
1387           275-294.

1388     Wells, R.E., Jayko, A.S., Niem, A.R., Black, G., Wiley, T., Baldwin, E., Molenaar, K.M., Wheeler,  
1389           K.L., DuRoss,C.B., and Givler, R.W., 2000, Geologic map and database of the Roseburg 30

1390 x 60' Quadrangle, Douglas and Coos Counties, Oregon: U.S. Geological Survey Open-File  
1391 report 00-376, <https://pubs.usgs.gov/of/2000/0376/>.

1392 Wells, R., Bukry, D., Friedman, R., Pyle, D., Duncan, R., Haeussler, P., and Wooden, J., 2014,  
1393 Geologic history of Siletzia, a large igneous province in the Oregon and Washington  
1394 Coast Range: Correlation to the geomagnetic polarity time scale and implications for a  
1395 long-lived Yellowstone hotspot: *Geosphere*, v. 10, p. 692-719, doi: 10.1130/GES01018.1.

1396 Wernicke, B.P., and Getty, S.R., 1997, Intracrustal subduction and gravity currents in the deep  
1397 crust; Sm-Nd, Ar-Ar, and thermobarometric constraints from the Skagit Gneiss Complex,  
1398 Washington: *Geological Society of America Bulletin*, v. 109, p. 1149-1166.

1399 Whalen, J.B., and Hildebrand, R.S., 2019, Trace element discrimination of arc, slab failure, and  
1400 A-type granitic rocks: *Lithos*, v. 348-349, doi.org/10.1016/j.lithos.2019.105179.

1401 White, A., Tepper, J.H., and Dawes, R.L., 2021, Geochemistry and petrology of Eocene to  
1402 Miocene rocks in a rear-arc setting, central Cascades, Washington: *Geological Society of*  
1403 *America Abstracts with Programs*, v. 53, no. 6. <https://doi.org/10.1130/abs/2021AM-367697>.

1405 White, P.J., 1986, Geology of the Island Mountain area, Okanogan County, Washington  
1406 [M.S. Thesis]: Seattle, Washington, University of Washington, 80 p.

1407 Whitney, D.L., 1992, High-pressure metamorphism in the Western Cordillera of North America:  
1408 an example from the Skagit Gneiss, North Cascades: *Journal of Metamorphic Geology*, v.  
1409 10, p. 71-85.

1410 Whitney, D.L., Paterson, S.R., Schmidt, K.L., Glazner, A.F., and Kopf, C.F., 2004, Growth and  
1411 demise of continental arcs and orogenic plateaux in the North American Cordillera: from  
1412 Baja to British Columbia: Geological Society, London, Special Publication 227, p. 167-175.

1413 Whittaker, J.M., Müller, R.D., Leitchenkov, G., Stagg, H., Sdrolias, M., Gaina, C., and Goncharov,  
1414 A., 2007, Major Australian-Antarctic plate reorganization at Hawaiian-Emperor bend time:  
1415 *Science*, v. 318, p. 83-86.

1416 Wintzer, N.E., 2012, Deformational episodes recorded in the Skagit Gneiss Complex, North  
1417 Cascades, Washington, USA: *Journal of Structural Geology*, v. 42, p. 127-139.

1418 Woods, M T., and Davies, G.F., 1982, Late Cretaceous genesis of the Kula plate: *Earth and*  
1419 *Planetary Science Letters*, v. 58, p. 161-166.

1420 Wright, N.M., Muller, R.D., Seton, M., and Williams, S.E., 2015, Revision of Paleogene plate  
1421 motions in the Pacific and implications for the Hawaiian-Emperor bend: *Geology*, v. 43,  
1422 p. 455-458.

1423 Wu, J. T-J., and Wu, J., 2019, Izanagi-Pacific ridge subduction revealed by a 56 to 46 Ma  
1424 magmatic gap along the northeast Asian margin: *Geology*, v. 47, 953-957.

1425 Wyld, S.J., Umhoefer, P.J., and Wright, J.E., 2006, Reconstructing northern Cordilleran terranes  
1426 along known Cretaceous and Cenozoic strike-slip faults: Implications for the Baja British  
1427 Columbia hypothesis and other models, *in* Haggart, J.W., Enkin, R.J., and Monger, J.W.H.,  
1428 eds., *Paleogeography of the North American Cordillera: Evidence for and Against Large-*  
1429 *scale Displacements*: Geological Association of Canada, Special Papers, v. 46, p. 277-298.

1430 Yeats, R.S., and Engels, J.C., 1971, Potassium-argon ages of plutons in the Skykomish-  
1431 Stillaguamish areas, north Cascades, Washington: U.S. Geological Survey Professional  
1432 Paper 750-D, p. D34-D38.

1433

1434 **TABLE**

1435 Table 1. STRIKE-SLIP FAULT OFFSETS ACROSS WASHINGTON CASCADES.

1436

1437 **FIGURE CAPTIONS**

1438 Figure. 1. Simple plate reconstruction models of the NE Pacific at 60 Ma and 52 Ma showing  
1439 locations of triple junctions. A. Kula – Farallon – North America triple junction. Note the  
1440 southward sweep of the Kula – Farallon Ridge from 60 Ma to 52 Ma in this model (e.g., Bradley  
1441 et al, 2003). B. Two triple junctions result from the hypothetical Resurrection plate (e.g.,  
1442 Hauessler et al., 2003). Note that in either model there is a triple junction near central to  
1443 southern Vancouver Island at ca. 52 Ma (e.g., Breitsprecher et al., 2003) and that the Kula ridge  
1444 interacted with the continental margin back to ca. 83 Ma (e.g., Engebretson et al., 1985;  
1445 Thorkelson and Taylor (1989). The hypothetical Orcas plate model is on a coarser scale and is  
1446 not shown; it calls for the final consumption of the plate at ~50 Ma (Clennett et al., 2020).  
1447 Sanak-Baranof is a belt of near-trench intrusions, which provide part of the evidence of a ridge  
1448 interacting with a trench (e.g., Bradley et al., 2003).

1449

1450 Figure 2. Generalized tectonic map of Paleogene rock types, structures, and tectonics of the  
1451 greater Pacific Northwest region considered in this study. Note the location of Siletzia (including  
1452 subsurface), near-trench intrusions, major dextral strike-slip faults, basins, magmatic rocks, and  
1453 metamorphic core complexes and bounding normal faults. Western, Central, and Eastern belts  
1454 are subdivisions used in text. An = Anaconda core complex; Br = Bitterroot lobe of Idaho  
1455 batholith; Cb = Chelan block of North Cascades crystalline core; Csz = Coast shear zone; Ef =  
1456 Entiat fault; Ff = Fraser fault; K = Kettle core complex; LCfz = Lewis and Clark fault zone; Ok =  
1457 Okanogan core complex; P = Priest River core complex; Pf = Pasayten fault; RLf = Ross Lake  
1458 fault; SCf = Straight Creek fault; Sh = Shuswap core complex; V = Valhalla complex. VI =  
1459 Vancouver Island; Wb = Wenatchee block of North Cascades crystalline core; Yf = Yalakom fault.  
1460 Box shows location of Fig. 3. States and Provinces: BC = British Columbia; ID = Idaho; MT =  
1461 Montana; OR = Oregon; WA = Washington.

1462

1463 Figure 3. Simplified geologic map of central and northern Washington State, and adjacent  
1464 southern British Columbia (modified from Eddy et al., 2016a). BP=Barlow Pass Formation;  
1465 Ccb=Chilliwack batholith; CHK=Chuckanut Formation; CM=Cooper Mountain pluton; CP=Castle  
1466 Peak stock; CRb=Columbia River Basalt Group; DD=Dinkelman decollement; DH=Duncan Hill  
1467 pluton; Ef=Entiat fault; Epc=Eagle Plutonic Complex; FDfz = Foggy Dew fault zone; FRfz=Frazer  
1468 River fault zone; GH=Golden Horn batholith; GPSz=Gabriel Peak shear zone; HZf=Hozameen  
1469 fault; Lfz=Leavenworth fault zone; LP=Lost Peak stock; MO=Mount Outram pluton;  
1470 MP=Monument Peak stock; MPS=Mount Pilchuck stock; N=Naches Formation; NP=Needle Peak  
1471 pluton; NWcts=Northwest Cascades thrust system; OP=Oval Peak pluton; Orb=Okanogan Range

1472 batholith; PC=Pipestone Canyon Formation; Pf=Pasayten fault; PG=Puget Group; Pv=Princeton  
1473 volcanics; R=Roslyn Formation; RC=Railroad Creek pluton; RLf=Ross Lake fault; SW=Swauk  
1474 Formation; SWG=Swakane Gneiss; T=Teanaway Formation; WEMB=Western and eastern  
1475 mélange belts; Yi=Yale intrusions.

1476

1477 Figure 4. Reconstruction map at ca. 55 Ma based on features in Figures 2 and 3 (see text for  
1478 details). Note that the western belt has been offset 150 km to the south relative to the central  
1479 zone and >300 km to the south relative to the eastern belt. The ridge which Siletzia formed on  
1480 is near central to southern Vancouver Island and the Swauk basin has formed inboard of Siletzia  
1481 in the western belt. There is a lull in magmatism in the southern part of the Coast Mountains  
1482 and North Cascades arc. B. Proposed plate tectonic setting at ca. 55 Ma based on features in  
1483 Figures 2 and 3. Note the position of major faults (both active and non-active) in gray for  
1484 reference. Br = Bitterroot lobe of Idaho batholith; Cb = Chelan block of North Cascades  
1485 crystalline core; Csz = Coast shear zone; Ef = Entiat fault; K = Kettle core complex; Ok =  
1486 Okanogan core complex; P = Priest River core complex; Pf = Pasayten fault; RLf = Ross Lake  
1487 fault; Sh = Shuswap core complex; V = Valhalla complex; VI = Vancouver Island; Wb =  
1488 Wenatchee block of North Cascades crystalline core; Yf = Yalakom fault. States and Provinces:  
1489 BC = British Columbia; MT = Montana; WA = Washington.

1490

1491 Figure 5. A. Reconstruction map at ca. 51 Ma based on features in Figures 2 and 3. By 51 Ma,  
1492 the ridge has reached Vancouver Island and Siletzia has collided with the continental margin.

1493 The Swauk basin has begun to invert and Challis-Kamloops magmatism is active, as are core  
1494 complexes and extensional basins in the eastern zone. B. Proposed plate tectonic setting. An =  
1495 Anaconda core complex; Br = Bitterroot core complex; Cb = Chelan block of North Cascades  
1496 crystalline core; Csz = Coast shear zone; Ef = Entiat fault; K = Kettle core complex; LCfz = Lewis  
1497 and Clark fault zone; Ok = Okanogan core complex; P = Priest River core complex; Pf = Pasayten  
1498 fault; RLf = Ross Lake fault; Sh = Shuswap core complex; V = Valhalla complex; VI = Vancouver  
1499 Island; Wb = Wenatchee block of North Cascades crystalline core; Yf = Yalakom fault. States and  
1500 Provinces: BC = British Columbia; CA = California; ID = Idaho; MT = Montana; NV = Nevada; UT =  
1501 Utah; WA = Washington.

1502

1503 Figure 6. A. Reconstruction map at ca. 48 Ma based on features in Figures 2 and 3. The  
1504 subduction zone has shifted outboard of Siletzia. Some of the dextral strike-slip faults in the  
1505 North Cascades have accelerated or initiated, and major dike swarms intruded in the central  
1506 and northern Washington Cascades coincident with a magmatic flare-up. Challis-Kamloops  
1507 magmatism continued, but is beginning to wane, as is extension associated with core  
1508 complexes. B. Proposed plate tectonic setting. The approximate location of the idealized slab  
1509 window assumes that the Farallon plate was moving NE and the Kula-Farallon ridge intersected  
1510 the continental margin as shown. C. Eocene magmatism across NE to north-central Washington  
1511 and the pattern of inferred rollback magmatism to the southwest are shown. Filled circles are  
1512 localities of U-Pb zircon ages of plutonic rocks. Heavy dashed lines are contours of the U-Pb  
1513 zircon ages (references cited in text). An = Anaconda core complex; Br = Bitterroot core  
1514 complex; Cb = Chelan block of North Cascades crystalline core; Chb = Chumstick basin; Csz =

1515 Coast shear zone; Ef = Entiat fault; Fa = Farallon plate; Ff = Fraser fault; K = Kettle core complex;  
1516 LCfz = Lewis and Clark fault zone; Ok = Okanogan core complex; P = Priest River core complex;  
1517 Pab = Pasco basin; Pf = Pasayten fault; RLf = Ross Lake fault; SCf = Straight Creek fault; Sh =  
1518 Shuswap core complex; V = Valhalla complex; VI = Vancouver Island; Wb = Wenatchee block of  
1519 North Cascades crystalline core. States and Provinces: BC = British Columbia; ID = Idaho; MT =  
1520 Montana; NV = Nevada; UT = Utah; WA = Washington.

1521

1522 Figure 7. Reconstruction map and proposed plate tectonic setting at ca. 44–40 Ma based on  
1523 features in Figures 2 and 3. The ancestral Cascades arc (“Cascadia”) has initiated, scattered  
1524 basins extend from the western to eastern belts, and magmatism has ended in the North  
1525 Cascades and almost all of the Challis-Kamloops belt. The Farallon – Pacific ridge is migrating to  
1526 the northwest relative to North America. Ff = Fraser River fault; LCfz = Lewis and Clark fault  
1527 zone; PG = Puget Group; Rb = Roslyn basin; SCf = Straight Creek fault. VI = Vancouver Island; Yf  
1528 = Yalakom fault. States and Provinces: BC = British Columbia; ID = Idaho; MT = Montana; OR =  
1529 Oregon; WA = Washington.

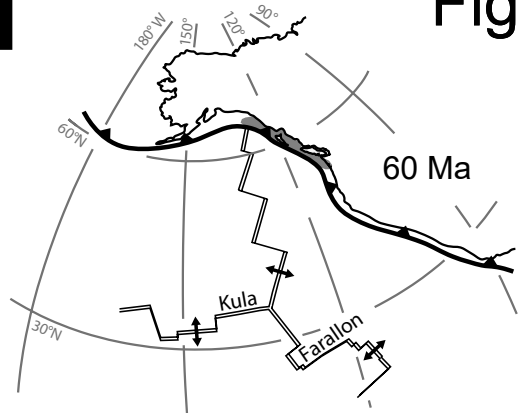
1530

1531 Figure 8. Summary of timing of major events described in the text. Within the magmatism,  
1532 sedimentation and deformation panels, features are generally arranged from west (left) to east  
1533 (right). Arrows designate where processes began before 60 Ma or ended after 40 Ma.

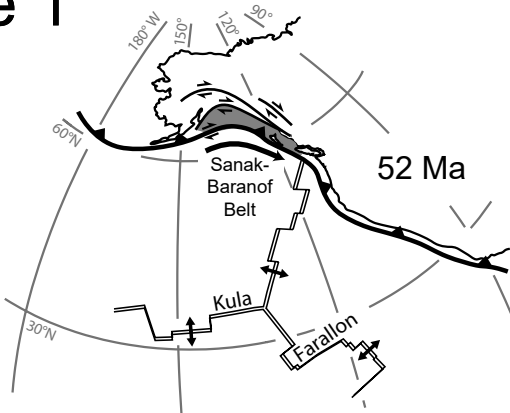
1534

1535 Figure 9. Tectonic model for 49.5–45 Ma magmatic flare-up in the Washington Cascades. The  
1536 star schematically shows the location of the northern Washington Cascades where the slab has  
1537 broken, south of the postulated slab window to the north. See text for explanation.

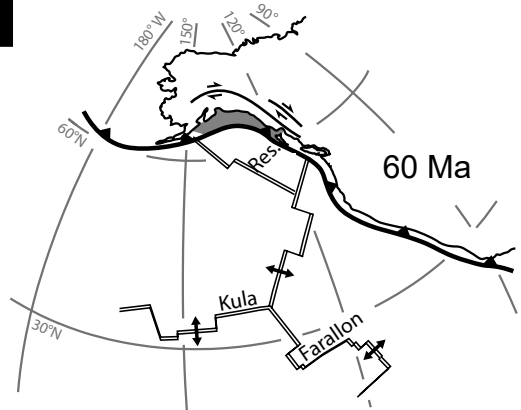
# Figure 1

**A**

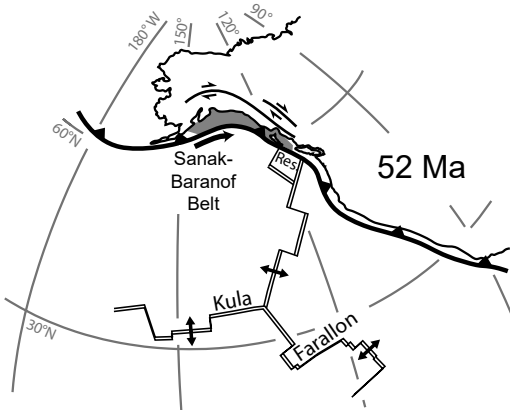
60 Ma



52 Ma

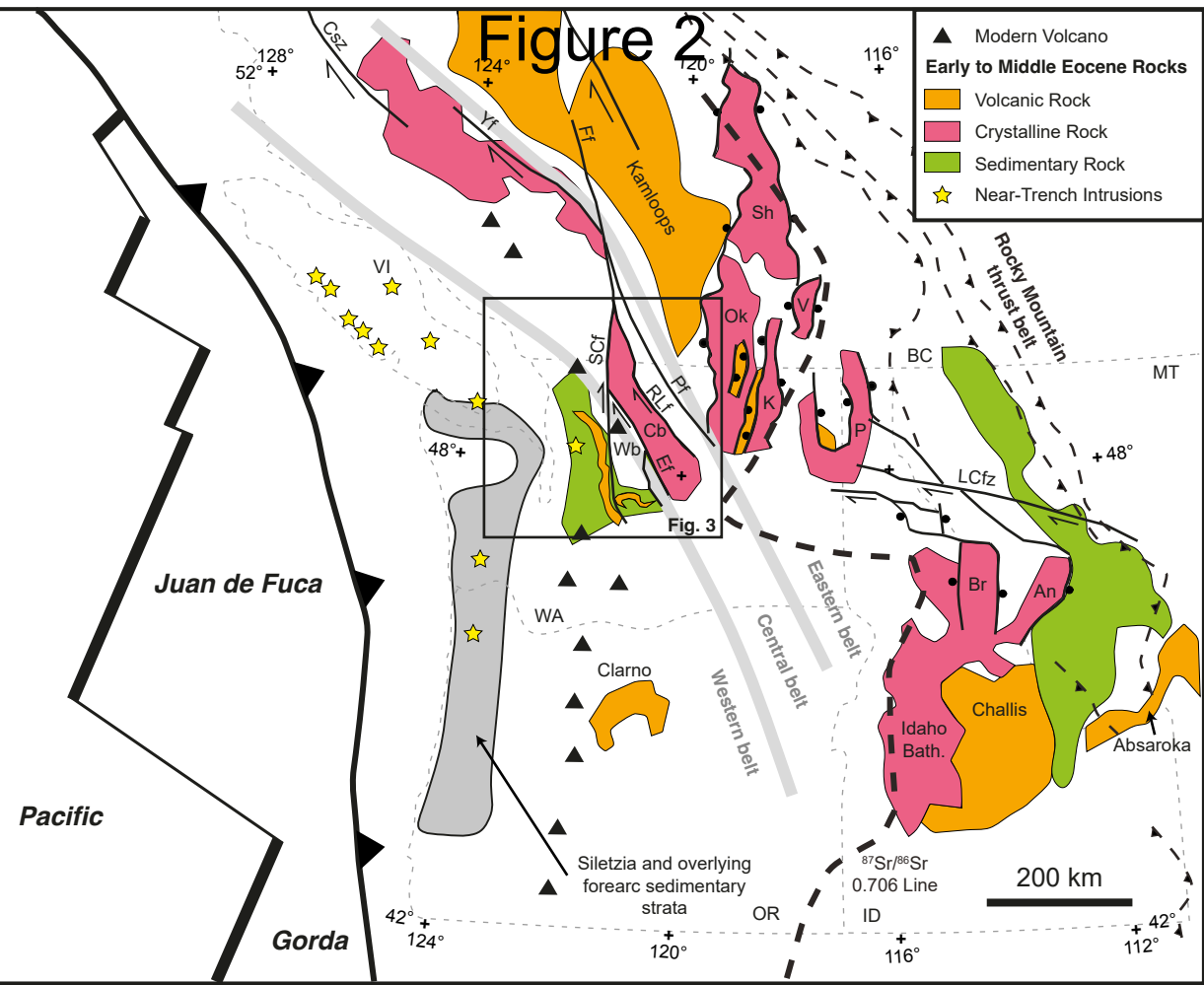
**B**

60 Ma



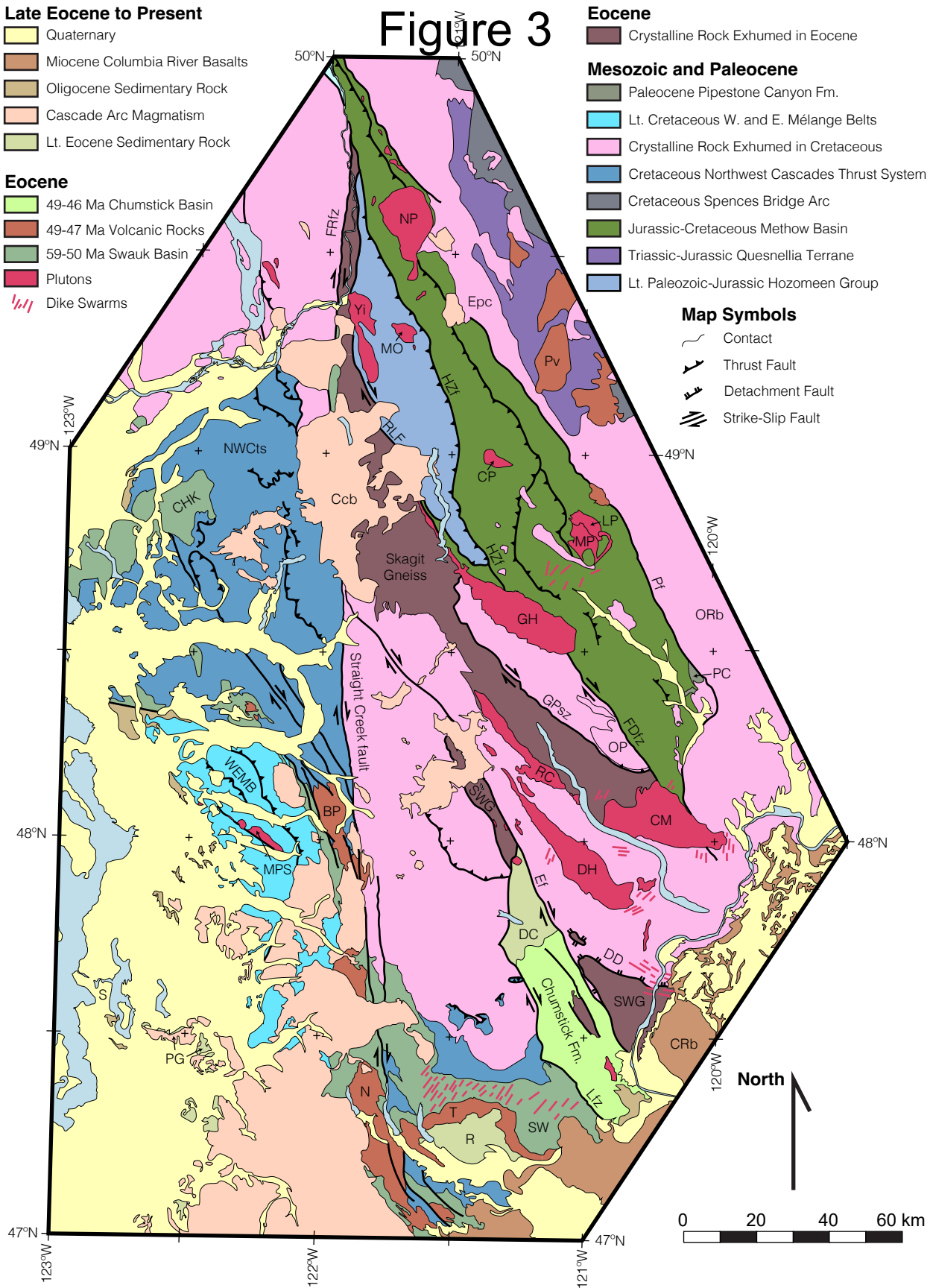
52 Ma

# Figure 2

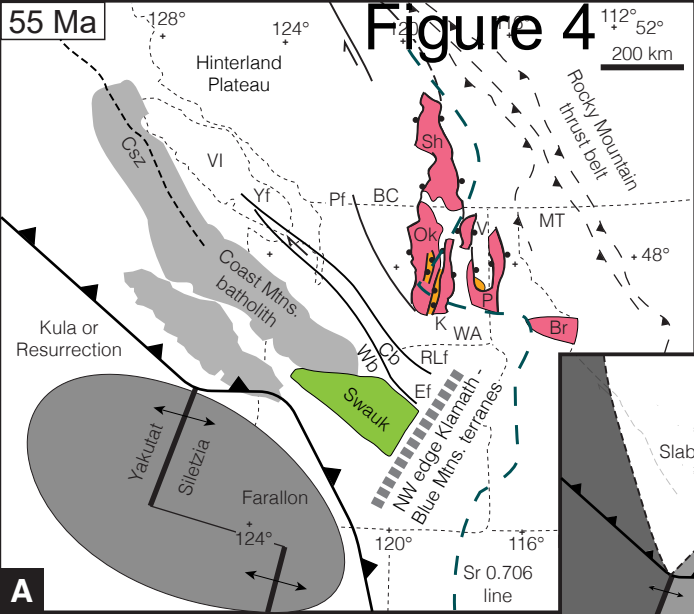
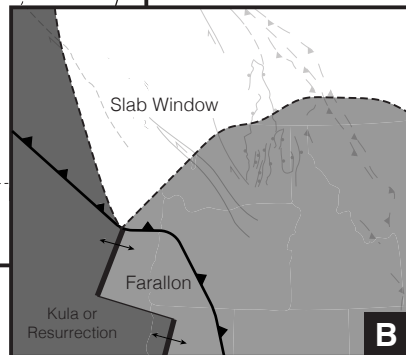


## Figure 3

## Late Eocene to Present



# Figure 4

**A****B**

51 Ma Figure 5

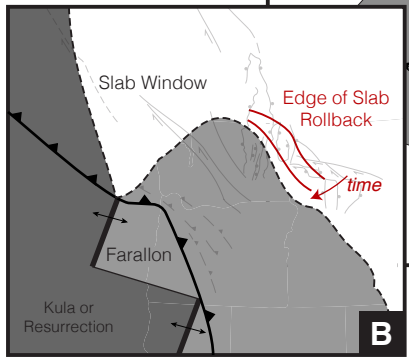
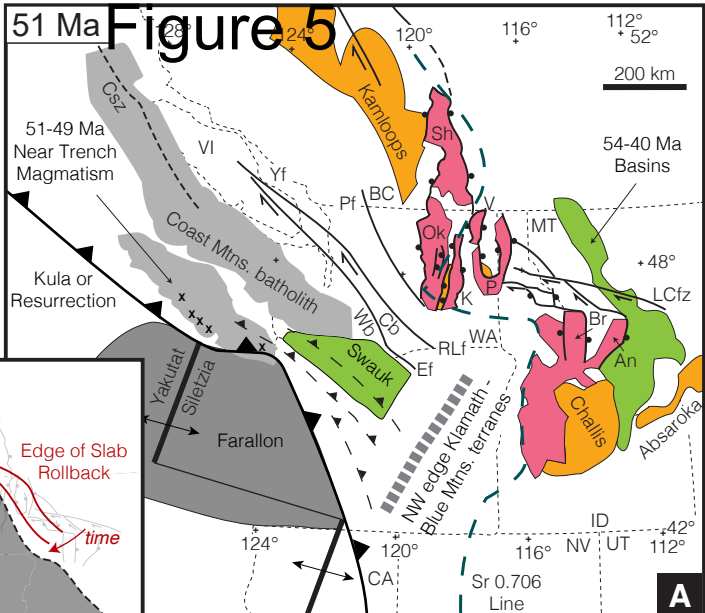


# Figure 6

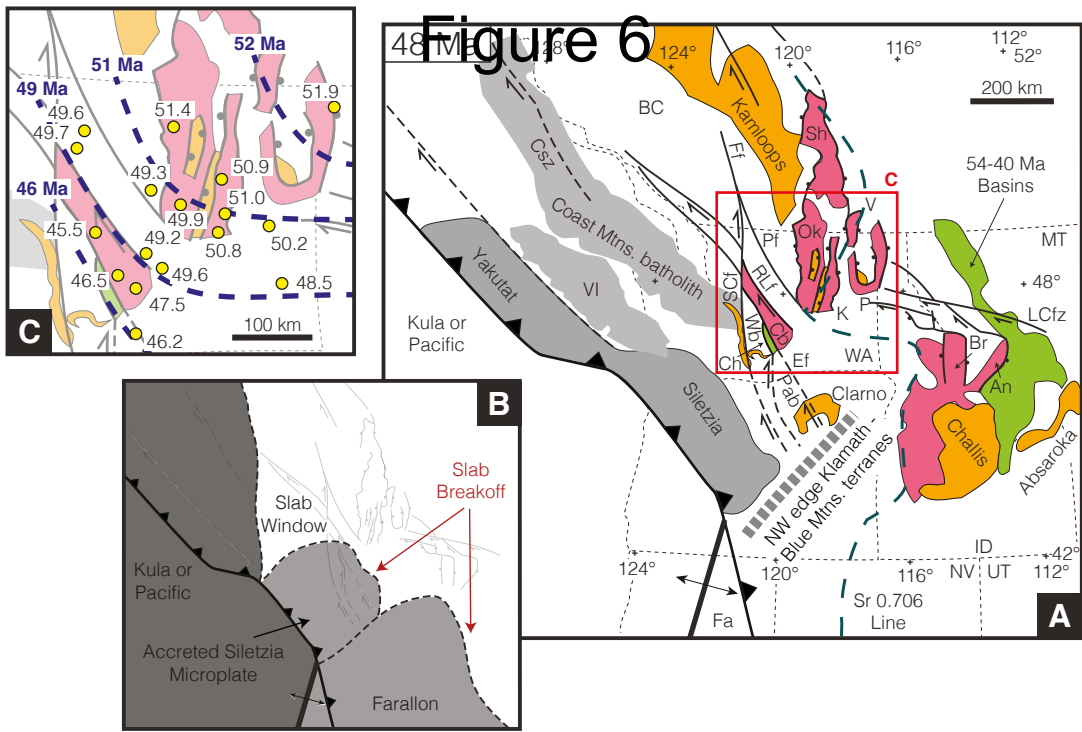


# Figure 7

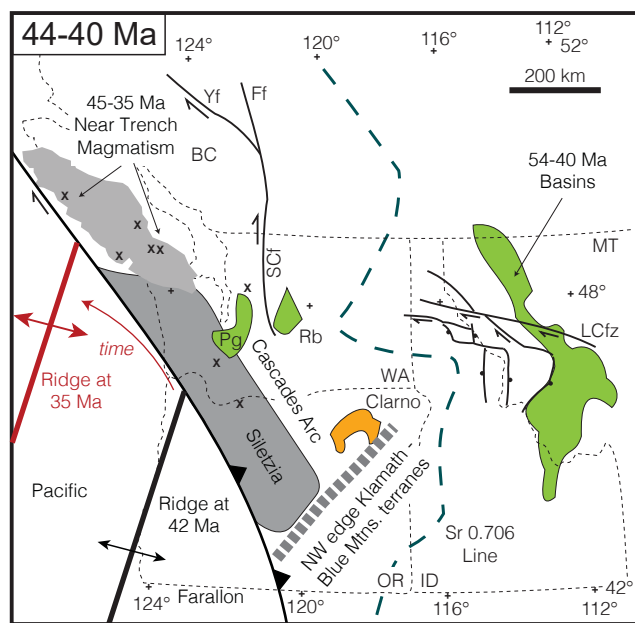


## Figure 8

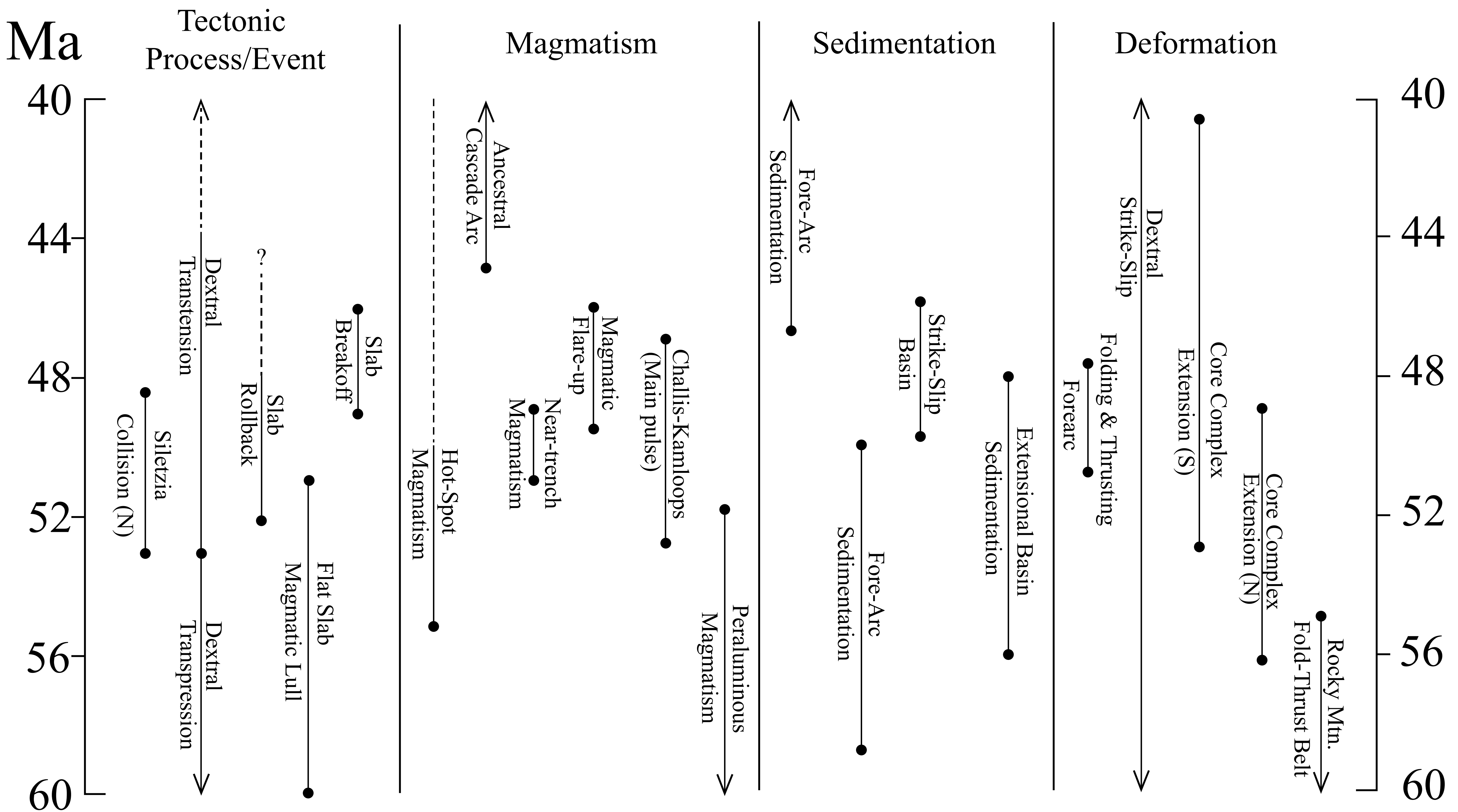
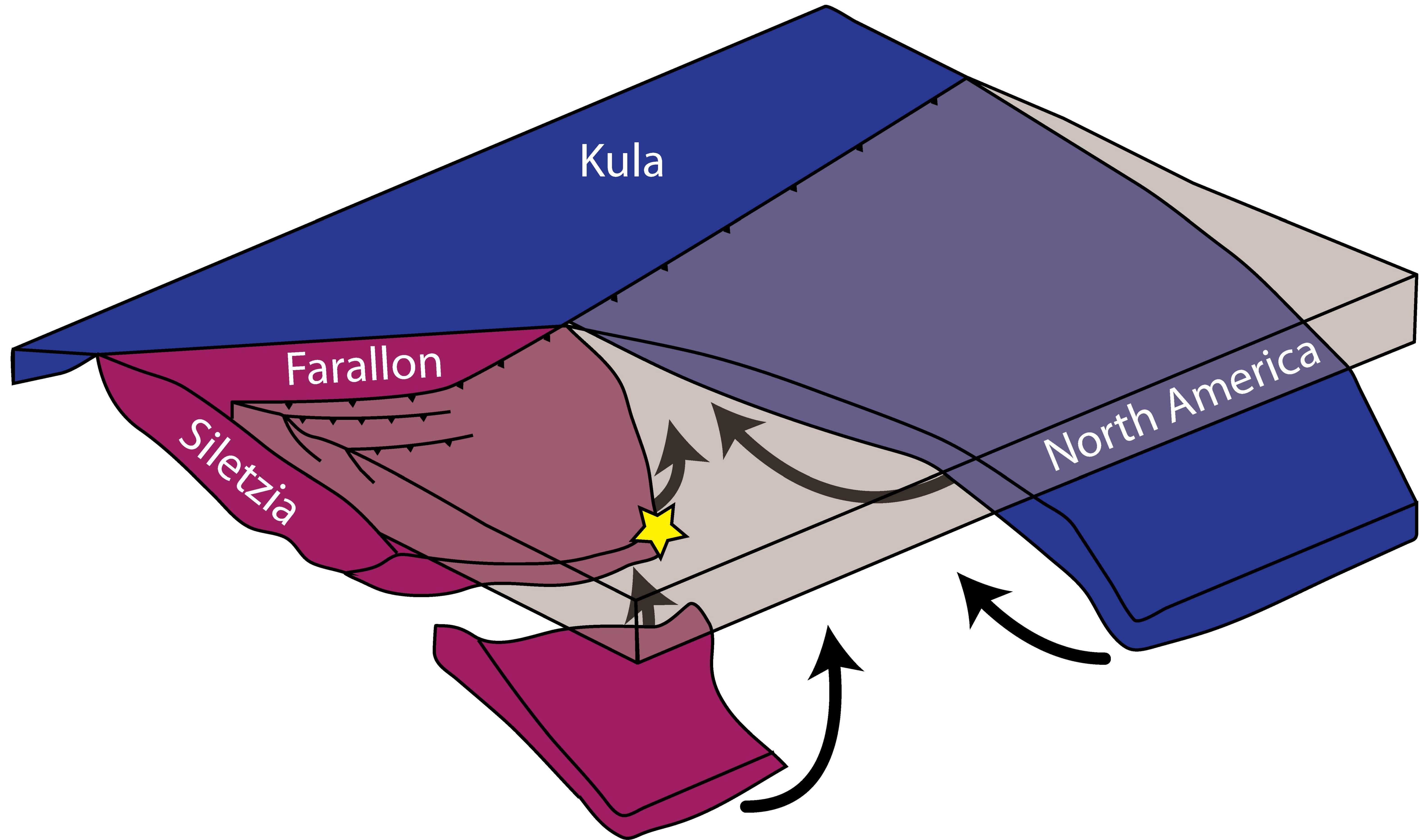


Figure 9



**TABLE 1. STRIKE-SLIP FAULT OFFSETS ACROSS WASHINGTON CASCADES**

	FAULT		OFFSETS		KM		<b>TOTALS</b>
	70-60 Ma	60 - 50 Ma	50 - 45 Ma	45 - 40 Ma	40 - 35 Ma		
Straight Creek fault			50	65	35	150	
Leavenworth fault			30			30	
Entiat fault			10	20		30	
Ross Lake - Hozameen - Foggy Dew faults	10	60	45	10		115	
<b>TOTAL OFFSET</b>	<b>10</b>	<b>60</b>	<b>135</b>	<b>95</b>	<b>35</b>	<b>325</b>	

We appreciate the thoughtful and constructive comments (in italics below) by the reviewers. Our responses directly follows each of the comments.

#### **Response to Comments by Gene Humphreys (Reviewer 1)**

Reviewer #1 (Comments to the Author):

*This was a well written and organized paper that was easy to read. More important, it is a thoughtful and comprehensive synthesis of a complex area. it represents an enormous amount of previous research that has been brought together by people who understand the geology and the geological relations better than anyone, and who also have a geographically broad perspective within which to place the North Cascades. The area is important to the making of the PNW, and to observations bearing on ridge-continent interaction and terrane accretion.*

*Practically speaking, the compilation of observational support for a PNW history will be useful to many, and their synthesis of the tectonic history through the use of tectonic reconstructions provides a good reference model for the area.*

=====

*Detailed comments for the authors to consider-*

53. *end of line needs a word or two to make sense.*

“Coast Mountains” added to clarify wording.

*58-61 & 98-100. Another possibility that has been suggested by the Muller and Sigloch groups is what they call the Orcas plate (Clennett et al., GGG, 2020). I don't know what to make of their models; while there seem to be clear errors when looking at a local level of their model, the arguments for a different plate tectonic setting in the NE Pacific basin (based on mantle tomography images of ocean slab) demand a different plate configuration and history.*

We don't explore the implications of this recent model in detail, but now refer to the Orcas plate in the introduction (line 59) and Clennett et al. (2020) is cited. The potential Orcas plate is also referred to on lines 104, 110, and 119 of the text and in the caption to Fig. 1.

*95. First paragraph of Plate Tectonic Setting. What's the point? And missing is anything about the transport of Baja/BC, which is an important point for the North Cascades. Also, since strongly oblique subduction is required, the subducting plate is more oblique than the Farallon plate. The plate subducting beneath the North Cascades region must be the Kula, Resurrection, Orcas, or whatever plate is north of Farallon. (I think a lot is not known about what was happening west of North America north of the Farallon plate, but the important thing is that a spreading center defines the northern limit of the Farallon plate.).*

Reviewer 2 also commented on the transport of Baja BC in his second and third general comments. In response to these comments, we have made our most extensive edits in the sections on “Plate Tectonic Setting” (lines 97-105) and “Restoration of Strike-Slip Faults” (lines 192-201). For the plate tectonic

setting we now state that the northern boundary of the Farallon plate was a ridge, regardless of whether the northern plate was the Kula, Resurrection, or Orcas plates, and added a phrase that emphasized the motion of the northern plate was more oblique than that of the Farallon plate relative to N.A.

“...northward translation of the Washington Cascades may have been rapid as the southern part of the Insular superterrane (the Baja BC hypothesis; e.g., Cowan et al., 1997; Umhoefer and Blakey, 2006). Relative to North America, motion of the Farallon plate was to the NE to ENE, and motion of the Kula (Resurrection or Orcas?) plate was to the N to NNE, and thus more oblique than that of the Farallon plate. Both oceanic plates were moving rapidly (50 – 150 km/Myr) during this time (e.g., Engebretson et al., 1985; Doubrovine and Tarduno, 2008; Wright et al., 2015; Fuston and Wu, 2021).”

The paleomagnetic data indicating major dextral translation is addressed more extensively in the section on strike-slip offsets (lines 192 to 201) – see response to Reviewer #2, general comment #3 for more detail

*111. To state "One explanation" is too weak, considering the abundance of different observations that support Well's basic interpretation.*

Replaced “one explanation for this feature is that” with “probably is.”

*135. Which rocks in Fig. 3 are being referred to?*

The Northwest Cascades system is labelled on Fig. 3., but to clarify we have slightly modified the text so that it reads “Paleozoic and Mesozoic oceanic and island arc rocks and overlapping Jura-Cretaceous marine clastic rocks, which were deformed in the mid-Cretaceous Northwest Cascades thrust system (shown as a single Cretaceous unit on Fig. 3).”

*137. It should be "which are."*

With the comma after “which”, we think that the use of the singular for “mélange belt” is proper?

*147, 156, 167, 172. Which rocks in Fig. 3 are being referred to? It's hard to go from the text to Fig. 3.*

All of the features on these lines are on Fig. 3 and we are not quite certain on how to clarify this figure. We made the following additions to help clarify locations. We did add some words to help guide the reader and added an abbreviation to Fig. 3.

Line 142, ... Northwest Cascades thrust system “(shown as a single Cretaceous unit on Fig. 3)”

For line 147, we added “of the central belt”.

For line 167, we added “of the western belt” to help the reader find these features on Fig. 3.

For line 172, "Hzf" was added along the southern part of the Hozameen fault in Fig. 3, which complements the label already present on the northern part.

*200-567 'PALEOGENE TECTONIC HISTORY.' A thorough presentation of the relevant observations. I learned a lot.*

*582-83. I don't know why the approach of Siletzia would help flatten the Farallon slab. I could believe that some of Siletzia that subducted north of the suture on southern Vancouver Island or east of the Crescent formation could provide some local buoyancy. Or that the flat Farallon beneath Wyoming helped hold up the adjacent Farallon.*

This material has been deleted. We have also shortened the subsequent text and added a reference to the Laramide. "The shallowing of the slab may be attributable to the rapid subduction of young buoyant lithosphere. Strong suction in the mantle wedge may have played a role, as proposed for the Laramide belt (Humphreys, 2009; O'Driscoll et al., 2009). Note that the Laramide belt in northern Wyoming was directly east of Siletzia at 55 Ma in our reconstruction (Fig. 4)."

*585-89. I thought Schellart's idea is that a wide slab acts like a parachute. But since about 85 Ma, the Farallon's northern end (beneath western U.S.) is defined by a ridge, and would not be parachute like. Nonetheless, I think the important thing is that the geological observations support the presence of a flat-slab beneath the PNW at this time.*

Our interpretation of the wide slab and shallowing has been deleted in response to Humphreys' comment.

*649. Why does the approach of Siletzia influence magmatism? I can imagine this if Siletzia extended beyond the boundaries of what we know today, and that this area was being subducted. I suspect this was likely. It would be remarkable if the entirety of Siletzia accreted, as though subduction stopped at the first encounter of Siletzia with the subduction zone.*

We deleted "approach of" following the reviewer's comment.

*677-699. As I understand it, the North Cascades basins trend into the Pasco basin area, which was very volcanically active at this time (Catchings and Mooney, 1988). This supports the idea that the flareup was not simply arc related, but related to the removal of the Farallon flat slab in some fashion.*

We have added the Pasco basin area to our interpretation (lines 707-712) and consulted with the reviewer (Gene Humphreys) to make certain we understood his comment.

"A speculative additional interpretation is that the breakoff-related magmatism continued to the southeast beneath the Columbia River Basalt Group in the Pasco basin to the Clarno Formation of NE Oregon (Figs. 2, 6). The Pasco basin is on strike with the Eocene Chumstick basin and seismic velocities suggest that beneath the Miocene basalt is a thick, asymmetric sedimentary basin of probable Eocene

age and an associated mafic underplate (Catchings and Mooney, 1988; Gao et al., 2011). These mafic rocks may be similar to the Teanaway Basalt of the flare-up.”

**Reviewer #2 (Comments to the Author):**

*Review by D.J. Thorkelson, January 19, 2023*

*The submission by Miller et al., on the Paleogene plate tectonic and geologic history of the Pacific Northwest and related areas is very good and should be published with few revisions.*

*The paper stands out as being well written, with complex ideas expressed simply and effectively. It is a pleasure to read and provides the reader with a near-encyclopedic source of information linked to larger ideas and tectonic models. The paper does not purport to solve all of the interesting local and regional geological problems, but neither does it set it to do so. It is a comprehensive statement on the current state of knowledge and provides a balanced and fair depiction of geological features, history and processes.*

*Although the paper is good, it could use a little improvement in a few areas, and I hope the authors will take the time to consider my remarks and to act on them.*

*I have annotated the manuscript using the sticky-notes function. I expect the authors to scroll through the annotated file and read my remarks.*

*Here, I will summarize four issues that need a little attention.*

*First, there are a couple of key references missing. I know, not all references can be cited, but please try to include the 2013 paper by McCrory and Wilson (Tectonics) and the 1980 paper by Tom Ewing (Journal of Geology). The Ewing paper is remarkable and is the first paper to try to pull a story of Paleogene evolution together. The McCrory and Wilson paper is a modern view of the region that attempts to do much of what the current submission does. The reader should be alerted to both.*

We now cite the papers omitted from the introduction. Ewing (1980) is cited on line 69 of the introduction. This paper was cited in 5 other places in the original manuscript. The paper by McCrory and Wilson (2013) is now cited on line 67 of the introduction and line 117 elsewhere in the text.

*Second, the plate tectonic setting is reasonably covered for the Paleogene, but that information could be set within a broader context, more clearly than it is. Specifically, the interaction between the Kula-Farallon ridge and North America in the Paleogene is quite an easy sell, and has been well utilized from Thorkelson and Taylor (1989) onwards. However, the work by Engebretson and colleagues in the mid-1980s and Woods and Davies in 1982 (and subsequently Thorkelson and Taylor) show that the Kula-Farallon ridge began as an oceanic rift in the late Cretaceous, circa 1983, and that the Kula-Farallon ridge would have intersected the western North American margin from that point on - until plate consumption and reorganization in the Eocene. However, one would never know that from the current submission. Instead, the notion of Paleogene ridge subduction is moved to the front of the discussion without being placed in a broader, longer tectonic history. I sincerely hope that the authors do their readers a favour by making the earlier history of K-F-NA interactions a little better known, even if all the*

*answers regarding exact locations and consequences are imperfectly known. The Paleogene ridge system was connected both physically and thematically to the late Cretaceous one. A possible diachronous scenario was provided by Thorkelson and Taylor and, although it need not be taken as unique, it does provide a foundation that could and should be built upon.*

We have added material on the Late Cretaceous history in the plate tectonic setting (lines 97-102) and in the caption to Fig. 1 (figure on tectonic models). “There is general agreement that the Kula plate originated from rifting of the Pacific plate at ~83 Ma and that the northern boundary of the Farallon plate was a ridge, which intersected the continental margin at a poorly constrained location (e.g., Atwater, 1970; Wood and Davies, 1982; Engebretson et al., 1985; Stock and Molnar, 1988; Thorkelson and Taylor, 1989).” The caption now states “Note that in either model there is a triple junction near central to southern Vancouver Island at ca. 52 Ma (e.g., Breitsprecher et al., 2003) and that a ridge in either scenario interacted with the continental margin back to ca. 83 Ma (e.g., Engebretson et al., 1985; Thorkelson and Taylor (1989).”

*Third, the thorny notion of dextral translation is a subject that the authors take on, and kudos to them for including it in the geological history and restorations. However, I think they could be a little more forthcoming by including a brief statement on the broader aspects of the dextral translation debate, specifically the much larger magnitudes of displacement indicated in paleomagnetic studies (and I believe in some detrital zircon studies). The authors are basing their estimates of translation on studies of specific fault zones, and that is an adequate approach to take. However, distributed strain along much small features is also worth considering, and the 1000-3000 km (or more) magnitudes are still, in some people's minds, not out of the question. Adding up displacement on specific faults will, most likely, provide only a minimum. Look at the GPS data for the region and marvel at how much displacement is currently taking place along distributed minor or cryptic structures. I am not asking the authors to re-do their estimates, but they should be more open on this subject and write a few sentences about the fact that the actual amounts of overall displacement, and how they vary from east to west, and temporally from mid-K to Eocene, are not perfectly understood, and may be much larger than fault-only based restorations.*

The following sentences were added to the section on lines 193-201 to satisfy this comment. “We note that this is likely a conservative estimate and does not include any distributed dextral ductile displacement or movement on minor cryptic structures. Paleomagnetic data indicate much larger cumulative dextral displacements between ~85–55 Ma of 2000 km or more between the easternmost part of the eastern belt and the central and western belts, and perhaps 1000 km between the western part of the eastern belt and rocks to the west (e.g., Enkin, 2006; Tikoff et al., 2023). From the paleomagnetic data, major displacements of the outboard rocks ended by 55 Ma (e.g., Cowan et al., 1997; Tikoff et al., 2023). Thus, uncertainties are much lower for the positions of units in the region in the 55 Ma and younger reconstructions (Figs. 4-7).” An additional phrase was also added to the introduction to the pre-Paleogene geologic setting on lines 138-39. “The arc and forearc were originally farther south relative to the inboard rocks by more than 300 km (e.g., Umhoefer and Blakey, 2006; Wyld et al., 2006), and potentially a much greater distance as discussed below.”

*Fourth, the shape of the slab window as shown in their Figure 6 is adequate but is not specifically mentioned in the caption. In fact, the three frames, A, B and C, are not individually addressed in the caption, and must be. For the slab window shape, the authors, I will bet, did not do any modeling of their own, and instead have chosen to show a stylized one. That is OK, but tell the reader exactly that - not modeled, but schematic, based on ... give references.*

Each frame is now addressed, as was the caption for Fig. 5. Added to the caption – “The approximate location of the idealized slab window assumes that the Farallon plate was moving NE and the Kula-Farallon ridge intersected the continental margin near the Oregon-Washington state boundary.”

#### Response to Comments on pdf by Derek Thorkelson (Reviewer 2)

##### LINES

20. *Is this a new finding or have others made the call, and you are supporting it?*

This lull has been pointed out by two of the authors (Miller et al., 2016; 2021) in two papers published in *Geosphere*. A flat slab has been proposed by others for the Pacific Northwest, but relating it to a flat slab is new in this manuscript. To clarify without adding details in an abstract, the text now reads “interpreted to reflect” rather than “we attribute”.

71 and 94. Compliments – no response needed (though appreciated).

94. – *The 1980 *Journal of Geology* article by Tom Ewing should be cited in this introduction. It was the first paper to cover the Paleogene story on both sides of the international border and was the first, I believe, to illustrate core complex formation at that time.* Ewing (1980) is now cited in the introduction on line 69. The paper was cited four times in the text in the original manuscript and these citations remain.

94 – *Surely the paper by McCrory and Wilson, *Tectonics*, 2013, should be cited as a previous attempt to make sense of the Paleogene history in the region.*

McCrory and Wilson (2013) is now cited on lines 67 and 117.

108. *Yes, but it would appear that the K-F triple junction first formed when the K plate broke from the Farallon in the 85-80 Ma range, and so the Paleogene history of ridge subduction and slab window formation is likely to be part of a continuum of interactions extending back to the mid-Cretaceous. An entirely plausible model was put forward by Thorkelson and Taylor in 1989. It accounts for the younging of the adjacent oceanic slabs and the subsequent flat-slab configuration. I bet readers would benefit from knowing that the Paleogene slab window history belongs to a longer history. Just inform the reader that the Paleogene situation is part of a broader history that goes beyond "transpression."*

We have added the following about the Cretaceous history and the intersection of a ridge bounding the Farallon plate with North America. "There is general agreement that the Kula plate originated from rifting of the Pacific plate at ~83 Ma and that the northern boundary of the Farallon plate was a ridge, which intersected the continental margin at a poorly constrained location (e.g., Atwater, 1970; Wood and Davies, 1982; Engebretson et al., 1985; Stock and Molnar, 1988; Thorkelson and Taylor, 1989)."

109. Better: "*Formation of the Siletzia Terrane was a major...*". We now start the sentence with "Formation of the Siletzia terrane" as suggested.

113. *Infer? Rather, "we support previous work that...."*

Now reads: "We support previous work that infers the triple junction"

185. *It would be good to tell the reader that your geologically based estimates are lower than those identified by paleomagnetism. The Spences Bridge Group may have been 1000 km farther south when it formed, and units farther west have been shown to have greater displacements from the south. I don't think you should feel obliged to make a comprehensive review of the information (which includes detrital mineral studies), but you should alert the reader that the estimates of translation from the south are on the low end, given all the information available. Displacement estimates on specific faults and fault sets will likely be less than the sum of those displacements plus distributed strain from less prominent.*

This comment amplifies the third general comment by Reviewer Thorkelson. The potential for much larger offsets of outboard rocks is now addressed on lines 193 to 201. See the response to the third general comment above.

206. *Again, since the Kula broke from the Farallon at about 83 Ma, it stands to reason that there would have been a K-F-NA triple junction and slab window somewhere along the coastline. No, we don't know exactly where it was, but do we know it wasn't near, or within, the study area?*

This paragraph at the beginning of the section focuses on the geologic evidence for oblique convergence. We hope that the material on lines 97-102, which mentions the earlier history, including the uncertain location of the triple junction, and the addition to the caption for Fig. 1 are sufficient. "There is general agreement that the Kula plate originated from rifting of the Pacific plate at ~83 Ma and that the northern boundary of the Farallon plate was a ridge, which intersected the continental margin at a poorly constrained location (e.g., Atwater, 1970; Wood and Davies, 1982; Engebretson et al., 1985; Stock and Molnar, 1988; Thorkelson and Taylor, 1989)." The caption now states "Note that in either model there is a triple junction near central to southern Vancouver Island at ca. 52 Ma (e.g., Breitsprecher et al., 2003) and that a ridge in either scenario interacted with the continental margin back to ca. 83 Ma (e.g., Engebretson et al., 1985; Thorkelson and Taylor (1989)."

241. *But no slab window despite the lack of proper arc magmatism?*

We are not certain if this is a parenthetical statement. This section describes the basic geologic features and reports on work by others on petrogenesis without focusing on tectonic setting.

325. *Surely, the K-F ridge is responsible for the younging and shallowing of the F and possibly the K slabs. So, where was the continental triple junction? Can you show that it wasn't involved? Doesn't seem like a bad fit to me.*

We didn't change this paragraph as we suggested that low-angle subduction accounted for the cessation of arc plutonism. Younging of the subducting slab is proposed for the cause of the low angle in the discussion and references to others whom have stated this for the greater region are cited (lines 597-599). "The shallowing of the slab may be attributable to the rapid subduction of young buoyant lithosphere, as also proposed by others for the greater region (e.g., Thorkelson and Taylor, 1989; Haeussler et al., 2003)."

418. *See attachments to this review -- Thorkelson 1995 GAC abstract and figures.*

We appreciate getting the abstract and figure. We mention "passage of a slab window" as one of the mechanisms proposed for Challis-Kamloops magmatism.

420. Humphreys now spelled correctly.

438. *Are we certain that the triple junction and slab window had nothing to do with these features? OIB -- a common composition of slab window volcanism -- see review in Thorkelson, Encyclopedia of Geology article on slab windows.*

Lines 434-5 mentioned a slab window as one of the mechanisms proposed by others in the original text. We emphasize this a little more with the underlined text. "Slab rollback and breakoff, and slab window evolution are the most widely cited scenarios (see review by Humphreys and Grunder, 2022)." We deleted the phrase stating our preference in this paragraph, which just summarizes models in the literature.

516. Changed "but" to "and" as requested.

579. We are not clear what the "and/or" refers to

582. *"ridge close to the trench"... a little vague. Knowing what we do about the K and F Cretaceous history, what is meant by "close to the trench"? What argument do you know of that would position the ridge offshore, and not in contact with the continent? It would seem unavoidable that the ridge would have intersected the continental margin, so, again, what does "ridge close to the trench" even mean?*

Reviewer Humphreys also criticized this idea and the statement has been deleted and a few other lines have been added in response to his comment (see new lines 597-602). Also see the response to Humphreys' comment above.

596. *Cite the papers which dealt with this and proposed a location something like this. This is not something new.*

The following reference is added (underlined) "in which case the latter would be kinematically tied to the Tintina fault – Rocky Mountain trench (Price and Carmichael, 1986) and magmatism would occur in a slab window (e.g., Breitsprecher et al., 2003)." We note that our interpretation is based on our strike-slip restorations and matching up parts of the southern Coast Mountains-North Cascades Cretaceous arc using compilations of recent U-Pb ages, which is new.

598. Made the minor wording change.

679. *I'm going to include an abstract with key figures from a 1995 GAC talk for you to consider.*

We have now stated that the magmatism to the east has been attributed to a slab window and reference Thorkelson and Taylor (1989) and Breitsprecher et al. (2003). We then give our preferred rollback and breakoff model, which takes into account new age data from NE Washington and the Cascades, as well as the tomographic information from Schmandt and Humphreys (2011).

"The Eocene Cascades core plutons have been considered the latest pulse of arc magmatism in the North Cascades by earlier workers (e.g., Matzel et al., 2008; Miller et al., 2009), and magmatism to the east in the Challis-Kamloops belt has been interpreted to occur within a slab window (e.g., Thorkelson and Taylor, 1989; Breitsprecher et al., 2003). In our view, the flare-up is related to the Farallon slab rollback and breakoff."

1395. *In this model -- OK -- but say where it comes from.*

Bradley et al. (2003) is now cited for model A and Haeussler et al. (2003) for model B. Madsen et al. (2006) is cited for location of ridge intersection on Vancouver Island.

1396. *from inclusion of the*

Phrase added as requested.

1399. *History from 83-60 not shown, and that's OK, but somewhere in the paper you need to let the reader know that a RTT triple junction did exist prior to 60.*

Please see the response to the second general comment.

1454. You need to have separate statements about each of the frames, A, B and C.

Each frame is now described separately. Also, please see response to general comment #4.

1        **UPPER PLATE RESPONSE TO RIDGE SUBDUCTION AND OCEANIC PLATEAU ACCRETION,**  
2        **WASHINGTON CASCADES AND SURROUNDING REGION: IMPLICATIONS FOR PLATE TECTONIC**  
3        **EVOLUTION OF THE PACIFIC NORTHWEST (U.S.A. AND SW CANADA) IN THE PALEOGENE**

4        **Miller, Robert B.**, Department of Geology, San José State University, One Washington Square,  
5        San Jose, CA 95192; **\*Umhoefer, Paul J.**, School of Earth & Sustainability, Northern Arizona  
6        University, P.O. Box 4099, Flagstaff, AZ 86011; **Eddy, Michael P.**, Earth, Atmospheric, and  
7        Planetary Sciences Department, Purdue University, 550 Stadium Mall Drive, West Lafayette, IN  
8        47907; **Tepper, Jeffrey H.**, Geology Department, University of Puget Sound, 1500 N. Warner St,  
9        Tacoma, WA 98416-1048

10        \*Deceased

11        **ABSTRACT**

12        The interaction between subduction zones and oceanic spreading centers is a common  
13        tectonic process, and yet our understanding of how it is manifested in the geologic record is  
14        limited to a few well-constrained modern and ancient examples. In the Paleogene, at least one  
15        oceanic spreading center interacted with the northwestern margin of North America. Several  
16        lines of evidence place this triple-junction near Washington and southern British Columbia in  
17        the early-middle Eocene and we summarize a variety of new datasets that permit us to track  
18        the plate tectonic setting and geologic evolution of this region from 65 to 40 Ma. The North  
19        Cascades segment of the voluminous Coast Mountains continental magmatic arc experienced a  
20        magmatic lull between ca. 60-50 Ma that we attribute interpreted to reflect low-angle  
21        subduction. During this period of time the Swauk basin began to subside inboard of the paleo-

22 trench in Washington and the Siletzia oceanic plateau began to develop along the Farallon-Kula  
23 or Farallon-Resurrection spreading center. Farther east, peraluminous magmatism occurred in  
24 the Omineca belt and Idaho batholith. Accretion of Siletzia and ridge-trench interaction  
25 occurred between ca. 53–49 Ma, as indicated by: (i) near-trench magmatism from central  
26 Vancouver Island to NW Washington; (ii) disruption and inversion of the Swauk basin during a  
27 short-lived contractional event; (iii) voluminous magmatism in the Kamloops – Challis belt  
28 accompanied by major E-W extension east of the North Cascades in metamorphic core  
29 complexes and supra-detachment basins and grabens; and (iv) southwestward migration of  
30 magmatism across NE Washington. These events suggest that flat slab subduction from ~60–52  
31 Ma was followed by slab rollback and breakoff during accretion of Siletzia. A dramatic magmatic  
32 flare-up was associated with rollback and breakoff between ca. 49.4 Ma and 45 Ma, and  
33 included bimodal volcanism near the eastern edge of Siletzia, intrusion of granodioritic to  
34 granitic plutons in the crystalline core of the North Cascades, and extensive dike swarms in the  
35 North Cascades. Transtension during and shortly before the flare-up led to >300 km of total  
36 offset on dextral strike-slip faults, formation of the Chumstick strike-slip basin, and  
37 subhorizontal ductile stretching and rapid exhumation of 8–10 kb metamorphic rocks in the  
38 North Cascades crystalline core. By ca. 45 Ma, the Farallon – Kula (or Resurrection) – North  
39 American triple-junction was likely located in Oregon, subduction of the Kula or Resurrection  
40 plate was established outboard of Siletzia, and strike-slip faulting was localized on the north-  
41 striking Straight Creek – Fraser River fault. Motion of this structure terminated by 35 Ma. These  
42 events culminated in the establishment of the modern Cascadia convergent margin.

43

44 **INTRODUCTION**

45 Plate tectonic margins vary from long-lived stable settings to those that change rapidly  
46 from one type of boundary to another over only a few million years. The modern Cascadia  
47 subduction zone, in the Pacific Northwest (U.S.A) and southwest British Columbia (Canada), has  
48 been a convergent plate margin since the mid-Eocene ( $\leq 45$  Ma) (du Bray and John, 2011).

49 Earlier, the northern Washington Cascades was part of a long-lived continental magmatic arc  
50 that is also manifested as the Coast Mountains batholith and parts of the Idaho batholith (e.g.,  
51 Gehrels et al., 2009). The North Cascades segment of the Coast Mountains arc was active from  
52 about 96–60 Ma, and changed from a contractional-convergent to oblique-convergent regime  
53 during that time (e.g., Brown and Talbot, 1989; Miller et al., 2009, 2016). Between the older

54 [Coast Mountains](#) and Cascadia magmatic arc regimes was an  $\sim 25$  m.y. period, from ca. 65 – 40  
55 Ma, during which the Washington Cascades and the surrounding region experienced many  
56 dynamic changes that can be linked to two major Paleogene tectonic events: spreading ridge –  
57 trench interaction and the formation and accretion of an oceanic plateau.

58 Plate reconstructions suggest that the Farallon – Kula [or](#) Farallon – Resurrection, [or](#)  
59 [Farallon – Orcas](#) spreading ridge(s) interacted with North America near the Pacific Northwest  
60 during the Paleogene (e.g., Atwater, 1970; Wells et al., 1984; Engebretson et al., 1985;  
61 Haeussler et al., 2003; Madsen et al., 2006; [Clennett et al., 2020](#); Fuston and Wu, 2021) (Fig. 1).  
62 Based on ca. 51-49 Ma near-trench magmatism from central Vancouver Island to northwestern  
63 Washington, a ridge is assumed to have intersected North America near these locations at that  
64 time (e.g., Cowan, 2003; Madsen et al., 2006), although how this triple-junction migrated along  
65 the margin prior to 52 Ma is poorly understood. The Siletzia terrane, a basaltic oceanic plateau,

66 formed along this oceanic spreading center and was accreted to the Pacific Northwest ca. 50  
67 Ma (e.g., [McCrory and Wilson, 2013](#); Wells et al., 2014). Farther inland there was a change from  
68 a long-lived thrust belt (e.g., Mudge and Earhart, 1980; Price, 1981) to east-west extension and  
69 widespread magmatism at ca. 55–53 Ma (e.g., [Ewing, 1980](#); Parrish et al., 1988). These and  
70 other changes in the upper plate of the system are the basis for our attempt at a  
71 comprehensive model of the 65 – 40 Ma tectonic evolution of the Washington Cascades and  
72 Pacific Northwest.

73 In this paper, we synthesize data on the ages and types of sedimentary basins (Evans,  
74 1984; Johnson, 1984; Eddy et al., 2016a; Donaghy et al., 2021), age, geochemistry, and spatial  
75 patterns of magmatism (e.g., Breitsprecher et al., 2003; Madsen et al., 2006; Miller et al., 2009),  
76 and deformation styles and exhumation patterns across Vancouver Island to the Washington  
77 Cascades (e.g., Johnston and Acton, 2003; Miller et al., 2016) (Figs. 2, 3). We present this 25  
78 m.y. geologic history in a series of time slices and place the discussion in the context of the  
79 greater region from northern California to southern British Columbia and inland to the Rocky  
80 Mountains (Fig. 2). Integrated within this discussion are a series of new maps that restore slip  
81 on the major Paleocene - Eocene strike-slip faults (Figs. 4-7). Boundaries between time slices  
82 coincide with transitional periods in at least one of the major processes emphasized in the  
83 synthesis (i.e. magmatism, sedimentation, metamorphism, deformation, exhumation). A critical  
84 aspect of this work is the incorporation of new high-precision U-Pb zircon age constraints tied  
85 to detailed field observations (e.g., Eddy et al., 2016a; 2017a; b; Miller et al., 2016, 2022), which  
86 enables the construction of a detailed time line not previously possible. Moreover, the varied  
87 levels of exhumation within the region allow us to study how the changing tectonic setting was

88 manifested at a wide range of Eocene crustal levels. In particular, we explore the upper-plate  
89 events in the Washington Cascades and surrounding region in relation to changing plate  
90 boundaries, especially the formation and accretion of Siletzia (Wells et al., 2014), and the  
91 shifting location of ridge – trench interaction. The study area is described in terms of western,  
92 central, and eastern regions, which roughly correspond to the forearc, arc, and backarc regions  
93 of the North Cascades segment of the Coast Mountains batholith in the Late Cretaceous (Fig. 2).  
94 We utilize these geographic terms because the dynamic tectonic changes described herein  
95 make it difficult to define regions typically associated with a stable subduction zone.

## 96 PLATE TECTONIC SETTING

97 There has long been uncertainty about the [Late Cretaceous to](#) early Cenozoic plate  
98 configuration in the northeast Pacific basin. [There is general agreement that the Kula plate](#)  
99 [originated from rifting of the Pacific plate at ~83 Ma and that the northern boundary of the](#)  
100 [Farallon plate was a ridge, which intersected the continental margin at a poorly constrained](#)  
101 [location \(, including the location of the Kula – Farallon – North America triple junction \(e.g.,](#)  
102 Atwater, 1970; [Wood and Davies, 1982;](#) Engebretson et al., 1985; [Stock and Molnar, 1988;](#)  
103 [Thorkelson and Taylor, 1989\), and Subsequent models proposed](#) the potential existence of a  
104 now-subducted Resurrection plate (e.g., Haeussler et al., 2003; Madsen et al., 2006; Fuston and  
105 Wu, 2021) (Fig. 1) [or Orcas plate \(Clennett et al., 2020\)](#). During the [interval Late Cretaceous to](#)  
106 [earliest Cenozoic](#), from ca. 85 Ma to 60 Ma, the northern Cordillera was an oblique,  
107 transpressional convergent margin (e.g., Engebretson et al., 1985; Doubrovine and Tarduno,  
108 2008), and northward translation of the Washington Cascades may have been rapid as the  
109 southern part of the Insular superterrane (the Baja BC hypothesis; e.g., Cowan et al., 1997;

110 Umhoefer and Blakey, 2006). Relative to North America, motion of the Farallon plate was to the  
 111 NE to ENE, and motion of the Kula ([and Resurrection](#) [or ?Orcas?](#)) plate was to the N to NNE, [and](#)  
 112 [thus more oblique than that of the Farallon plate](#). Both oceanic plates were moving rapidly (50  
 113 – 150 km/Myr) during this time (e.g., Engebretson et al., 1985; Doubrovine and Tarduno, 2008;  
 114 Wright et al., 2015; Fuston and Wu, 2021).

115 [Formation of the Siletzia terrane was Aa](#) major factor in the Paleogene tectonic  
 116 evolution of the Pacific Northwest [was the formation of the Siletzia terrane](#). This terrane  
 117 represents a large igneous province that developed between 56–49 Ma near an oceanic  
 118 spreading center, [and it is probably One explanation for this feature is that it represents](#) an  
 119 early manifestation of the Yellowstone hotspot (e.g., [Gao et al., 2011; McCrory and Wilson,](#)  
 120 [2013; Wells et al., 2014; Camp and Wells, 2021](#)). We [infer support previous work](#) that [infers](#) the  
 121 [triple junction between the Kula \(or Resurrection\) – Farallon – North America – Kula \(or](#)  
 122 [Resurrection or Orcas\) plates triple junction](#) lay along central Vancouver Island by 55–53 Ma  
 123 [\(e.g., Madsen et al., 2006\)](#) (Figs. 1, 4). From 52–49 Ma, a triple junction is interpreted to have  
 124 interacted with the continental margin along central to southern Vancouver Island (Fig. 1), as  
 125 this interval is marked by near-trench magmatism (Groome et al., 2003; Madsen et al., 2006),  
 126 geochemically anomalous backarc magmatism ([Ewing, 1980; Breitsprecher et al., 2003; Ickert et](#)  
 127 [al., 2009; Dostal and Jutras, 2021](#)), and disruption of non-marine basins (Eddy et al., 2016a). The  
 128 collision of Siletzia, which started by 53 Ma in SW Oregon (Wells et al., 2014) and by 51 Ma in  
 129 northern Washington and southernmost Vancouver Island, led to a major change in plate  
 130 geometries and profound changes in the upper plate of the system from 52–48 Ma, which we  
 131 describe in more detail below. The plate boundary later shifted outboard (west) of Siletzia,

**Formatted:** Font: 12 pt

132 resulting in the new Cascadia subduction system at ca. 45–40 Ma (e.g., [Wells et al., 1984, 2014](#);  
133 [Schmandt and Humphreys, 2011](#); [McCrory and Wilson, 2013](#); [Eddy et al., 2017a](#); [Kant et al.,](#)  
134 [2018](#)).

135

### 136 PRE-PALEOGENE GEOLOGIC SETTING

137 Prior to 65 Ma, the Pacific Northwest was characterized by a typical convergent margin  
138 with a forearc, continental magmatic arc, back-arc basin, and fold-and-thrust belt that  
139 deformed a Paleozoic passive margin sequence (e.g., [Burchfiel et al., 1992](#)). The arc and forearc  
140 were originally farther south relative to the inboard rocks by [at least more than](#) 300 km (e.g.,  
141 [Umhoefer and Blakey, 2006](#); [Wyld et al., 2006](#)), [and potentially a much greater distance](#) as  
142 discussed below.

143 In the forearc (western belt of Fig. 2) are Paleozoic and Mesozoic oceanic and island arc  
144 rocks and overlapping Jura-Cretaceous marine clastic rocks, which were deformed in the mid-  
145 Cretaceous Northwest Cascades thrust system ([shown as a single Cretaceous unit on](#) Fig. 3)  
146 ([Misch, 1966](#); [Brown, 1987](#); [Brandon et al., 1988](#)). Structurally above these rocks are mostly  
147 Jura-Cretaceous rocks of the western mélange belt ([Fig. 3](#)), which is interpreted as an  
148 accretionary complex ([Tabor, 1994](#)) and contains rocks at least as young as 72 Ma ([Dragovich et](#)  
149 [al., 2014](#); [Sauer et al., 2017a](#)). The Upper Cretaceous to Paleocene Nanaimo Group (e.g.,  
150 [Mustard, 1994](#)), exposed mostly on southern Vancouver Island, is interpreted as a foreland  
151 basin to the Northwest Cascades thrust system ([Brandon et al., 1988](#)), and has depositional  
152 ages extending from at least ca. 84 Ma to 63 Ma (e.g., [Matthews et al., 2017](#); [Coutts et al.,](#)  
153 [2020](#)).

154 The Cretaceous arc in northern Washington and southern British Columbia is  
155 represented by medium- to high-grade metamorphic and plutonic rocks in the crystalline core  
156 of the North Cascades and southern British Columbia (central belt of Fig. 2). The crystalline  
157 rocks are subdivided into the Wenatchee and Chelan blocks, which are separated by the high-  
158 angle Eocene Entiat fault [and bounded to the west by the Straight Creek-Fraser River fault](#) (Fig.  
159 3). Magmatism in the Wenatchee block occurred from 96–87 Ma, and most biotite Ar/Ar and  
160 K/Ar cooling ages are >60 Ma, whereas magmatism in the Chelan block ranges from 92–45 Ma  
161 and Eocene cooling ages are common (e.g., Walker and Brown, 1991; Matzel, 2004; Miller et  
162 al., 2009, 2016). The Chelan block also records Paleogene ductile deformation and partial  
163 melting in the highest-grade rocks of the Skagit Gneiss Complex (Gordon et al., 2010a).

164 [Pre-Cenozoic rocks](#) ~~directly~~ east of the North Cascades in the eastern belt ~~pre-~~  
165 [Cenozoic rocks](#) include: the Mesozoic Methow basin; ca. 160–105 Ma arc plutonic rocks of the  
166 Eagle Complex and Okanogan Range batholith; ca. 105 Ma arc volcanic rocks of the Spences  
167 Bridge Group; and arc volcanic and sedimentary rocks of the Quesnellia terrane (Fig. 3) (e.g.,  
168 Greig, 1992; Hurlow and Nelson, 1993). Farther east are plutonic and metamorphic rocks of the  
169 Omineca belt, including multiple metamorphic core complexes, the Idaho batholith, and  
170 Cordilleran passive margin sediments involved in the Rocky Mountain-Sevier fold-and-thrust  
171 belt (Fig. 2).

172

173 **RESTORATION OF STRIKE-SLIP FAULTS**

174 Dextral strike-slip faulting occurred in the northern Cordillera in the Late Cretaceous to  
175 Eocene (e.g., Gabrielse, 1985; Wyld et al., 2006), and within our study region displacements of  
176 ~325 km on strike-slip faults active from ca. 60 – 35 Ma are well documented (Table 1). In the  
177 west, the N-S-striking Straight Creek – Fraser River fault separates the North Cascades  
178 crystalline core [of the central belt](#) from the outboard Paleozoic and Mesozoic Northwest  
179 Cascades system, mélange belts, and Paleogene rocks [of the western belt](#) (Fig. 3). The most  
180 recent estimate of dextral offset on this fault is ~150 km (Monger and Brown, 2016). The  
181 Leavenworth and Entiat faults ([Fig. 3](#)) involve the Cascades core and have a total displacement  
182 of ~60 km (Eddy et al., 2017b). The Entiat fault separates the Wenatchee and Chelan blocks  
183 within the core (see above) and the NE boundary of the Cascades core is the Ross Lake fault  
184 system (Ross Lake fault, Gabriel Peak tectonic belt, Hozameen fault, and Foggy Dew fault) (Fig.  
185 3), which probably has ~115 km of dextral offset (Umhoefer and Miller, 1996).

186 These known displacements of ~325 km must be considered in tectonic restorations,  
187 particularly before 50 Ma. To summarize, after 50 Ma there is approximately 1) 150 km of  
188 offset between the western belt and Cascades core of the central belt; 2) 60 km of  
189 displacement within the core; 3) 50 km (of total 115 km) of offset between the core and the  
190 eastern belt; and 4) a cumulative offset of ~265 km between the western and eastern belts  
191 after 50 Ma (Table 1). If we assume that the strike-slip offset from 60 to 50 Ma occurred at  
192 rates comparable to those of the ~50–40 Ma interval, the implication is that another  
193 approximately 250–300 km of offset occurred across Washington from 60 to 50 Ma. About 60  
194 km of this slip has been documented on the Ross Lake fault system (Miller and Bowring, 1990)  
195 and Yalakom fault during that time (Umhoefer and Schiarizza, 1996); precise timing and offset

196 of faults are difficult to document. From this reasoning, at 55 Ma we ~~show~~ Vancouver  
 197 Island and the western belt about 450 km south of the eastern belt (Fig. 4). We note that this is  
 198 likely a conservative estimate and does not include any distributed dextral ductile displacement  
 199 or movement on minor cryptic structures. Paleomagnetic data indicate much larger cumulative  
 200 dextral displacements between ~85–55 Ma of 2000 km or more between the easternmost part  
 201 of the eastern belt and the central and western belts, and ~1000 km between the western part  
 202 of the eastern belt and rocks to the west (e.g., Enkin, 2006; Tikoff et al., 2023). From the  
 203 paleomagnetic data, major displacements of the outboard rocks ended by 55 Ma (e.g., Cowan  
 204 et al., 1997; Tikoff et al., 2023). Thus, uncertainties are much lower for the positions of units in  
 205 the region in the 55 Ma and younger reconstructions (Figs. 4–7).

**Formatted:** Not Highlight  
**Formatted:** Not Highlight  
**Formatted:** Not Highlight  
**Formatted:** Not Highlight

206 Another potential complication is the rotation in the Oregon Coast Ranges and  
 207 Cascades, which is probably related to distributed dextral strike slip and Basin and Range  
 208 extension (e.g., Beck, 1984; Wells and Heller, 1988; Colgan and Henry 2009; Wells and  
 209 McCaffrey, 2013; Wells et al., 2014). Rotation increases westward and decreases from the  
 210 Klamath Mountains northward to the Olympic Peninsula. Statistically significant vertical axis  
 211 rotation has not occurred after ca. 50 Ma in the Washington Cascades, at least as far south as  
 212 the present latitude of Seattle (e.g., Beske et al., 1973; Beck et al., 1982; Fawcett et al., 2003).  
 213 In our reconstructions, we utilize the present trends of structures in the north and restore the  
 214 Klamath Mountains to northeastern-most California to account for Basin and Range extension  
 215 (e.g., Colgan and Henry, 2009) and rotation. The resulting trend and position of Siletzia  
 216 (Washington and Oregon Coast Ranges) in our reconstructions (Figs. 4–7) after accretion is

217 more northerly than in Wells et al. (2014), which suggests that a portion of the rotation in  
218 Siletzia was taken up on more local blocks at a scale of a few tens of km or less.

219

## 220 PALEOGENE TECTONIC HISTORY

221 In this section, we synthesize the Paleogene tectonic evolution across the Pacific  
222 Northwest (Fig. 3), and divide this ~25 Myr history into five intervals. The time slices are  
223 generally considered from west to east. The major events from 60–40 Ma are summarized on  
224 Fig. 8.

### 225 65 – 60 Ma

226 During this interval the plate boundary was one of oblique convergence. This  
227 interpretation is based on the arc-type tonalitic intrusions (Miller and Bowring, 1990; Miller et  
228 al., 2009), transpressional deformation in the North Cascades and southern Coast Mountain  
229 batholith arc (e.g., Brown and Talbot, 1989; Miller and Bowring, 1990), and contractional  
230 deformation (e.g., Brown et al., 1986; Simony and Carr, 2011) in the hinterland (eastern belt).

231 The forearc (western belt) record is sparse and the timing of deformation in this belt is  
232 poorly known (Tabor, 1994; Sauer et al., 2017a). The only known forearc rocks of this age are  
233 the uppermost clastic strata of the Nanaimo Group [on Vancouver Island](#), which have maximum  
234 depositional ages (MDAs) as young as ca. 63 Ma (Coutts et al., 2020). The youngest dated  
235 (MDA) sandstone in the western mélange belt is ca. 72 Ma (Sauer et al., 2017a), and younger  
236 rocks may be present in this belt, as the upper limit for the mélange is only indicated by an  
237 angular unconformity with Eocene strata.

238 The 65 – 60 Ma interval includes the final stage of a magmatic flare-up in the North  
239 Cascades core (Chelan block) that began ca. 78 Ma (Miller et al., 2009), and was directly  
240 preceded by rapid burial and metamorphism of Cretaceous (protolith age) metasedimentary  
241 rocks that comprise the deep-crustal (up to 12 kbar) Swakane Biotite Gneiss (Valley et al., 2003)  
242 and Skagit Gneiss Complex (7 – 10 kbar; Whitney, 1992; Hanson, 2022) (Fig. 3), between ca. 79  
243 – 66 Ma and 74 – 65 Ma, respectively (Sauer et al., 2017b, 2018). Tonalitic magmatism is  
244 recorded by the 65 Ma Oval Peak pluton (Fig. 3), which crystallized at 5 – 6 kbar (Miller and  
245 Bowring, 1990), and sheets (now orthogneisses) in the Skagit Gneiss Complex (Miller et al.,  
246 2016). Leucosomes of this age also are recognized in the Complex (Gordon et al., 2010a). K-Ar  
247 and Ar/Ar biotite cooling ages are sparse, but there is no evidence for major rapid cooling or  
248 exhumation of the Cascades core during this interval (Paterson et al., 2004), and no  
249 sedimentary or volcanic rocks of this age have been recognized in the arc. Dated deformation  
250 during this time interval is limited in the arc region where dextral and reverse shear in the  
251 Gabriel Peak tectonic belt of the Ross Lake fault system (Fig. 3) was inferred to be coeval with  
252 emplacement of the Oval Peak pluton (Miller and Bowring, 1990).

253 In the eastern belt, igneous activity was sparse during this interval and volcanic rocks  
254 are absent. In NE Washington, magmatism was limited to a few ca. 64–56 Ma plutons (e.g.,  
255 Stoffel et al., 1991). North of the international border, intrusion of the quartz monzonitic to  
256 granitic, peraluminous Ladybird granite suite into high-grade Shuswap Complex (Fig. 4) initiated  
257 at 62 Ma (Carr, 1992; Hinckley and Carr, 2006). In Idaho, peraluminous magmatism in the  
258 Bitterroot lobe (Fig. 4) of the Idaho batholith began at ca. 66 Ma and peaked at ca. 60 Ma  
259 (Gaschnig et al. (2010). These peraluminous rocks are part of the “Cordilleran anatetic belt” of

260 Chapman et al. (2021a), and the magmatism is ascribed to partial melting of crustal rocks  
261 (Mueller et al., 1996; Hinckley and Carr, 2006; Gaschnig et al., 2011).

262 Sedimentary rocks of this age are also very rare in NE Washington. Aside from a <30 km<sup>2</sup>  
263 body of Paleocene conglomerate (Pipestone Canyon Formation) directly west of the Pasayten  
264 fault (Fig. 3) (Kriens et al., 1995), no other strata have been recognized between central  
265 Washington and the Sevier foreland basins. The scarcity of sedimentary rocks, and the evidence  
266 of crustal melting, are compatible with the existence of a high-standing orogenic plateau in the  
267 hinterland during this interval (Whitney et al., 2004; Bao et al., 2014). Thrusting also occurred  
268 in the eastern belt in the Shuswap Complex and in the Rocky Mountain - Sevier fold and thrust  
269 belt (e.g., Price, 1981).

270 **60 – 52 Ma**

271 This interval is marked by major changes in magmatism and sedimentation throughout  
272 the region. Near-trench intrusions strongly suggest that an oceanic spreading center lay off  
273 central to southern Vancouver Island by 52 - 51 Ma (Fig. 5) (Groome et al., 2003; Madsen et al  
274 2006). Magmatism and sedimentation occurred in the western belt near the spreading ridge,  
275 but igneous activity was nearly absent in the Cascades core and eastern belt, until the onset of  
276 Challis-Kamloops magmatism at ca. 53 Ma (e.g., Ickert et al., 2009). The formation of  
277 metamorphic core complexes and associated basins in the eastern region also started at ca. 56  
278 Ma (e.g., Brown et al., 2012).

279 Basaltic magmatism began in the Siletzia terrane by ca. 55 Ma in the south (southwest  
280 Oregon) and by 53.2 Ma outboard of the Northwest Cascades system and mélange belts in  
281 western Washington and Vancouver Island in the north, where it continued until at least 48 Ma

282 (Crescent and Metchosin basalts) (Fig. 2) (Wells et al., 2014; Eddy et al., 2017a). Siletzia consists  
283 of thick sequences of basalt that transition from deep-water lava flows of normal mid-oceanic-  
284 ridge basalt (N-MORB) to shallow water and subaerial flows of enriched mid-oceanic-ridge  
285 basalt (E-MORB) and oceanic-island basalt (OIB) (e.g., Wells et al., 2014). Siletzia is comparable  
286 in volume to other large igneous provinces (Trehu et al., 1994; Wells et al., 2014) and this,  
287 combined with isotopic evidence, supports its formation over a 'plume-like' mantle source,  
288 thought to be the Yellowstone hot spot (e.g., Pyle et al., 2015; Phillips et al., 2017; Stern and  
289 Dumitru, 2019; Camp and Wells, 2021). In southern Oregon, the submarine basalts were  
290 overlain by deep-water sediments (Umpqua Group) in this time interval (Wells et al., 2014),  
291 while in Washington sedimentation was initiated in the non-marine Chuckanut and Swauk  
292 Formations of the greater Swauk basin (Fig. 3) (Eddy et al., 2016a). This basin developed on  
293 accreted Paleozoic and Mesozoic rocks of the Northwest Cascades thrust system and the  
294 southern end of the Cascades core. A 56.8 Ma tuff from the lower part of the Chuckanut  
295 Formation and a 59.9 Ma maximum depositional age (MDA) near the base of the Swauk  
296 Formation are compatible with sedimentation in the greater Swauk basin starting at 60 – 57 Ma  
297 (Eddy et al., 2016a). The 56.8 Ma tuff, a 53.7 Ma tuff higher in the Chuckanut section  
298 (Breedlovestrout et al., 2013), and a 53.7 Ma tuff with arc affinities (Summit Creek section; Kant  
299 et al., 2018) in the southern Washington Cascades are the only record of volcanism inboard of  
300 Siletzia in the western belt. There is also no well-documented deformation between 60 Ma and  
301 52 Ma, although a local angular unconformity in the middle to lower part of the Swauk  
302 Formation may be a link to the early collision of Siletzia (Doran, 2009).

303 In the North Cascades core a magmatic lull began at ca. 60 Ma (Miller et al., 2009), and  
304 that lull extended into the southern Coast Mountains to the northwest (Cecil et al., 2018). The  
305 transpressional Gabriel Peak belt (Fig. 3) of the Ross Lake fault system continued to be active  
306 between at least 60 – 55(?) Ma, and was cut by the transtensional Foggy Dew fault zone of the  
307 Ross Lake system at ca. 55–53 Ma (Miller and Bowring, 1990). Ductile deformation probably  
308 occurred in domains in the Skagit Gneiss Complex, but otherwise, deformation is not well  
309 documented.

310 In northeastern Washington, magmatism is represented only by scattered, small-volume  
311 intrusions until ~53 Ma, while small mafic bodies began intruding the Idaho batholith region at  
312 ca. 58 Ma (Foster and Fanning, 1997; Gaschnig et al., 2010). Peraluminous magmatism  
313 (Ladybird granite suite), metamorphism, and migmatization continued during the 60–52 Ma  
314 time interval in the Shuswap and Okanagan complexes (e.g., Crowley et al., 2001; Kruckenberg  
315 et al., 2008; Gervais et al., 2010; Brown et al., 2012), and peraluminous magmatism persisted in  
316 the Bitterroot lobe of the Idaho batholith until ca. 53 Ma (Gaschnig et al., 2010) and the  
317 Anaconda core complex of Montana until ca. 56 Ma (e.g., Howlett et al., 2021). This magmatism  
318 in Idaho was directly followed by the Challis magmatic event (ca. 53 – 43 Ma; e.g., Janecke and  
319 Snee, 1993; Ickert et al., 2009; Gaschnig et al., 2010), which extended from Oregon to South  
320 Dakota and Washington and into central British Columbia as the Kamloops belt (Figs. 5, 6) (e.g.,  
321 Ewing, 1980; Breitsprecher et al., 2003). Shallow plutons, dikes, and volcanic rocks characterize  
322 this magmatic event with geochemical affinities ranging from arc to within-plate, and some  
323 rocks being almost entirely crustal melts and others only weakly contaminated melts of the  
324 lithospheric mantle (Ewing, 1980; Thorkelson and Taylor, 1989; Lewis and Kiilsgaard, 1991;

325 Morris et al., 2000; Breitsprecher et al., 2003; Ickert et al., 2009; Dostal and Jutras, 2021). The  
326 alkalinity of magmas increases markedly south of ca. 51.5° N and the width of the belt widens  
327 south of the international border (e.g., Breitsprecher et al., 2003).

328 In the eastern belt, ductile deformation and thrusting continued in the hinterland of the  
329 Rocky Mountain fold and thrust belt for the early part of this interval (e.g., Simony and Carr,  
330 2011). A major transition from contraction to extension, which was time transgressive (e.g.,  
331 Parrish et al., 1988; Harlan et al., 1988; Brown et al., 2012), led to the formation of  
332 metamorphic core complexes and associated extensional basins in NE Washington, British  
333 Columbia, Idaho, and Montana (Fig. 4). Core complexes (e.g., Priest River, Okanogan) and  
334 associated basins initiated earlier north of the WNW-striking Lewis and Clark fault zone than to  
335 the south (Anaconda, Bitterroot) (Foster et al., 2007). Sedimentary basin formation initiated  
336 from ca. 56 Ma next to the Okanogan core complex directly east of the North Cascades to ca. 53  
337 Ma adjacent to the Bitterroot and Anaconda core complexes (e.g., Foster et al., 2007; Howlett  
338 et al., 2021), and in NE Washington continued to 48 Ma (Pearson and Obradovich, 1977;  
339 Suydam and Gaylord, 1997). The absence of sedimentary deposits between the Swauk basin in  
340 the west and the foreland basin east of the thrust belt until extension began and basins formed  
341 suggests that the hinterland region continued to be a high orogenic plateau until ca. 55 Ma  
342 (Whitney et al., 2004; Bao et al., 2014).

343 We postulate that the near complete termination of arc-type magmatism in the North  
344 Cascades core and southern Coast Mountains, and paucity of magmatism east of there, records  
345 a change to low-angle subduction of the Farallon plate at ca. 60 Ma. The peraluminous

346 magmatism in the east probably resulted mainly from concentrated crustal thickening (e.g.,  
347 Gaschnig et al., 2010).

348 In the eastern belt, the shift to shallow, widespread, and diverse magmatism at ca. 53  
349 Ma accompanied by extension points to a major change from the earlier peraluminous  
350 magmatism. This shift marks the onset of Challis activity and is discussed in more detail in the  
351 next section.

### 352 **52 – 49.5 Ma**

353 A fundamental change in plate boundary stresses occurred between 52 Ma and 49.5  
354 Ma, as Siletzia encountered the subduction zone in southern Oregon. Collision progressed  
355 northward during this time interval from Oregon to Washington and southern Vancouver Island  
356 (Wells et al., 2014). This collision was coincident with major changes in magmatism,  
357 sedimentation, and the strain field in the upper plate. The Siletzia collision also ultimately led to  
358 a westward shift in the location of the plate boundary (e.g., Schmandt and Humphreys, 2011).

359 The Siletzia collision was accompanied from central Vancouver Island to northwest  
360 Washington by near-trench magmatism from ca. 51 – 49 Ma (Madsen et al., 2006), which is  
361 thought to record the location of a subducting spreading ridge and the Kula-Farallon-North  
362 America or Resurrection-Farallon-North America triple junction (Fig. 5) (e.g., Cowan, 2003;  
363 Groome et al., 2003; Haeussler et al., 2003; Madsen et al., 2006) that would have been the  
364 northern boundary of Siletzia (Wells et al., 2014). This inference is also consistent with the 51  
365 Ma age of the ophiolitic Metchosin Complex on southern Vancouver Island (Massey, 1986, Eddy  
366 et al., 2017a). Near-trench magmatic rocks on Vancouver Island include: 51.2 – 50.5 Ma

367 bimodal, but dominantly dacitic rocks (Flores volcanics) (Irving and Brandon, 1990); 51.2–48.8  
368 Ma, hypabyssal tonalite, trondhjemite, and granodiorite (Clayquot intrusions) (Madsen et al.,  
369 2006); and in the south peraluminous 50.9 – 50.7 Ma intrusions (Walker Creek intrusions)  
370 (Groome et al., 2003). The Leech River Schist on southern Vancouver Island also records high  
371 T/low P metamorphism at ~51 Ma (Fairchild and Cowan, 1982; Groome et al., 2003). In NW  
372 Washington, local peraluminous magmatism occurred as the ca. 49 Ma Mt. Pilchuck stock (Fig.  
373 3) and nearby Bald Mountain pluton (Yeats and Engels, 1971).

374 Farther inland, but still west of the Cascades core, basaltic to rhyolitic volcanism began  
375 with the eruption of 51.4 Ma lavas and tuffs (Silver Pass member) of the upper Swauk  
376 Formation (Peterson and Tepper, 2021) and 51.3 Ma dacitic to rhyolitic lavas and pyroclastic  
377 rocks (Taneum Formation) which overlie clastic rocks correlative with the Swauk Formation (Fig.  
378 3) (Tabor et al., 1984; Eddy et al., 2016a; Wallenbrock and Tepper, 2017). These units represent  
379 the initiation of a magmatic belt that roughly parallels the leading edge of subducted Siletzia in  
380 the subsurface (Fig. 2) (Wells et al., 2014), and is attributed to tearing of the Farallon slab (Kant  
381 et al., 2018).

382 The approach and collision of Siletzia is also recorded in folding and changes in  
383 paleotopography in the western belt. Sedimentation in the Swauk basin persisted until at least  
384 ca. 50.8 Ma, the youngest MDA from stratigraphically high in the basin (Eddy et al., 2016a;  
385 Senes, 2019), but a drainage reversal from SW- to NE-flowing streams occurred at ca. 51 Ma  
386 (Eddy et al., 2016a) and may record the initial stages of collision of Siletzia at the latitude of the  
387 Swauk basin. A NW-vergent fold-and-thrust belt developed in SW Oregon in response to  
388 collision and involved Siletzia basalts, overlying Umpqua Group, and Klamath basement

389 terranes. Unconformably overlying marine strata (Tyee Formation) demonstrate that accretion  
390 was completed between 50.5 Ma and 49 Ma at that latitude (Wells et al., 2000, 2014). In the  
391 central Washington Cascades, the Swauk Formation is folded and locally faulted under a short-  
392 lived (<1.5 Myr) angular unconformity with the overlying Teanaway Formation (Foster, 1958).  
393 The Teanaway Formation includes a 49.3 Ma rhyolite near its base (Eddy et al., 2016a) and is  
394 dominated by subaerial basalts, in contrast to the marine strata in SW Oregon. Contractional  
395 structures also attributed to the accretion of Siletzia are folds in the Chuckanut Formation in  
396 the northwestern Swauk basin (Misch, 1966; Johnson, 1984), some of the upright folds in the  
397 Skagit Gneiss Complex of the North Cascades core (Miller et al., 2016), and the Cowichan fold-  
398 and-thrust belt on Vancouver Island, which is approximately the same age and has a similar  
399 northwesterly trend as the Chuckanut folds (Fig. 5) (Johnston and Acton, 2003).

400 The magmatic lull continued in the North Cascades core (Miller et al., 2009), although  
401 minor partial melting persisted in the Skagit Gneiss Complex (Gordon et al., 2010a). The deep-  
402 crustal (9-12 kbar) Swakane Gneiss in the crystalline core was probably rapidly exhumed during  
403 this interval, in part during distributed ductile shear and top-to-N to –NNE motion on the  
404 Dinkelman decollement (Fig. 3) (Paterson et al., 2004). Dextral-normal slip and associated  
405 mylonitization continued in the Foggy Dew fault zone, a southern strand of the Ross Lake fault  
406 system, and dextral displacement also occurred on the NW-striking Yalakom fault and other  
407 faults west of the Straight Creek-Fraser River fault (Fig. 5) (Miller and Bowring, 1990; Umhoefer  
408 and Schriazza, 1996).

409 East of the Cascades core, magmatism increased with the emplacement of granitoid  
410 plutons, and dominantly metaluminous tonalites and granodiorites. Although arc-like in

411 mineralogy, many of these plutons have trace element traits compatible with slab-breakoff  
412 magmas (e.g., Sr/Y>10, La/YbN>10; Whalen and Hildebrand, 2019) and Sr-Nd isotopic  
413 compositions indicative of significant contributions from older crust (Tepper and Eddy, 2017).  
414 The earliest U-Pb date associated with this renewed activity is 52 Ma in central Idaho, and  
415 subsequent plutonism appears to have migrated to the SW across NE Washington (Fig. 6C)  
416 (Tepper, 2016). Metamorphism and deformation continued in the metamorphic core  
417 complexes in southern British Columbia, NE Washington, Idaho, and Montana, as did Challis-  
418 Kamloops magmatism and sedimentation in extensional basins where MDAs of locally derived  
419 sediments cluster around 50 Ma in southern British Columbia and northeastern Washington  
420 (e.g., Ewing, 1980; Suydan and Gaylord, 1997; Foster et al., 2007; Brown et al., 2012; Rubino et  
421 al., 2021). In contrast to NE Washington, no pattern of magmatism migration is seen across the  
422 Challis to Absaroka area in Idaho and Wyoming (e.g., Feeley and Cosca, 2003). The thermal  
423 peak in the Shuswap metamorphism was at ca. 53–49 Ma (Crowley et al., 2001).

424 Deformation in the eastern belt was dominated by roughly east-west extension,  
425 although contraction may have continued at deep levels in the Shuswap metamorphic core  
426 complex until ca. 52–49 Ma (Crowley et al., 2001; Gervais et al., 2010; Gervais and Brown,  
427 2011). The peak of extension and exhumation in the Okanogan core complex occurred at 53 –  
428 50 Ma (Brown et al., 2012). Brittle slip of uncertain sense reactivated the high-angle,  $\geq 250$ -km-  
429 long Pasayten fault (Fig. 3) along the eastern boundary of the Methow basin, and ended in  
430 Washington before eruption of ca. 48 Ma volcanic rocks, which overlap the fault (White, 1986).

431 In summary, the transition from a low-angle, transpressional subduction regime to a  
432 dextral transtensional regime was largely complete by the end of this time interval. The

433 collision of Siletzia explains the deformation in the Swauk basin and along strike to the NW, and  
434 the southwestward migration of magmatism in NE Washington is consistent with rollback of the  
435 northern Farallon slab (Figs. 5, 6C). The slab ruptured west of the Cascades core and is marked  
436 in part by a belt of magmatism that started at the end of this time period and lasted until ca. 48  
437 Ma (Kant et al., 2018) (Fig. 6). Previous explanations for this Challis – Kamloops magmatism  
438 include a decrease in the rate of plate convergence (Constenius, 1996), passage of a slab  
439 window ([Thorkelson and Taylor, 1989](#); Breitsprecher, et al., 2003; Ickert et al., 2009), buckling  
440 and “sideways” slab rollback (Humphreys, 1995, 2009), and rollback and breakoff of the  
441 Farallon slab (Tepper, 2016). Slab rollback and breakoff, [and slab window evolution](#) are the  
442 most widely cited scenarios (see review by Humphreys and Grunder, 2022), [and we favor this](#)  
443 [interpretation as discussed below](#).

444 **49.5 – 45 Ma**

445 The short-lived deformation episode resulting from the collision of Siletzia was followed  
446 by profound changes in the tectonic evolution of the Pacific Northwest. A new subduction zone  
447 of the Kula or Resurrection plate beneath North America was established along the west side of  
448 Siletzia during this time interval (Fig. 6) (e.g., Schmandt and Humphreys, 2011). A dextral  
449 transtensional regime dominated, and a new non-marine strike-slip basin formed next to the  
450 Cascades core (Fig. 6). A magmatic flare-up occurred in the Cascades core and in the adjacent  
451 parts of the western belt, and magmatism and extension continued in the eastern belt, but  
452 were more arially restricted after ca. 48 Ma.

453 In the west, the effects of the collision of Siletzia were waning by this time as  
454 magmatism ended in the southern part of Siletzia at ca. 50-49 Ma (Wells et al., 2014), and in  
455 northern Siletzia at ca. 48 Ma (Eddy et al., 2017a). The collision was followed in the Olympic  
456 Mountains (northern Siletzia) by deposition of turbidites (Blue Mountain unit) that have  
457 maximum depositional ages ranging from 47.8 to 44.7 Ma (Eddy et al., 2017a).

458 To the east of Siletzia, magmatism attributed to slab rollback, tear, and breakoff  
459 continued until ca. 45 Ma, producing compositionally diverse volcanic and plutonic rocks that in  
460 part formed parallel to the edge of Siletzia in the subsurface and are commonly near the  
461 Straight Creek fault and its splays (Fig. 6) (Trehu et al., 1994; Kant et al., 2018). Distinctive traits  
462 of these rocks include their bimodal nature, with OIB affinities of the mafic lavas and crustal  
463 signatures of the silicic rocks. On the west side of the Straight Creek fault are basalt and lesser  
464 rhyolite flows interbedded with nonmarine sedimentary rocks in the Naches and Barlow Pass  
465 units (Fig. 3). East of the Straight Creek fault, the prolific Teanaway dike swarm intruded the  
466 deformed rocks of the Swauk basin (Fig. 3) (Tabor et al., 1984; Miller et al., 2022), and is  
467 interpreted to be related to the dominantly basaltic, ca. 49.3 Ma Teanaway Formation. The  
468 mafic rocks are medium-K tholeiitic basalts and basaltic andesites (Clayton, 1973; Peters and  
469 Tepper, 2006; Roepke et al., 2013), which are derived from mantle that is inferred to have been  
470 metasomatized during earlier subduction (Tepper et al., 2008). The NNE (035°) average  
471 orientation of the dikes provides the most robust evidence for initiation of right-lateral strike-  
472 slip on the Straight Creek fault at ~49 Ma (e.g., Miller, et al., 2022).

473 Starting at 49.2 Ma, the Chumstick basin formed between the right-stepping  
474 Leavenworth and Entiat strike-slip faults, directly west of the Chelan block (Evans, 1994; Eddy et

475 al., 2016a) (Fig. 3). Abundant stratigraphic, paleocurrent, and detrital geochronologic data  
476 suggest that the basin formed during strike-slip faulting (Eddy et al., 2016a; Donaghy et al.,  
477 2021). The main western subbasin formed from 49.2 to ~46.5 Ma, and fault reorganization at  
478 ~46.5 - 44 Ma started inversion of the western subbasin and the formation of a narrow eastern  
479 subbasin next to the Entiat fault (Fig. 3). After this reorganization, strike-slip faulting localized  
480 on the Entiat and Straight Creek faults. The youngest (<45.9 Ma) sediments of the Chumstick  
481 Formation top the Leavenworth fault and probably correlate with the arkosic Roslyn Formation,  
482 which overlies the Teanaway Formation (Evans, 1994; Eddy et al., 2016a) (Fig. 3).

483 The magmatic lull in the Cascades core ended at ~49.4 Ma, close in time to the eruption  
484 of Teanaway volcanic rocks south of the Cascades core. The ensuing short-lived (until ca. 45  
485 Ma) flare-up has the highest magmatic addition rate and the shortest duration of the three  
486 flare-up events in the North Cascades since the mid-Cretaceous. It began with the ca. 49.6 Ma  
487 Lost Peak stock, followed by two large (ca. 300 km<sup>2</sup> each) plutons, the Cooper Mountain and  
488 Golden Horn batholiths, which intruded at 49.3-47.9 Ma and 48.5-47.7 Ma (Eddy et al., 2016b;  
489 Miller et al., 2016), respectively, across the Ross Lake fault zone and into both the Cascades  
490 core and the Methow basin (Fig. 3). These plutons and coeval variably deformed 49.4–47.2 Ma  
491 intrusions (now orthogneisses) in the Skagit Gneiss Complex are commonly granodioritic in  
492 contrast to the mainly Cretaceous tonalitic intrusions of the two older flare-ups (e.g., Misch,  
493 1966; Haugerud et al., 1991; Miller et al., 2009). The ca. 49–48 Ma intrusions also range from  
494 gabbro to granite, and include alkaline granites. Between ~47.9–46.5 Ma, magmatism in the  
495 core migrated westward from the Ross Lake fault zone. The ~46.5 Ma Duncan Hill pluton and  
496 45.5 Ma Railroad Creek pluton (Fig. 3) were the last of the large intrusions in the North

497 Cascades (Miller et al., 2021), and on the basis of their age and location, they appear to be the  
498 youngest sizable elements related to slab rollback (Fig. 6C). The youngest magmatic rocks are  
499 ca. 44.9 Ma lineated granite sheets (Misch, 1968; Haugerud et al., 1991; Wintzer, 2012; Miller  
500 et al., 2016).  $\epsilon_{\text{Nd}}$  values for some of the 49.3–45 Ma intrusive rocks are the least radiogenic  
501 values for North Cascades intrusions, and imply a greater crustal component than in earlier  
502 flare-ups (Matzel et al., 2008).

503 Extensive dike intrusion into a  $\geq 600 \text{ km}^2$  region of the Cascades core and adjacent rocks  
504 to the east and south began at ca. 49.3 with the Teanaway dikes and at least one other dike  
505 swarm, and continued until ca. 45 Ma (Miller et al., 2022). The largest number of dikes intruded  
506 between ca. 49.3–47 Ma. Many of these rhyolitic to basaltic dikes overlap spatially with the 49–  
507 46.5 Ma granodioritic plutons of the core. Some of the dikes have trace element signatures of  
508 arc magmas and some are adakites; they are interpreted to be the product of melting of  
509 eclogitic lower crust in response to intrusion of mantle-derived basalts (Davidson et al., 2015).

510 Metamorphism during this time interval is restricted to domains in the Skagit Gneiss  
511 Complex of the Cascades core where metamorphic monazite growth continued at least locally  
512 until 46 Ma (Gordon et al., 2010a). NW-striking foliation and subhorizontal lineation formed in  
513 the Complex from ca. 49.5–45 Ma (Haugerud et al., 1991; Wintzer, 2012; Miller et al., 2016),  
514 and foliation was deformed into upright gentle to open, generally SE- or NW-plunging folds of  
515 foliation between ca. 49 Ma to 47 Ma (Miller et al., 2016). Motion of the Ross Lake fault zone  
516 ended at ca. 49 Ma, but the Entiat fault was active until at least 46.9 Ma and ended by 44.4 Ma,  
517 and the N-S-trending Straight Creek fault experienced dextral slip from ca. 49 Ma and was  
518 sealed by 35 Ma (Misch, 1966; Tabor et al., 1984; Miller and Bowring, 1990). Excision and top-

519 to-the north motion continued on the Dinkelman decollement at least until ca. 49–47 Ma  
520 (Matzel, 2004; Paterson et al., 2004). The Eocene dikes also provide information on the strain  
521 field. Their average orientation is  $\sim 035^\circ$ , and the resultant extension direction ( $305^\circ$ – $125^\circ$ ) is  
522 oblique to the strike ( $\sim 320^\circ$ ) of the North Cascades orogen and to the stretching lineation  
523 (average trend of  $330^\circ$ – $150^\circ$ ) in the Skagit Gneiss Complex (Miller et al., 2022). Overall, these  
524 structures are compatible with the regional dextral transtensional tectonic regime.

525 The 49.5–45 Ma interval was marked by rapid cooling and exhumation of parts of the  
526 Cascades core. The 8–12 kbar Swakane Gneiss was in part exhumed by the Dinkelman  
527 decollement and was at the surface in the Chumstick basin by 48.5 Ma (Tabor et al., 1987; Eddy  
528 et al., 2016a). Most of the  $^{40}\text{Ar}/^{39}\text{Ar}$  and K-Ar hornblende, biotite, and muscovite cooling ages in  
529 the 7–10 kbar Skagit Gneiss Complex are ca. 50–44 Ma (Engels et al., 1976; Wernicke and Getty,  
530 1997; Tabor et al., 2003; Gordon et al., 2010b), and thermochronology indicates very rapid  
531 cooling in some areas, with rates of perhaps  $100^\circ\text{C}/\text{m.y.}$  at ca. 47–45 Ma (Wernicke and Getty,  
532 1997).

533 In the eastern belt, magmatism, sedimentation, and extension all continued during the  
534 early part of this interval, but and magmatism and extension were largely waning by the end.  
535 Igneous activity was still migrating southwestward across NE Washington (Fig. 6C). In British  
536 Columbia, the  $>200 \text{ km}^2$ , granodioritic Needle Peak pluton intruded the Methow basin at ca. 48  
537 Ma (Monger, 1989), but and Challis-Kamloops magmatism to the east had largely ended by ca.  
538 47 Ma (Ickert et al., 2009; Dostal and Jutras, 2021).

539 Extension and sedimentation related to the metamorphic core complexes in NE  
540 Washington and British Columbia were on the wane during this interval. Termination of

541 sedimentation at ~48 in NE Washington was roughly coeval with the end of volcanism (Suydam  
542 and Gaylord, 1997). Mylonitization in the Okanogan Complex ended at ca. 49 Ma with cooling  
543 through 47 Ma (Kruckenberg et al., 2008). The Priest River Complex was rapidly exhumed from  
544 ca. 50–48 Ma (Doughty and Price, 2000; Stevens et al., 2016), but extension and exhumation  
545 continued through this interval in Idaho and Montana in the Bitterroot and Anaconda core  
546 complexes (Foster et al., 2007, 2010; Howlet et al., 2021). The Lewis and Clark fault zone  
547 continued to act as a boundary between the older core complexes to the north and the  
548 younger complexes to the south.

549 **45 - 40 Ma**

550 This interval marks the end of slab foundering and the establishment of a new north-  
551 south subduction zone and arc that became Cascadia. Subduction was occurring beneath much,  
552 if not all, of Oregon and Washington by the end of this period (Fig. 7). Sedimentation occurred  
553 in the western belt, but ended in the Chumstick basin, as did Challis-Kamloops magmatism in  
554 the eastern belt.

555 Arc magmatism began at ca. 45 Ma in southwest Washington where local basaltic  
556 andesites and andesites erupted (du Bray and John, 2011) and by 40 Ma in southwest Oregon  
557 (e.g., Darin et al., 2022). In northwestern Washington, similar volcanic rocks occur in a belt that  
558 lies west of the younger part of the Cascades arc and also includes 45 – 35 Ma granodioritic  
559 intrusions, and abundant 45–40 Ma tuffs occur in the Puget Group (Fig. 3) (Vine, 1969; Tabor et  
560 al., 1993, 2000; Dragovich et al., 2009, 2011, 2013, 2016; MacDonald et al., 2013). Within this  
561 belt the oldest rocks appear to be at the northern end, but there is a lack of precise dates for

562 units in the south. Local dacite and rhyolite domes (Wenatchee domes) intruded the Chumstick  
563 basin to the east at ca. 44.5 Ma (Gilmour, 2012; Eddy et al., 2017b) and may be the youngest  
564 intrusive rocks related to slab rollback and/or breakoff (White et al., 2021). In SW Washington  
565 and Oregon, the Tillamook magmatic episode occurred from 42 to 34 Ma (Parker et al., 2010;  
566 Chan et al., 2012; Wells et al., 2014). This episode included volcanic rocks (Tillamook Volcanics,  
567 Yachats basalt, and Grays River Volcanics) in NW Oregon and SW Washington, which are  
568 interpreted by some workers to be related to the Yellowstone hotspot, and were synchronous  
569 with margin-parallel extension (e.g., Wells et al., 2014; Camp and Wells, 2021).

570 Sedimentation in the western belt includes both deep and shallow marine deposits on  
571 the Olympic Peninsula (Einarsen, 1987; Babcock et al., 1994). Inboard, in the Puget Sound  
572 region, the deltaic to shallow marine middle(?) to late Eocene Puget Group (Fig. 3; Vine, 1969;  
573 Buckovic, 1979; Johnson and O'Connor, 1994) was deposited on Siletzia on the west and the  
574 older rocks of the western North Cascades on the east. The Puget Sound basin likely formed in  
575 the forearc to the early Cascadia arc.

576 Sedimentation ended in the Chumstick basin, but continued in the overlying, ca. 44–42  
577 Ma arkosic Deadhorse Canyon unit and the Roslyn Formation (Evans, 1994; Eddy et al., 2016a).  
578 (Fig. 3). The latter, which rests on the Teanaway Formation south of the Cascades core, may be  
579 the easternmost part of the regional depositional system that included the Puget Group.

580 Magmatism ceased in the Cascades core at ca. 44.9 Ma and ductile deformation in the  
581 Skagit Gneiss Complex had also ended at ca. 45 Ma (Miller et al., 2016). Dextral strike slip ended  
582 between 46.9 Ma and 44.5 Ma on the Entiat fault (Evans, 1994; Eddy et al., 2016a) and

583 continued to a later time on the Straight Creek fault, which is intruded by a 34 Ma pluton (e.g.,  
584 Tabor et al., 2003).

585 East of the Cascades core, Challis magmatism terminated at ca. 43 Ma (Gaschnig et al.,  
586 2010). Extension and cooling of the Bitterroot and Anaconda core complexes continued until ca.  
587 39 Ma, as did sedimentation (Foster et al., 2010; Howlett et al., 2021). Motion on the Lewis and  
588 Clark fault zone presumably ended as well.

589

## 590 **DISCUSSION**

591 We emphasized in the introduction that the Pacific Northwest in the Paleogene is an  
592 excellent place to examine a variety of processes resulting from ridge-trench interaction and  
593 oceanic plateau collision. In the following, we explore the upper-plate response shortly before,  
594 during, and after the Farallon- Kula or Farallon-Resurrection ridge encountered the trench  
595 bordering North America near Vancouver Island, and the consequences of the collision of  
596 Siletzia.

### 597 **Relation of the 60 – 50 Ma Magmatic Lull to Slab Dynamics**

598 It is likely that the end of long-lived arc magmatism in the Cascades core at ca. 60 Ma  
599 and the overall low volume of magmatism from ca. 60–50 Ma eastward to the Idaho batholith  
600 resulted from flat-slab subduction. Moreover, magmatism in the Idaho batholith during this  
601 interval probably resulted from crustal thickening and not subduction-related processes  
602 (Gaschnig et al., 2010). [The shallowing of the slab may be attributable to the subduction of](#)

603 young buoyant lithosphere The shallowing of the slab may be attributable to the rapid  
604 subduction of young buoyant lithosphere, as also proposed by others for the greater region  
605 (e.g., Thorkelson and Taylor, 1989; Haeussler et al., 2003). ~~generated at a ridge close to the~~  
606 ~~trench, and by the approach of overthickened oceanic crust of Siletzia~~. Strong suction in the  
607 mantle wedge ~~due to approach of the slab with its decreasing dip toward the craton~~ may have  
608 played a role, as proposed for the Laramide belt ~~to the south~~ (Humphreys, 2009; O'Driscoll et  
609 al., 2009). Note that the Laramide belt in northern Wyoming was directly east of Siletzia at 55  
610 Ma in our reconstruction (Fig. 4). Another explanation for the postulated flat-slab subduction is  
611 that the Farallon subduction zone was old and wide (Schellart, 2020), which is viable if the flat  
612 slab before an approximately 60 Ma plate reorganization was a smaller part of the northern  
613 Farallon plate subducting beneath western North America since at least the earliest Cretaceous  
614 (Engebretson et al., 1985).

615 The northern boundary of the flat slab is inferred to be northeast of central Vancouver  
616 Island (Fig. 4) where there is a transition in pluton ages within the Coast Mountains batholith.  
617 The southern Coast Mountains have a 60 – 50 Ma magmatic lull much like the Cascades core of  
618 this study, whereas to the north, a high magma addition event attributed to arc magmatism  
619 occurred from 61–48 Ma (Cecil et al., 2018). A projection of the triple junction off central  
620 Vancouver Island through the boundary in the Coast Mountains to the NE may run to the  
621 northern edge of the Shuswap Complex at this time, which potentially explains the location of  
622 the belt of major extension along the eastern edge of the flat slab from British Columbia to  
623 southern Idaho and western Montana. Alternatively, the flat slab may underlie have underlain  
624 the region of the magmatic lull, but just south of most of the Shuswap to Okanagan extensional

625 belt (Fig. 4), in which case the latter would be kinematically tied to the Tintina fault – Rocky  
626 Mountain trench (Price and Carmichael, 1986) and magmatism would occur in a slab window  
627 (e.g., Breitsprecher et al., 2003). Seismic tomography and reconstructions of plate motions in  
628 the NE Pacific also suggest a major boundary inboard from Vancouver Island (Fuston and Wu,  
629 2021). Plate motion models suggest indicate rapid northward rates of either the Kula or  
630 Resurrection plates from ca. 65–50 Ma that were highly oblique to the North American plate  
631 boundary (Engebretson et al. 1985; Matthews et al., 2016), and this may have produced a large  
632 slab window under western Canada (Fuston and Wu, 2021; cf. Madsen et al., 2006) north of the  
633 proposed flat slab.

634 The magmatic lull and flat slab extended to the south of the crystalline core of the North  
635 Cascades, which on the basis of known strike-slip faults (Wyld et al., 2006; this study) was at the  
636 latitude of current central Oregon to the Oregon – Washington border at ca. 60–50 Ma. Post-50  
637 Ma volcanic and sedimentary strata obscure relations to the south and east of the Wenatchee  
638 block; in our reconstruction at 55 Ma (Fig. 4), and projecting faulting back to 60 Ma, the North  
639 Cascades would have lain near the NW edge of the Klamath – Blue Mountains terranes and the  
640 flat slab beneath the Pacific Northwest would be continuous with the well-established Laramide  
641 flat slab to the south (see Tikoff et al.,[2023] for an alternative hypothesis).

642

643 **Consequences of Collision of Siletzia**

644 The inferred position of the intersection of the Farallon – Resurrection/Kula ridge with  
645 the trench is complicated by the eruption of Siletzia basalts and the construction of an oceanic

646 plateau above a hot spot mantle plume (e.g., Wells et al., 2014). In the region of the  
647 Washington Cascades, major changes occurred in the upper plate of the system due to collision  
648 of this oceanic plateau.

649 Notable aspects of Siletzia collision are the short duration of the associated  
650 deformation, its profound inboard influence, and the subsequent change in plate boundary  
651 stresses along the newly established North America margin. The most important structural  
652 response was the brief shortening that migrated from southwest Oregon to central Washington  
653 and Vancouver Island during the 51 – 49 Ma interval (Fig. 5) (Wells et al., 2014). In the Swauk  
654 basin, folding and formation of an angular unconformity is tightly bracketed between ~50.8 Ma  
655 and 49.3 Ma (Eddy et al., 2016a). The reversal of drainage in the Swauk basin at ~51 Ma is  
656 probably one of the first signs of Siletzia collision at that latitude (Eddy et al., 2016a). Younger  
657 upright folding continued until ca. 48 Ma at deeper crustal-levels in the Skagit Gneiss Complex  
658 of the Chelan block of the Cascades core ~175 km inboard of Siletzia (Miller et al., 2016).  
659 Folding only bracketed between ca. 65 Ma and 48 Ma (Kriens et al., 1995) in the Methow basin  
660 farther to the northeast may have been induced by collision. In contrast, in the eastern belt,  
661 ≥235 km inboard of Siletzia, extension in most of the core complexes continued unabated.  
662 Peak metamorphism of the voluminous Shuswap Complex and several other core complexes at  
663 ~53–49 Ma was roughly coincident with the proposed flat slab and Siletzia collision. One  
664 explanation for the widespread eastern extension and timing of magmatism and  
665 metamorphism may be the rollback of the flat slab, which we propose was underway in  
666 Washington by ca. 52 Ma (Figs. 5, 6C).

667 In the western belt, sedimentation continued in the early stages of collision after the  
668 drainage reversal in the Swauk basin at 51 Ma, but presumably ended during folding and  
669 certainly before the Swauk-Teanaway unconformity and eruption of Teanaway volcanic rocks at  
670 49.3 Ma. Note that the youngest Swauk Formation strata are in lake and fluvial facies in the far  
671 eastern end of the Swauk basin near the Leavenworth fault (Tabor et al., 1982; Senes, 2019),  
672 and their position may be related to an eastward migration of late basin subsidence related to  
673 the collision. In the eastern belt, sedimentation continued in the supra-detachment extensional  
674 basins and grabens until ca. 48 Ma, just after this slab is inferred to have rolled back to the SW.

675 The [approach-and](#)-collision of Siletzia with the continental margin influenced  
676 magmatism much farther eastward than it influenced deformation and sedimentation. We  
677 attribute this to the shut off of northeastward flat subduction caused by the collision-related  
678 plate reorganization (e.g., Schmandt and Humphreys, 2011). Magmatism migrated to the  
679 southwest across NE Washington and reached the Golden Horn batholith at the northeast  
680 margin of the Cascades core at ca. 48.3 Ma (Figs. 3, 6C). This migration has been interpreted to  
681 result from slab rollback (Tepper, 2016) and breakoff, as the Farallon plate detached and  
682 formed the subvertical “slab curtain” currently imaged seismically beneath Idaho and eastern  
683 Washington (Schmandt and Humphreys, 2011).

684

685 **What Drove the 49.3 Ma to 45.5 Ma Magmatic Flare-up?**

686 Plutons in the North Cascades crystalline core and dike swarms across the study area  
687 record a major magmatic flare-up at 49.3–45.5 Ma (Miller et al., 2009), shortly after Siletzia

688 collision. This flare-up is concentrated in the Chelan block of the core, but also includes plutons  
689 that intruded the Methow basin directly east and northward of the core for ca. 70 km into  
690 Canada (e.g., Needle Peak pluton), volcanic rocks on the west and south sides of the core, and  
691 voluminous dike swarms (Figs. 3, 6) (e.g., Tabor et al., 1984; Eddy et al., 2016b; Miller et al.,  
692 2016, 2022). The Eocene flare-up is marked by the highest magmatic addition rate and shortest  
693 duration of any of the magmatic events in the North Cascades.

694 The factors that control initiation and termination of magmatic 'flare-ups', such as the  
695 Eocene event, are controversial (e.g., Chapman et al., 2021b). Isotopic data from intrusions  
696 emplaced during flare-ups in some arcs imply increased crustal melting and have led to the  
697 orogenic cycle hypothesis in which flare-ups are driven by melting of fertile backarc crustal  
698 material thrust into the deep levels of an arc or underlying mantle (e.g., Ducea and Barton,  
699 2007; DeCelles et al., 2009). Others have argued that voluminous melting results dominantly  
700 from processes external to the arc, including slab break-off and ridge subduction, and largely  
701 involves mantle-derived melts (e.g., Decker et al., 2017; Schwartz et al., 2017; Ardila et al.,  
702 2019), which in turn can drive an increase of partial melting of the crust.

703 The Eocene Cascades core plutons have been considered the latest pulse of arc  
704 magmatism in the North Cascades by earlier workers (e.g., Matzel et al., 2008; Miller et al.,  
705 2009), and magmatism to the east in the Challis-Kamloops belt has been interpreted to occur  
706 within a slab window (e.g., Thorkelson and Taylor, 1989; Breitsprecher et al., 2003). but in our  
707 view, the flare-up is related to the Farallon slab rollback and breakoff. At ~49.5 Ma, the  
708 southwest-migrating rollback magmatism had reached the northeast margin of the Cascades  
709 core (Tepper, 2016) and the edge of a large slab window may have lain nearby to the north (Fig.

710 6). The accretion of Siletzia and termination of subduction led the slab to break off, as shown in  
711 part by the belt of bimodal volcanic rocks lacking an arc signature near the Straight Creek fault  
712 (Figs. 3, 6, 9) (Kant et al., 2018). The Eocene age Cascades core plutons have a wider isotopic  
713 range than earlier plutons (Matzel et al., 2008), but their geochemistry does not permit  
714 distinguishing between an arc or slab break-off origin as the crustal component of melt during  
715 break-off would be mafic lower crust of the Late Cretaceous arc. Dextral strike-slip, slab  
716 rollback, and breakoff were concentrated in and near the Cascades core, and we infer that the  
717 slab was ripped apart leading to upwelling of asthenospheric mantle and decompression  
718 melting (Fig. 9).

719 A speculative additional interpretation is that the breakoff-related magmatism  
720 continued to the southeast beneath the Columbia River Basalt Group in the Pasco basin to the  
721 Clarno Formation of NE Oregon (Figs. 2, 6). The Pasco basin is on strike with the Eocene  
722 Chumstick basin and seismic velocities suggest that beneath the Miocene basalt is a thick,  
723 asymmetric sedimentary basin of probable Eocene age and an associated mafic underplate  
724 (Catchings and Mooney, 1988; Gao et al., 2011). These mafic rocks may be similar to the  
725 Teanaway Basalt of the flare-up. A speculative additional interpretation is that the breakoff-  
726 related magmatism continued to the southeast to the Clarno Formation of NE Oregon (Figs. 2,  
727 6). The Clarno Formation is not well dated, but available ages suggest that the volcanic rocks  
728 erupted starting at ca. 53–50 Ma (Bestland et al., 2002). Note that in our reconstruction for 48  
729 Ma the Clarno area is about 100 km SE of the North Cascades flare-up and the western breakoff  
730 belt west of the Straight Creek fault would have been about 40–50 km closer to the Clarno at 50  
731 Ma. If the Siletzia terrane lay on a small microplate within the shrinking northern Farallon plate

732 as we show (Fig. 6), then the southeast edge of the slab that rolled back and broke off may have  
733 been near the Clarno volcanics (cf. Humphreys, 2009).

734

735 **Upper Plate Deformation After Siletzia Collision**

736 The ca. 49–45 Ma structural record west of the Fraser River-Straight Creek fault is  
737 largely restricted to high-angle NW-striking faults and associated local folds, whereas in the  
738 central and eastern belts a wide array of structures can be used to evaluate deformation.  
739 Eocene dikes, dextral strike-slip faults, basins, and ductile structures in the Cascades are broadly  
740 coeval with dikes, faults bounding non-marine basins, and ductile fabrics in metamorphic core  
741 complexes in NE Washington and southern British Columbia (Fig. 6) (e.g., Ewing, 1980; Parrish  
742 et al., 1988; Eddy et al., 2016a; Miller et al., 2016). Dikes in the eastern belt are not well dated,  
743 but most K-Ar dates from volcanic rocks in NE Washington range between 51–48 Ma (Pearson  
744 and Obradovich, 1977), and thus overlap temporally with the older (49.3–47.5 Ma) dikes in the  
745 Cascades and the magmatic flare-up. Dikes intruding the Kettle metamorphic core complex,  
746 ~140 km east of the North Cascades, strike ~012°–022° (McCarley Holder et al., 1990; their Fig  
747 1). These dikes are subparallel to the normal faults that separate the Kettle and Okanogan core  
748 complexes from Eocene grabens (Keller, Republic, and Toroda), which strike 008–020°. Farther  
749 east, ENE-WSW (~075°–255°) brittle slip occurred on the Newport fault, which is the upper  
750 boundary of the Priest River Complex (Harms and Price, 1992), and east and south of the Lewis  
751 and Clark fault zone, slip on the Bitterroot and Anaconda detachments is top-to-the-east-  
752 southeast (~100–110°) (Kalakay et al., 2003; Foster et al., 2007). Brittle extension directions  
753 from the dikes and faults bounding the grabens suggest that they are oblique (ca. 15°–50°

754 counter clockwise) to those of the voluminous N–NE-striking (average of 035°), ~49.3–47.5 Ma  
755 dikes in the Cascades.

756 A major difference between faults in the eastern belt and those in the western and  
757 central belts is that the eastern faults are apparently purely dip slip, whereas faults (Ross Lake,  
758 Entiat, Leavenworth, Straight Creek) in the central and western belts are dextral strike slip, and  
759 most have a subordinate component of normal slip. Dextral slip does occur to the east on the  
760 Lewis and Clark fault zone (Figs. 2, 6), but this structure strikes ~E-W and transfers slip between  
761 the Anaconda, Bitterroot, and Priest River core complexes (e.g., Foster, et al., 2007). The  
762 combination of dextral strike-slip faults and dike swarms of the Cascades core region is most  
763 compatible with a N-S dextral shear and related WNW – ESE extension.

764 Eocene ductile stretching in mylonites in core complexes ranges from ~105–285° in the  
765 Bitterroot and Anaconda complexes in Montana (Foster et al. 2007), to 074-254° in the Priest  
766 River Complex (Harms and Price, 1992; Doughty and Price, 1999) near the Washington – Idaho  
767 border, to E-W in the Kettle Complex (Rhodes and Cheney (1981), to W-NW – E-SE (~295-115°)  
768 in the Okanogan Complex (Kruckenberg, 2008; Brown et al., 2012) ~ 40 km east of the Cascades  
769 core. Broadly coeval, subhorizontal Eocene ductile stretching in the North Cascades is ~330 -  
770 150° in the Skagit Gneiss Complex to close to N-S in the Swakane Gneiss. Thus, ductile extension  
771 directions rotate progressively clockwise by ~75° from east to west. The sense of rotation is the  
772 same, but the magnitude of rotation is greater, then that of the upper-crustal structures.

773 Rotation of extension directions fits with the progressively greater influence of dextral  
774 shear closer to the plate margin in response to the plate reorganization at ~49.5 Ma after  
775 Siletzia collision. Extension and transtension led to orogenic collapse in the core complexes

776 (e.g., Price and Carmichael, 1986; Parrish et al., 1988; Vanderhaege and Teyssier, 2001),  
777 whereas strike slip occurred to the west on the faults bounding and cutting the North Cascades  
778 core.

779

780 **Eocene Global Plate Reorganization**

781 The dramatic tectonic transitions in the Pacific Northwest region at ca. 52–49 Ma  
782 coincide with a fundamental plate reorganization in the Pacific Basin and a global change in  
783 plate vectors at ~53–47 Ma (e.g., Whittaker et al., 2007; O'Connor et al., 2013; Seton et al.,  
784 2015). This plate reorganization in the Pacific may have been driven by subduction of the  
785 Izanagi-Pacific ridge at ca. 60–46 Ma (Wu and Wu, 2019), with the ensuing initiation of  
786 subduction in the Tonga-Kermadec and Izu-Bonin-Mariana system occurring at ca. 53–50 Ma  
787 (Sharp and Clague, 2006; Whittaker et al., 2007a; Tarduno et al., 2009). The ~50 Ma bend in the  
788 Hawaiian–Emperor seamount chain also coincides with a change in Pacific plate motion and  
789 Australian-Antarctic plate reorganization at that time (Sharp and Clague, 2006; Whittaker et al.,  
790 2007). It has been suggested that Pacific – Kula plate spreading also changed at ca. 53.3 Ma to  
791 43.8 Ma (Lonsdale, 1988), and that Kula – North America relative motion became more  
792 northerly and faster at 57 Ma (Doubrovine and Tarduno, 2008). Other major global events  
793 roughly coeval with the fundamental changes in the Pacific Northwest region include initiation  
794 of the Aleutian arc and the dramatic slowing of Greater India at ca. 50 Ma resulting from  
795 collision with Asia (e.g., Copley et al., 2010; van Hinsbergen et al., 2011).

796 It appears that the significant changes in the tectonics of the Pacific Northwest at 52 –  
797 49 Ma are the consequence of both a global plate reorganization and the regional collision of  
798 the ridge-centered Siletzia oceanic plateau. The global plate changes resulted in faster and  
799 perhaps more northerly relative plate motion in the Pacific Northwest, which in turn resulted in  
800 the formation of the new N-S- striking strike-slip Straight Creek – Fraser River fault. However,  
801 most of the complex changes summarized here are the result of the profound changes due to  
802 the Siletzia collision and westward stepping of the subduction zone, and triple-junction  
803 migration during the 60 – 40 Ma interval.

804

#### 805 **ACKNOWLEDGEMENTS**

806 This research was supported by National Science Foundation grants EAR-1119358 and  
807 EAR-1945352 to R.B. Miller, EAR-1945260 to M.P. Eddy, EAR-1119252 to J.H. Tepper, EAR-  
808 1119063 to P.J. Umhoefer, and EAR-1118883 to S. Bowring. Our late colleague and friend Paul  
809 Umhoefer was a driving force for much of this synthesis and particularly the fault  
810 reconstructions. The late Sam Bowring also played an important role in the research presented  
811 here. M.S. and B.S thesis students at Northern Arizona University, San Jose State University, and  
812 the University of Puget Sound contributed to our research project and include Katie Bryant, Erin  
813 Donaghy, Melissa Gunderson, Lisa Kant, Jen Pence, and Francesca Senes. We thank Stacia  
814 Gordon, Margi Rusmore, and Noah McLean for helpful discussions. We thank Gene Humphreys  
815 and Derek Thorkelson for their thorough and very helpful reviews of the manuscript.

816

817 **References Cited**

818 Ardila, A.M.M., Paterson, S.R., Memeti, V, Parada, M.A., and Molina, P.G., 2019, Mantle driven  
819 Cretaceous flare-ups in Cordilleran arcs: *Lithos*, v. 326-327, p. 19-27.

820 Atwater, T., 1970, Implications of plate tectonics for the Cenozoic tectonic evolution of western  
821 North America: *Geological Society of America Bulletin*, v. 81, p. 3513–3536.

822 Babcock, R.S., Suczek, C.A., and Engebretson, D.C., 1994, The Crescent “Terrane,” Olympic  
823 Peninsula and Southern Vancouver Island: *Washington Division of Geology and Earth*  
824 *Resources Bulletin* 80, p. 141–157.

825 Bao, X., Eaton, D.W., and Guest, B., 2014, Plateau uplift in western Canada caused by  
826 lithospheric delamination along a craton edge: *Nature Geoscience*, v. 7, p. 830–833.

827 Beck, M.E., 1984, Has the Washington-Oregon coast range moved northward?: *Geology*, v. 12,  
828 p. 737–740.

829 Beck, M.E., Burmester, R.F., and Schoonover, R., 1982, Tertiary paleomagnetism of the North  
830 Cascade Range, Washington: *Geophysical Research Letters*, v. 9, p. 515-518.

831 Beske, S.J., Beck, M.E., and Noson, L., 1973, Paleomagnetism of the Miocene Grotto and  
832 Snoqualmie batholiths, central Cascades, Washington: *Journal of Geophysical Research*, v.  
833 78, p. 2601-2608.

834 Bestland, E.A., Hammond, P.E., Blackwell, D.L.S., Kays, M.A., Retallack, G.J., and Stimac, J., 2002,  
835 Geologic framework of the Clarno unit, John Day Fossil Beds National Monument,  
836 central Oregon: *Oregon Department of Geology and Mineral Industries, Open-file*  
837 Report, 0-02-03, 39 p.

838 [Bradley, D.C., Kusky, T.M., Haeussler, P.J., Goldfarb, R.J., Miller, M.L., Dumoulin, J.A., Nelson,](#)  
839 [S.W., and Karl, S.M., 2003, Geologic signature of early Tertiary ridge subduction in](#)  
840 [Alaska, \*in\* Sisson, V.B., Roeske, S.M., and Pavlis, T.L., eds., Geology of a Transpressional](#)  
841 [Orogen Developed During Ridge-trench InteractionAlong the North Pacific Margin:](#)  
842 [Geological Society of America Special Paper 371, p. 19–49, <https://doi.org/10.1130/0-8137-2371-X.19>.](#)

**Formatted:** Font: Italic

843 Brandon, M.T., Cowan, D.S., and Vance, J.A., 1988, The Late Cretaceous San Juan thrust system,  
844 San Juan Islands, Washington: Geological Society of America Special Paper, v. 221, 81 p.

845 Breedlovestrout, R.L., Evaerts, B.J., and Parrish, J.T., 2013, New Paleogene paleoclimate analysis  
846 of western Washington using physiognomic characteristics from fossil leaves:  
847 Palaeogeography, Palaeoclimatology, Palaeoecology, v. 392, p. 22–40, doi: 10.1016/j.  
848 .palaeo.2013.08.013 .

849 Breitsprecher, K., Thorkelson, D.J., Groome, W.G., and Dostal, J., 2003, Geochemical  
850 confirmation of the Kula-Farallon slab window beneath the Pacific Northwest in Eocene  
851 time: Geology, v. 31, p. 351-354.

852 Brown, E.H., 1987, Structural geology and accretionary history of the Northwest Cascades  
853 system, Washington and British Columbia: Geological Society of America Bulletin, v. 99, p.  
854 201–214.

855 Brown, E.H., and Talbot, J.L., 1989, Orogen-parallel extension in the North Cascades crystalline  
856 core, Washington: Tectonics, v. 8, p. 1105–1114, doi: 10.1029/TC008i006p01105 .

858 Brown, R.L., Journeay, J.M., Lane, L.S., Murphy, D.C., and Rees, C.J., 1986, Obduction,  
859 backfolding and piggyback thrusting in the metamorphic hinterland of the southeastern  
860 Canadian Cordillera: *Journal of Structural Geology*, v. 8, p. 255-268.

861 Brown, S.R., Gibson, H.D., Andrews, G.D.M., Thorkelson, D.J., Marshall, D.M., Vervoort, J.D., and  
862 Rayner, N., 2012, New constraints on Eocene extension within the Canadian Cordillera  
863 and identification of Phanerozoic protoliths for footwall gneisses of the Okanagan Valley  
864 shear zone: *Lithosphere*, v. 4, p. 353-377.

865 Buckovic, W.A., 1979, The Eocene deltaic system of west-central Washington, *in* Armentrout, J.,  
866 Cole, M.R., and Terbest, H., eds., *Cenozoic Paleogeography of the Western United States:*  
867 *Society of Economic Paleontologists and Mineralogists Pacific Section, Pacific Coast*  
868 *Paleogeography Symposium 3*, p. 147–163.

869 Burchfiel, B.C., Cowan, D.S., and Davis, G.A., 1992, Tectonic overview of the Cordilleran orogen  
870 in the western United States, *in* Burchfiel, B.C., Lipman, P.W., and Zoback, M., eds., *The*  
871 *Cordilleran Orogen: Coterminous U.S. in the Western United States: Boulder, Colorado,*  
872 *Geological Society of America, The Geology of North America*, v. G-3, p. 407-479.

873 Camp, V.E., and Wells, R.E., 2021, The case for a long-lived and robust Yellowstone hot spot:  
874 *GSA Today*, v. 31, <https://doi.org/10.1130/GSATG477A.1>.

875 Carr, S.D., 1992, Tectonic setting and U-Pb geochronology of the Early Tertiary Ladybird  
876 Leucogranite Suite, Thor-Odin - Pinnacles Area, Southern Omineca Belt, British Columbia:  
877 *Tectonics*, v. 11, p. 258-278.

878 [Catchings, R.D., and Mooney, W.D., 1988, Crustal structure of the Columbia Plateau: Evidence](#)

879 [for continental rifting: Journal of Geophysical Research, v. 93, p. 459-474.](#)

880 Cecil, M.R., Rusmore, M.E., Gehrels, G.E., Woodsworth, G.J., Stowell, H.H., Yokelson, I.N.,

881 Chisom, C., Trautman, M., and Homan, E., 2018, Along-strike variation in the magmatic

882 tempo of the Coast Mountains batholith, British Columbia, and implications for processes

883 controlling episodicity in arcs: *Geochemistry, Geophysics, Geosystems*, v. 19, p. 4274–

884 4289. <https://doi.org/10.1029/2018GC007874> 2018.

885 Chan, C.F., Tepper, J.H., and Nelson, B.K., 2012, Petrology of the Grays River volcanics,

886 southwest Washington: Plume-influenced slab window magmatism in the Cascadia

887 forearc: *Geological Society of America Bulletin*, v. 124, p. 1324-1338.

888 Chapman, J.B., 2021a, Runyon, S.E., Shields, J.E., Lawler, B.L., Pridmore, C.J., Scoggin, S.H.,

889 Swaim, N.T., Trzinski, A.E., Wiley, H.N., Barth, A.P., and Haxel, G.B., 2021a, The North

890 American Cordilleran anatetic belt: *Earth Science Reviews*, v. 215,

891 <https://doi.org/10.1016/j.earscirev.2021.103576>.

892 Chapman, J.B., Shields, J.E., Ducea, M.N., Paterson, S.R., Attia, S., and Ardill, K.E., 2021b, The

893 causes of continental arc flare ups and drivers of episodic magmatic activity in Cordilleran

894 orogenic systems: *Lithos*, v. 398-399, doi.org/10.1016/j.lithos.2021.106307.

895 Clayton, D.N., 1973, Volcanic history of the Teanaway Basalt, east-central Cascade Mountains,

896 Washington [M.S. thesis]: Seattle, Washington, University of Washington, 55 p.

897 [Clennett, E.J., Sigloch, K., Mihalynuk, M.G., Seton, M., Henderson, M.A., Hosseini, K.,](#)

898 [Mohammadzaheri, A., Johnston, S.T., Müller, R.D., 2020, A quantitative tomotectonic](#)

← → Formatted: Line spacing: Double

899 [plate reconstruction of western North America and the eastern Pacific Basin:](#)  
900 [Geochemistry, Geophysics, Geosystems, e2020GC009117,](#)  
901 [https://doi.org/10.1029/2020GC009117.](https://doi.org/10.1029/2020GC009117)

902 Colgan, J.P., and Henry, C.D., 2009, Rapid middle Miocene collapse of the Mesozoic orogenic  
903 plateau in north-central Nevada: International Geology Review, v. 51, p. 920-961.

904 Constenious, K.N., 1996, Late Paleogene extensional collapse of the Cordilleran foreland fold  
905 and thrust belt: Geological Society of America Bulletin, v. 108, p. 20-39.

906 Copley, A., Avouac, J.P., and Royer, J-Y., 2010, The India-Asia collision and the Cenozoic  
907 slowdown of the Indian plate; implications for the forces: Journal of Geophysical  
908 Research, v.115, B03410, doi:10.1029/2009JB006634.

909 Coutts, D.S., Matthews, W.A., Englert, R.G., Brooks, M.D., Boivin, M-P, and Hubbard, S.M., 2020,  
910 Along-strike variations in sediment provenance within the Nanaimo basin reveal  
911 mechanisms of forearc basin sediment influx events: Lithosphere, v. 12, p. 180-197.

912 Cowan, D.S., 2003, Revisiting the Baranof–Leech River hypothesis for early Tertiary coastwise  
913 transport of the Chugach–Prince William terrane: Earth and Planetary Science Letters, v.  
914 213, p. 463-475.

915 Cowan, D.S., Brandon, M.T., and Garver, J.I., 1997, Geologic tests for hypotheses for large  
916 coastwise displacements – A critique illustrated by the Baja British Columbia  
917 controversy: American Journal of Science, v. 279, p. 117-173.

918 Crowley, J.L., Brown, R.L., and Parrish, R.R., 2001, Diachronous deformation and a strain  
919 gradient beneath the Selkirk allochthon, northern Monashee complex, southeastern  
920 Canadian Cordillera: *Journal of Structural Geology*, v. 23, p. 1103-1121.

921 Darin, M., Armentrout, J.M., and Dorsey, R.J., 2022, Oligocene onset of uplift and inversion of  
922 the Cascadia forearc basin, southern Oregon Coast Range, USA: *Geology*, v. 50, p. 603–  
923 609.

924 Davidson, P., Tepper, J.H., and Nelson, B.K., 2015, Petrology of Eocene dikes near Lake Chelan,  
925 WA; evidence of mantle and crustal melting during the Challis event: *American  
926 Geophysical Union Fall Meeting*, Abstract V23B-B312.

927 DeCelles, P.G., Ducea, M.N., Kapp, P., and Zandt, G., 2009, Cyclicity in Cordilleran orogenic  
928 systems: *Nature Geoscience*, v. 2, p. 251–257.

929 Decker, M., Schwartz, J.J., Stowell, H.H., Klepeis, K.A., Tulloch, A.J., Kitajima, K., Valley, J.W., and  
930 Kylander-Clark, A.R.C., 2017, Slab-triggered arc flare-up in the Cretaceous Median  
931 Batholith and the growth of lower arc crust, Fiordland, New Zealand: *Journal of  
932 Petrology*, v. 58, p. 1145–1172.

933 Donaghay, E.E., Umhoefer, P.J., Eddy, M.P., Miller, R.B., and LaCasse, T., 2021, Stratigraphy,  
934 age, and provenance of the Eocene Chumstick Basin, Washington Cascades; implications  
935 for paleogeography and regional tectonics: *Geological Society of America Bulletin*, v.  
936 133, p. 2418-2438. <https://doi.org/10.1130/B35738.1>.

937 Doran, B.A., 2009, Structure of the Swauk Formation and Teanaway dike swarm, Washington

938 Cascades [M.S. thesis]: San Jose, California, San Jose State University, 97 p.

939 Dostal, J.D., and Jutras, P., 2021, Tectonic and petrogenetic settings of the Eocene Challis-

940 Kamloops volcanic belt of western Canada and the northwestern United States:

941 International Geology Review; doi.org/10.1080/00206814.2021.1992800.

942 Doubrovine, P.V., and Tarduno, J.A., 2008, A revised kinematic model for the relative motion

943 between Pacific oceanic plates and North America since the Late Cretaceous: Journal of

944 Geophysical Research, v. 113, B12101, doi.org/10.1029/2008JB005585.

945 Doughty, P.T., and Price, R.A., 1999, Tectonic evolution of the Priest River complex, northern

946 Idaho and Washington- A reappraisal of the Newport fault with new insights on

947 metamorphic core complex formation: Tectonics, v. 18, p. 375-393.

948 Doughty, P.T., and Price, R.A., 2000, Geology of the Purcell Trench rift valley and Sandpoint

949 Conglomerate: Eocene en echelon normal faulting and synrift sedimentation along the

950 eastern flank of the Priest River metamorphic complex, northern Idaho: Geological Society

951 of America Bulletin, v. 112, p. 1356-1374.

952 Dragovich, J.D., Littke, H.A., Anderson, M.L., Hartog, R., Wessel, G.R., DuFrane, S.A. Walsh, J.,

953 MacDonald, J.H., Jr., Mangano, J.F., and Cakir, R., 2009, Geologic map of the Snoqualmie

954 7.5-minute quadrangle, King County, Washington: Washington Division of Geology and

955 Earth Resources Geologic Map GM-75, 2 sheets, scale 1:24,000.

956 Dragovich, J.D., Anderson, M.L., Mahan, S.A., Koger, C.J., Saltonstall, J.H., MacDonald, J H., Jr.,

957 Wessel, G.R., Stoker, B.A., Bethel, J.P., Labadie, J.E., Cakir, R., Bowman, J.D., and DuFrane,

958 S.A., 2011, Geologic map of the Monroe 7.5-minute quadrangle, King and Snohomish

959 Counties, Washington: Washington Division of Geology and Earth Resources Open File

960 Report 2011-1, 1 sheet, scale 1:24,000, with 24 p. text.

961 [[http://www.dnr.wa.gov/publications/ger\\_ofr2011-1\\_geol\\_map\\_mon-roe\\_24k.zip](http://www.dnr.wa.gov/publications/ger_ofr2011-1_geol_map_mon-roe_24k.zip)]

962 Dragovich, J.D., Mahan, S.A., Anderson, M.L., MacDonald, J.H., Jr., Cakir, R., Stoker, B.A., Koger,

963 C.J., Bethel, J.P., DuFrane, S.A., Smith, D.T., and Villeneuve, N.M., 2013, Geologic map of

964 the Sultan 7.5-minute quadrangle, King and Snohomish Counties, Washington:

965 Washington Division of Geology and Earth Resources Map Series 2013-01, 1 sheet, scale

966 1:24,000, 52 p. text.

967 [http://www.dnr.wa.gov/publications/ger\\_ms201301\\_geol\\_map\\_sultan\\_24k.zip](http://www.dnr.wa.gov/publications/ger_ms201301_geol_map_sultan_24k.zip).

968 Dragovich, J.D., Frattali, C.L., Anderson, M.L., Mahan, S.A., MacDonald, J.H., Jr., Stoker, B.A.,

969 Smith, D.T., Koger, C.J., Cakir, R., Dufrane, S.A., and Sauer, K.B., 2014, Geologic map of the

970 Lake Chaplain 7.5-minute quadrangle, Snohomish County, Washington: Washington

971 Division of Geology and Earth Resources Map Series 2014-01, 1 sheet, scale 1:24,000, 51

972 p. text.

973 Dragovich, J.D., Mavor, S.P., Anderson, M.L., Mahan, S.A., MacDonald, J.H., Jr., Tepper, J.H.,

974 Smith, D.T., Stoker, B.A., Koger, C.J., Cakir, R., DuFrane, S.A., Scott, S.P., and Justman,

975 B.P., 2016, Geologic map of the Granite Falls 7.5-minute quadrangle, Snohomish County,

976 Washington: Washington Division of Geology and Earth Resources Map Series 2016-01,

977 1 sheet, scale 1:24,000, 63 p. text.

978 du Bray, E.A., and John, D.A., 2011, Petrologic, tectonic, and metallogenic evolution of the  
979 Ancestral Cascades magmatic arc, Washington, Oregon, and northern California:  
980 *Geosphere*, v. 7, p. 1102-1133.

981 Ducea, M.N., and Barton, M.D., 2007, Igniting flare-up events in Cordilleran arcs: *Geology*, v. 35,  
982 p. 1047-1050.

983 Eddy, M.P., Bowring, S.A., Umhoefer, P.J., Miller, R.B., McLean, N.M., and Donaghy, E.E., 2016a,  
984 High-resolution temporal and stratigraphic record of microplate accretion and ridge-  
985 trench interaction preserved in non-marine sedimentary basins in central and western  
986 Washington: *Geological Society of America Bulletin*, v. 128, p. 425-441.

987 Eddy, M.P., Bowring, S.A., Miller, R.B., and Tepper, J.H., 2016b, Rapid assembly and  
988 crystallization of a fossil large-volume silicic magma chamber: *Geology*, v. 44, p. 341-344.

989 Eddy, M.P., Clark, K.P., and Polenz, M., 2017a, Age and volcanic stratigraphy of the Eocene  
990 Siletzia oceanic plateau in Washington and on Vancouver Island: *Lithosphere*, v. 9, p. 652-  
991 664.

992 Eddy, M.P., Umhoefer, P.J., Miller, R.B., Donaghy, E.E., Gundersen, M., and Senes, F.I., 2017b,  
993 Sedimentary, volcanic, and structural processes during triple-junction migration: Insights  
994 from the Paleogene record in central Washington, *in* Haugerud, R.A., and Kelsey, H.M.,  
995 eds., From the Puget Lowland to East of the Cascade Range: Geologic Excursions in the  
996 Pacific Northwest: *Geological Society of America Field Guide* 49, p. 143-173,  
997 doi:10.1130/2017.0049(07).

998 Einarsen, J.M., 1987, The petrography and tectonic significance of the Blue Mountain unit,  
999 Olympic Peninsula, Washington (M.S. thesis): Bellingham, Washington, Western  
1000 Washington University, 175 p.

1001 Engebretson, D.C., Cox, A., and Gordon, R.G., 1985, Relative motions between oceanic and  
1002 continental plates in the Pacific basin: Geological Society of America Special Paper 206,  
1003 59 p.

1004 Engels, J.C., Tabor, R.W., Miller, F.K., and Obradovich, J.D., 1976, Summary of K-Ar, Rb-Sr, U-Pb,  
1005 and fission track ages of rocks from Washington State prior to 1975 (exclusive of Columbia  
1006 Plateau Basalts): U.S. Geological Survey Miscellaneous Field Studies Map MF-710.

1007 [Enkin, R.J., 2006, Paleomagnetism and the case for Baja British Columbia, in Haggart, J.W., Enkin](#)  
1008 [R.J., and Monger, J.W.H., eds., Paleogeography of the North American Cordillera: Evidence](#)  
1009 [For and Against Large-Scale Displacements: Geological Association of Canada Special](#)  
1010 [Paper 46, p. 233–254.](#)

1011 Evans, J.E., 1994, Depositional history of the Eocene Chumstick Formation: Implications of  
1012 tectonic partitioning for the history of the Leavenworth and Entiat-Eagle Creek fault  
1013 systems, Washington: Tectonics, v. 13, p. 1425-1444.

1014 Ewing, T., 1980, Paleogene tectonic evolution of the Pacific Northwest: Journal of Geology, v.  
1015 88, p. 619-638.

Formatted: Font: Italic

1016 Fawcett, T.C., Burmester, R.F., Housen, B.A., and Iriondo, A., 2003, Tectonic implications of  
1017 magnetic fabrics and remanence in the Cooper Mountain pluton, North Cascade  
1018 Mountains, Washington: Canadian Journal of Earth Sciences, v. 40, p. 1335-1356.

1019 Fairchild, L.H., and Cowan, D.S., 1982, Structure, petrology, and tectonic history of the Leech  
1020 River complex northwest of Victoria, Vancouver Island: Canadian Journal of Earth  
1021 Sciences, v. 19, p. 1817-1835.

1022 Feeley, T.C., and Cosca, M.A., 2003, Time vs. composition trends of magmatism at Sunlight  
1023 volcano, Absaroka volcanic province, Wyoming: Geological Society of America Bulletin, v.  
1024 115, p. 714-728.

1025 Foster, D.A., and Fanning, C.M., 1997, Geochronology of the northern Idaho batholith and the  
1026 Bitterroot metamorphic core complex: Magmatism preceding and contemporaneous with  
1027 extension: Geological Society of America Bulletin, v. 109, p. 379-394.

1028 Foster, D.A., Doughty, P.T., and Kalakay, T.J., 2007, Kinematics and timing of exhumation of  
1029 metamorphic core complexes along the Lewis and Clark fault zone, northern Rocky  
1030 Mountains, USA, in Sisson, V.B., Roeske, S.M., and Palvis, T.L., eds., Geology of a  
1031 Transpressional Orogen Developed During Ridge-trench Interaction along the North  
1032 Pacific Margin: Geological Society of America Special Paper 371, p. 205-229.

1033 Foster, D.A., Grice, W.C., Jr., and Kalakay, T.J., 2010, Extension of the Anaconda metamorphic  
1034 core complex:  $40\text{Ar}/39\text{Ar}$  thermochronology and implications for Eocene tectonics of  
1035 the northern Rocky Mountains and the Boulder batholith: Lithosphere, v. 2, p. 232-246.

1036 Foster, R.J., 1958, The Teanaway dike swarm of Central Washington: American Journal of  
1037 Science, v. 256, p. 644-653.

1038 Fuston, S., and Wu, J., 2021, Raising the Resurrection plate from an unfolded-slab plate tectonic  
1039 reconstruction of northwestern North America since early Cenozoic time: Geological  
1040 Society of America Bulletin, v. 133, p. 1128-1140.

1041 Gabrielse, H., 1985, Major dextral transcurrent displacements along the Northern Rocky  
1042 Mountain Trench and related lineaments in north-central British Columbia: Geological  
1043 Society of America Bulletin, v. 96, p. 1-14.

1044 [Gao, H., Humphreys, E.D., Yao, H., and van der Hilst, R.D., 2011, Crust and lithosphere structure](#)  
1045 [of the northwestern U.S. with ambient noise tomography: Terrane accretion and Cascade](#)  
1046 [arc development: Earth and Planetary Science Letters, v. 304, p. 202-211.](#)

1047 Gaschnig, R.M., Vervoort, J.D., Lewis, R.S., and McClelland, W.C., 2010, Migrating magmatism in  
1048 the northern US Cordillera: in situ U-Pb geochronology of the Idaho batholith:  
1049 Contributions to Mineralogy and Petrology, v. 159, p. 863-883.

1050 Gaschnig, R.M., Vervoort, J.D., Lewis, R.S., and Tikoff, B., 2011, Isotopic evolution of the Idaho  
1051 batholith and Challis Intrusive Province, northern US Cordillera: Journal of Petrology, v.  
1052 52, p. 2397-2429.

1053 Gehrels, G., Rusmore, M., Woodsworth, G., Crawford, M., Andronicos, C., Hollister, L., Patchett,  
1054 J., Ducea, M., Butler, R., Klepeis, K., Davidson, C., Friedman, R., Haggart, J., Mahoney, B.,  
1055 Crawford, W., Pearson, D., and Girardi, J., 2009, U-Th-Pb geochronology of the Coast

1056 Mountains batholith in north-coastal British Columbia: Constraints on age and tectonic  
1057 evolution: Geological Society of America Bulletin, v. 121, p. 1341-1361, doi:  
1058 10.1130/B26404.1.

1059 Gervais, F., and Brown, R.L., 2011, Testing modes of exhumation in collisional orogens:  
1060 Synconvergent channel flow in the southeastern Canadian Cordillera: *Lithosphere*, v. 3, p.  
1061 55–75.

1062 Gervais, F., Brown, R.L., and Crowley, J.L., 2010, Tectonic implications for a Cordilleran orogenic  
1063 base in the Frenchman Cap dome, southeastern Canadian Cordillera: *Journal of Structural  
1064 Geology*, v. 34, p. 941-959.

1065 Gilmour, L.A., 2012, U/Pb ages of Eocene and younger rocks on the eastern flank of the central  
1066 Cascade Range, Washington, USA (M.S. thesis): Seattle, Washington, University of  
1067 Washington, 48 p.

1068 Gordon, S.M., Bowring, S.A., Whitney, D.L., Miller, R.B., and McLean, N., 2010a, Timescales of  
1069 metamorphism, deformation, and crustal melting in a continental arc, North Cascades,  
1070 USA: Geological Society of America Bulletin, v. 122, p. 1308–1330.

1071 Gordon, S.M., Whitney, D.L., Miller, R.B., McLean, N., and Seaton, N.C.A., 2010b,  
1072 Metamorphism and deformation at different structural levels in a strike-slip fault zone,  
1073 Ross Lake fault, North Cascades, USA: *Journal of Metamorphic Geology*, v. 28, p. 117–136.

1074 Greig, C.J., 1992, Jurassic and Cretaceous plutonic and structural styles of the Eagle Plutonic  
1075 Complex, southwestern British Columbia, and their regional significance: Canadian Journal  
1076 of Earth Sciences, v. 29, p. 793-811.

1077 Groome, W.G., Thorkelson, D.J., Friedman, R.M., Mortensen, J.M., Massey, N.W.D., Marshall,  
1078 D.D., and Layer, P.W., 2003, Magmatic and tectonic history of the Leech River Complex,  
1079 Vancouver Island, British Columbia: Evidence for ridge-trench intersection and accretion  
1080 of the Crescent Terrane, *in* Sisson, V.B., Roeske, S.M., and Pavlis, T.L., eds., Geology of a  
1081 Transpressional Orogen Developed During Ridge-trench Interaction along the North  
1082 Pacific Margin: Geological Society of America Special Paper 371, p. 327–353.

1083 Haeussler, P.J., Bradley, D.C., Wells, R.E., and Miller, M.L., 2003, Life and death of the  
1084 Resurrection plate: Evidence for its existence and subduction in the northeastern Pacific  
1085 in Paleocene–Eocene time: Geological Society of America Bulletin, v. 115, p. 867-880.

1086 Hanson, A.E.H., Gordon, S.M., Ashley, K.T., Miller, R.B., and Langdon-Lassagne, E., 2022, Multiple  
1087 sediment incorporation events in a continental magmatic arc: insight from the  
1088 metasedimentary rocks of the northern North Cascades, Washington: Geosphere, v. 18,  
1089 <https://doi.org/10.1130/GES02425.1>.

1090 Harlan, S.S., Geissman, J.W.M., Lageson, D.R., and Snee, W.W., 1988, Paleomagnetic and  
1091 isotopic dating of thrust-belt deformation along the eastern edge of the Helena salient,  
1092 northern Crazy Mountains Basin, Montana: Geological Society of America Bulletin, v. 100,  
1093 p. 492-499.

1094 Harms, T.A., and Price, R.A., 1992, The Newport fault: Eocene listric normal faulting,  
1095 mylonitization, and crustal extension in northeast Washington and northwest Idaho:  
1096 Geological Society of America Bulletin, v. 104, p. 745-761.

1097 Haugerud, R.A., and Tabor, R.W., 2009, Geologic map of the North Cascade Range,  
1098 Washington: U.S. Geological Survey Scientific Investigations Map 2940, 2 sheets, scale  
1099 1:200,000; 2 pamphlets, 29 p. and 23 p.

1100 Haugerud, R.A., van der Heyden, P., Tabor, R.W., Stacey, J.S., and Zartman, R.E., 1991, Late  
1101 Cretaceous and early Tertiary plutonism and deformation in the Skagit Gneiss Complex,  
1102 North Cascade Range, Washington and British Columbia: Geological Society of America  
1103 Bulletin, v. 103, p. 1297-1307.

1104 Hinckley, A.M., and Carr, S.D., 2006, The S-type Ladybird leucogranite suite of southeastern  
1105 British Columbia: Geochemical and isotopic evidence for a genetic link with migmatite  
1106 formation in the North American basement gneisses of the Monashee complex: Lithos,  
1107 doi.org/10.1016/j.lithos.2006.03.003.

1108 Howlett, C.J., Reynolds, A.N., and Laskowski, A.K., 2021, Magmatism and extension in the  
1109 Anaconda metamorphic core complex of western Montana and relation to regional  
1110 tectonics: Tectonics, v. 40, p. 1-31, doi:10.1029/2020TC006431.

1111 Humphreys, E.D., 1995, Post-Laramide removal of the Farallon slab, western United States:  
1112 Geology, v. 23, p. 987-990.

1113 Humphreys, E.D., 2009, Relation of flat subduction to magmatism and deformation in the  
1114 western United States, *in* Kay, S.M., Ramos, V.A., and Dickinson, W.R., eds., Backbone of  
1115 the Americas: Shallow Subduction, Plateau Uplift, and Ridge and Terrane Collision:  
1116 Geological Society of America Memoir 204, p. 85–98, doi: 10.1130/2009.1204(04).

1117 Humphreys, E.D., and Grunder, A.L., 2022, Tectonic controls on the origin and segmentation of  
1118 the Cascade arc, USA: *Bulletin of Volcanology*, 84:102, <https://doi.org/10.1007/s00445-022-01611-2>.

1120 Hurlow, H.A., and Nelson, B.K., 1993, U-Pb zircon and monazite ages for the Okanogan Range  
1121 batholith, Washington: Implications for the magmatic and tectonic evolution of the  
1122 southern Canadian and northern United States Cordillera: *Geological Society of America*  
1123 *Bulletin*, v. 105, p. 231–240.

1124 Ickert, R.B., Thorkelson, D.J., Marshall, D.D., and Ullrich, T.D., 2009, Eocene adakitic volcanism  
1125 in southern British Columbia: Remelting of arc basalt above a slab window:  
1126 *Tectonophysics*, v. 464, p. 164-185.

1127 Irving, E., and Brandon, M.T., 1990, Paleomagnetism of the Flores volcanics, Vancouver Island,  
1128 in place by Eocene time: *Canadian Journal of Earth Sciences*, v. 27, p. 811-817.

1129 Janecke, S.U., and Snee, L.W., 1993, Timing and episodicity of middle Eocene volcanism and  
1130 onset of conglomerate deposition, Idaho: *The Journal of Geology*, v. 101, p. 603–621, doi:  
1131 10.1086/648252.

1132 Johnson, S.Y., 1984, Stratigraphy, age, and paleogeography of the Eocene Chuckanut  
1133 Formation, northwest Washington: Canadian Journal of Earth Sciences, v. 21, p. 92-106.

1134 Johnson, S.Y., and O'Connor, J.T., 1994, Stratigraphy, sedimentology, and provenance of the  
1135 Raging River Formation (Early and middle Eocene), King County, Washington: U.S.  
1136 Geological Survey Bulletin 2085-A, p. A-1 – A-33.

1137 Johnston, S.T., and Acton, S., 2003, The Eocene Southern Vancouver Island Orocline — a  
1138 response to seamount accretion and the cause of fold-and-thrust belt and extensional  
1139 basin formation: Tectonophysics, v. 365, p. 165-183.

1140 Kalakay, T.J., Foster, D.A., and Thomas, R.A., 2003, Geometry, kinematics and timing of  
1141 extension in the Anaconda extensional terrane, western Montana: Northwest Geology, v.  
1142 32, p. 42–72.

1143 Kant, L.B., Tepper, J.H., and Nelson, B.K., 2018, Eocene Basalt of Summit Creek: Slab breakoff  
1144 magmatism in the central Washington Cascades, USA: Lithosphere, v. 10, p. 792-805.

1145 Kriens, B.J., Hawley, D.L., Chappelear, F.D., Mack, P.D., and Chan, A.F., 1995, Spatial and  
1146 temporal relations between early Tertiary shortening and extension in NW Washington,  
1147 based on geology of the Pipestone Canyon Formation and surrounding rocks: Tectonics, v.  
1148 14, p. 719-735.

1149 Kruckenberg, S.C., Whitney, D.L., Teyssier, C., Fanning, C.M., and Dunlap, W.J., 2008, Paleocene-  
1150 Eocene migmatite crystallization, extension, and exhumation in the hinterland of the

1151 northern Cordillera: Okanogan dome, Washington, USA: Geological Society of America

1152 Bulletin, v. 120, p. 912-929.

1153 Lewis, R.S., and Kjelsgaard, 1991, Eocene plutonic rocks in south central Idaho: Journal of

1154 Geophysical Research: Solid Earth, v. 96, p. 13295-13311.

1155 Lonsdale, P., 1988, Paleogene history of the Kula plate: Offshore evidence and onshore

1156 implications: Geological Society of America Bulletin, v. 100, p. 733-754.

1157 MacDonald, J.H., Jr., Dragovich, J.D., Littke, H.A., Anderson, M., and Dufrane, S.A., 2013, The

1158 Eocene volcanic rocks of Mount Persis: An Eocene continental arc that contains adakitic

1159 magmas: Geological Society of America Abstracts with Programs, v. 45, no. 7, p. 392.

1160 Madsen, J.K., Thorkelson, D.J., Friedman, R.M., and Marshall, D.D., 2006, Cenozoic to Recent

1161 plate configurations in the Pacific Basin: Ridge subduction and slab window magmatism in

1162 western North America: Geosphere, v. 2, p. 11-34.

1163 Massey, N.W.D., 1986, Metchosin Igneous Complex, southern Vancouver Island: Ophiolite

1164 stratigraphy developed in an emergent island setting: Geology, v. 14, p. 602-605.

1165 Matthews, K.J., Maloney, K.T., Zahirovic, S., Williams, S.E., Seton, M., and Müller, R.D., 2016,

1166 Global plate boundary evolution and kinematics since the late Paleozoic: Global and

1167 Planetary Change, v. 146, p. 226-250.

1168 Matthews, W.A., Guest, B., Coutts, D., Bain, H., and Hubbard, S., 2017, Detrital zircons from the

1169 Nanaimo basin, Vancouver Island, British Columbia: An independent test of Late

1170 Cretaceous to Cenozoic northward translation: *Tectonics*, v. 36, p. 854–876, <https://doi.org/10.1002/2017TC004531>

1171

1172 Matzel, J.E.P., 2004, Rates of tectonic and magmatic processes in the North Cascades

1173 continental magmatic arc [Ph.D. thesis]: Cambridge, Massachusetts

1174 Institute of Technology, 249 p.

1175 Matzel, J.E.P., Bowring, S.A., and Miller, R.B., 2008, Spatial and temporal variations in Nd

1176 isotopic signatures across the crystalline core of the North Cascades, WA, *in* Shervais, J.,

1177 and Wright, J., eds., *Arcs, Ophiolites, and Batholiths: A Tribute to Cliff Hopson*: Geological

1178 Society of America Special Paper 438, p. 499–516.

1179 McCarley Holder, G.A., Holder, R.W., and Carlson, D.H., 1990, Middle Eocene dike swarms and

1180 their relation to contemporaneous plutonism, volcanism, core-complex mylonitization,

1181 and graben subsidence, Okanogan Highlands, Washington: *Geology*, v. 18, p. 1082-1085.

1182 [McCrory, P.A., and Wilson, D.S., 2013, A kinematic model for the formation of the Siletz-](#)

1183 [Crescent forearc terrane by capture of coherent fragments of the Farallon and](#)

1184 [Resurrection plates: \*Tectonics\*, v. 32, p. 718-736.](#)

1185 Miller, R.B., and Bowring, S.A., 1990, Structure and chronology of the Oval Peak batholith and

1186 adjacent rocks: Implications for the Ross Lake fault zone, North Cascades, Washington:

1187 Geological Society of America Bulletin, v. 102, p. 1361-1377.

1188 Miller, R.B., and Paterson, S.R., 1999, In defense of magmatic diapirs: *Journal of Structural*

1189 *Geology*, v. 21, p. 1161-1173.

1190 Miller, R.B., Paterson, S.R., and Matzel, J.P., 2009, Plutonism at different crustal levels: Insights  
1191 from the ~5-40 km (paleodepth) North Cascades crustal section, Washington, *in* Miller,  
1192 R.B., and Snoker, A.W, eds., Crustal cross sections from the western North America  
1193 Cordillera and elsewhere: Implications for tectonic and petrologic processes: Geological  
1194 Society of America Special Paper 456, p. 125–150.

1195 Miller, R.B., Gordon, S.M., Bowring, S.A., Doran, B.A., McLean, N., Michels, Z., Shea, E.K., and  
1196 Whitney, D.L., 2016, Linking deep and shallow crustal processes during regional  
1197 transtension in an exhumed continental arc, North Cascades, northwestern Cordillera  
1198 (USA): *Geosphere*, v. 12, p. 900-924.

1199 Miller, R.B., Bryant, K.I., Doran, B., Eddy, M.P., Raviola, F.P., Sylva, N., and Umhoefer, P.J., 2022,  
1200 Eocene dike orientations across the Washington Cascades in response to a major strike-  
1201 slip faulting episode and ridge-trench interaction: *Geosphere*, v. 18, no. 2, p. 1–29,  
1202 <https://doi.org/10.1130/GES02387.1>.

1203 Misch, P., 1966, Tectonic evolution of the northern Cascades of Washington State—a west  
1204 Cordilleran case history: Canadian Institute of Mining and Metallurgy, Special Volume 8, p.  
1205 101-148.

1206 Misch, P., 1968, Plagioclase compositions and non-anatetic origin of migmatitic gneisses in  
1207 Northern Cascade Mountains of Washington State: Contributions to Mineralogy and  
1208 Petrology, v. 17, p. 1-70.

1209 Monger, J.W.H., 1989, Geology of the Hope and Ashcroft map areas, British Columbia:  
1210 Geological Survey of Canada Maps 41-1989 and 42-1989.

1211 Monger, J.W.H., and Brown, E.H., 2016, Tectonic evolution of the southern Coast-Cascade  
1212 orogen, *in* Cheney, E.S., ed., The Geology of Washington and Beyond: From Laurentia to  
1213 Cascadia: Seattle, University of Washington Press, p. 101-130.

1214 Morris, G.A., Larson, P.B., and Hooper, P.R., 2000, 'Subduction style' magmatism in a  
1215 nonsubduction setting: The Colville igneous complex, NE Washington State, USA: Journal  
1216 of Petrology, v. 41, p. 43-67, <https://doi.org/10.1093/petrology/41.1.43>.

1217 Mudge, M.R., and Earhart, R.L., 1980, The Lewis thrust fault and related structures in the  
1218 Disturbed Belt, northwestern Montana: U.S. Geological Survey Professional Paper 1174,  
1219 18 p.

1220 Mueller, P.A., Heatherington, A.L., D'Arcy, K.A., Wooden, J.L., and Nutman, A.P., 1996,  
1221 Contrasts between Sm-Nd whole-rock and U-Pb zircon systematics in the Tobacco Root  
1222 batholith, Montana: implications for the determination of crustal age provinces:  
1223 Tectonophysics, v. 265, p. 169-179.

1224 Mustard, P. S., 1994, The Upper Cretaceous Nanaimo Group, Georgia Basin, *in* Monger, J.W.H.,  
1225 ed., Geology and Geological Hazards of the Vancouver Region, Southwestern British  
1226 Columbia: Geological Survey of Canada Bulletin, v. 481, p. 27-95.

1227 O'Connor, J.M, Steinberger, B, Regelous, M., Koppers, A.A.P., Wijbrans, J.R., Haase, K.M.,  
1228 Stoffers, P., Jokat, W., and Garbe-Schönberg, D., 2013, Constraints on past plate and

1229 mantle motion from new ages for the Hawaiian-Emperor Seamount Chain: Geochemistry,  
1230 Geophysics, and Geosystems, v. 14, no. 10, doi:10.1002/ggge.20267.

1231 O'Driscoll, L.J., Humphreys, E., and Saucier, F., 2009, Subduction adjacent to deep continental  
1232 roots: Enhanced negative pressure in the mantle wedge, mountain building and  
1233 continental motion: Tectonophysics, v. 280, p. 61-70.

1234 Parker, D.F., Hodges, F.N., Perry, A., Mitchener, M.E., Barnes, M.A., and Ren, M., 2010,  
1235 Geochemistry and petrology of late Eocene Cascade Head and Yachats Basalt and alkalic  
1236 intrusions of the central Oregon Coast Range, U.S.A.: Journal of Volcanology and  
1237 Geothermal Research, v. 198, p. 311-324.

1238 Parrish, R.R., Carr, S.D., and Parkinson, D.L., 1988, Eocene extensional tectonics and  
1239 geochronology of the southern Omineca Belt, British Columbia and Washington:  
1240 Tectonics, v. 7, p. 181-212

1241 Paterson, S.R., Miller, R.B., Alsleben, H., Whitney, D.L., Valley, P.M., and Hurlow, H., 2004,  
1242 Driving mechanisms for >40 km of exhumation during contraction and extension in a  
1243 continental arc, Cascades core, Washington: Tectonics, v. 23, TC3005, doi:  
1244 10.1029/2002TC001440.

1245 Pearson, R.C., and Obradovich, J.D., 1977, Eocene rocks in northeast Washington: Radiometric  
1246 ages and correlation: U.S. Geological Survey Bulletin 1433, 41 p.

1247 Peters, R.L., and Tepper, J.H., 2006, Petrology of the Teanaway dike swarm, central Cascades,  
1248 Washington: Geological Society of America Abstracts with Programs, v. 38, no. 5, p. 9.

1249 Peterson, P., and Tepper, J.H., 2021, Petrology and tectonic setting of the Silver Pass Volcanics,  
1250 Central Cascades, WA: early evidence of Farallon Slab breakoff: Geological Society of  
1251 America Abstracts with Programs, v. 53, no. 6, doi.org/10.1130/abs/2021AM-368972.

1252 Phillips, B.A., Kerr, A.C., Mullen, E.K., and Weis, D., 2017, Oceanic mafic magmatism in the Siletz  
1253 terrane, NW North America: Fragments of an Eocene oceanic plateau?: *Lithos*, v. 274–  
1254 275, p. 291–303, <https://doi.org/10.1016/j.lithos.2017.01.005>.

1255 Price, R., 1981, The Cordilleran foreland thrust and fold belt in the southern Canadian Rocky  
1256 Mountains, in McClay, K.R., and Price, N.J., eds., *Thrust and Nappe Tectonics*: Geological  
1257 Society, London, Special Publications, v. 9, p. 427-448.

1258 Price, R.A., and Carmichael, D.M., 1986, Geometric test for Late Cretaceous-Paleogene  
1259 intracontinental transform faulting in the Canadian Cordillera: *Geology*, v. 14, p. 468-471.

1260 Pyle D.G., Duncan, R.A., Wells, R.E., Graham, D.W., Hanan, B.B., Harrison, B.K., and Haileab, B.,  
1261 2015, Longevity of YHS volcanism: Isotopic evidence linking the Siletzia LIP (56 Ma) and  
1262 early Columbia River Basalt Group (17 Ma) to mantle sources: *American Geophysical  
1263 Union Fall Meeting*, Abstract V31E-3060.

1264 Rhodes, B.P., and Cheney, E.S., 1981, Low-angle faulting and the origin of Kettle dome, a  
1265 metamorphic core complex in northeastern Washington: *Geology*, v. 9, p. 366-369.

1266 Roepke, E., Tepper, J.H., and Ivener, D., 2013, A petrologic study of the Teanaway Basalt:  
1267 Eocene slab window volcanism in central WA: *American Geophysical Union Fall Meeting*,  
1268 2013, Abstract V31A-2667.

1269 Rubino, E., Leier, A., Cassel, E.J., Archibald, B., Foster-Baril, Z., and Barbeau Jr., D.L., 2021,  
1270 Detrital zircon U–Pb ages and Hf-isotopes from Eocene intermontane basin deposits of  
1271 the southern Canadian Cordillera: *Sedimentary Geology*, v. 422,  
1272 doi.org/10.1016/j.sedgeo.2021.105969.

1273 Sauer, K.B., Gordon, S.M., Miller, R.B., Vervoort, J.D., and Fisher, C.M., 2017a, Evolution of the  
1274 Jura-Cretaceous North American Cordilleran margin: Insights from detrital-zircon U-Pb  
1275 and Hf isotopes of sedimentary units of the North Cascades Range, Washington:  
1276 *Geosphere*, v. 13, no.6, p. 2094-2118, doi. doi.org/10.1130/GES01501.1

1277 Sauer, K.B., Gordon, S.M., Miller, R.B., Vervoort, J.D., and Fisher, C.M., 2017b, Transfer of  
1278 metasupracrustal rocks to midcrustal depths in the North Cascades continental  
1279 magmatic arc, Skagit Gneiss Complex, Washington: *Tectonics*, 10.1002/2017TC004728:

1280 Sauer, K.B., Gordon, S.M., Miller, R.B., Vervoort, J.D., and Fisher, C.M., 2018, Provenance and  
1281 metamorphism of the Swakane Gneiss: implications for incorporation of sediment into  
1282 the deep levels of the North Cascades continental magmatic arc, Washington:  
1283 *Lithosphere*, v. 10, p. 460–477, doi.org/10.1130/L712.1.

1284 Schellart, P., 2020, Control of subduction zone age and size on flat slab subduction: *Frontiers in*  
1285 *Earth Science*, doi.org./10.3389/feart/2020.00026.

1286 Schmandt, B., and Humphreys, E.D., 2011, Seismically imaged relict slab from the 55 Ma Siletzia  
1287 accretion to the northwest United States: *Geology*, v. 39, p. 175–178.

1288 Schwartz, J.J., Klepeis, K.A., Sadorski, J.F., Stowell, H.H., Tulloch, A.J., and Coble, M.A., 2017, The  
1289 tempo of continental arc construction in the Mesozoic Median Batholith, Fiordland, New  
1290 Zealand: *Lithosphere*, v. 9, p. 343-365.

1291 Senes, F.I., 2019, Deformation, sandstone detrital zircon ages, and provenance in and near the  
1292 Eocene Leavenworth fault zone, Washington [M.S. thesis]: San Jose, California, San Jose  
1293 State University, 114 p.

1294 Seton, M., Flament, N., Whittaker, J., Müller, R.D., Gurnis, M., and Bower, D.J., 2015, Ridge  
1295 subduction sparked reorganization of the Pacific plate-mantle system 60–50 million  
1296 years ago: *Geophysical Research Letters*, v. 42, p. 1732–1740,  
1297 doi:10.1002/2015GL063057.

1298 Sharp, W.D., and Clague, D.A., 2006, 50-Ma Initiation of Hawaiian-Emperor bend records major  
1299 change in Pacific plate motion: *Science*, v. 313, p. 1281-1284.

1300 Simony, P.S., and Carr, S.D., 2011, Cretaceous to Eocene evolution of the southeastern  
1301 Canadian Cordillera: Continuity of Rocky Mountain thrust systems with zones of “in-  
1302 sequence” mid-crustal flow: *Journal of Structural Geology*, v. 33, p. 1417-1434.

1303 Stern, R.J., and Dumitru, T.A., 2019, Eocene initiation of the Cascadia subduction zone: A second  
1304 example of plume-induced subduction initiation?: *Geosphere*, v. 15, no. 3, p. 659–681,  
1305 <https://doi.org/10.1130/GES02050.1>.

1306 Stevens, L.M., Baldwin, J.A., Crowley, J.L., Fisher, C.M., and Vervoort, J.D., 2016, Magmatism as  
1307 a response to exhumation of the Priest River complex, northern Idaho: Constraints from  
1308 zircon U-Pb geochronology and Hf isotopes: *Lithos*, v. 262, p. 285–297.

1309 Stock, J., and Molnar, P., 1988, Uncertainties and implications of the Late Cretaceous and  
1310 Tertiary position of North America relative to the Farallon, Kula, and Pacific plates:  
1311 *Tectonics*, v. 7, p. 1339-1384.

1312 Stoffel, K.L., Joseph, N.L., Waggoner, S.Z., Gulick, C.W., Korosec, M.A., and Bunning, B.B., 1991,  
1313 Geologic map of Washington—Northeast quadrant: Washington Division of Geology and  
1314 Earth Resources Geologic Map GM-39, 3 sheets, scale 1:250,000, with 36 p. text.

1315 Suydam, J.D., and Gaylord, D.R., 1997, Toroda Creek half graben, northeast Washington: Late-  
1316 stage sedimentary infilling of a synextensional basin: Geological Society of America  
1317 *Bulletin*, v. 109, p. 1333–1348.

1318 Tabor, R.W., 1994, Late Mesozoic and possible early Tertiary accretion in western Washington  
1319 State: The Helena-Haystack mélange and the Darrington-Devils Mountain fault zone:  
1320 *Geological Society of America Bulletin*, v. 106, p. 217-232.

1321 Tabor, R.W., Waitt, R.B., Jr., Frizzell, V.A., Jr., Swanson, D.A., Byerly, G.R., and Bentley, R.D., 1982,  
1322 Geologic map of the Wenatchee quadrangle, Washington: U.S. Geological Survey  
1323 Miscellaneous Investigations Map, MI-1311, scale 1:100,000, 1 sheet, 31 p. text.

1324 Tabor, R.W., Frizzell, V.A., Jr., Vance, J.A., and Naeser, C.W., 1984, Ages and stratigraphy of  
1325 lower and middle Tertiary sedimentary and volcanic rocks of the Central Cascades,

1326 Washington: Applications to the tectonic history of the Straight Creek fault: Geological  
1327 Society of America Bulletin, v. 95, p. 26-44.

1328 Tabor, R.W., Frizzell, V.A., Jr., Whetten, J.T., Waitt, R.B., Swanson, D.A., Byerly, G.R., Booth, D.B.,  
1329 Hetherington, M.J., and Zartman, R.E., 1987, Geologic map of the Chelan 30-minute by 60-  
1330 minute quadrangle, Washington: U.S. Geological Survey Geologic Investigation Series, I-  
1331 1661, scale 1:100,000, 1 sheet, 56 p. text.

1332 Tabor, R.W., Frizzell, V.A., Jr., Booth, D.B., Waitt, R.B., Whetten, J.T., and Zartman, R.E., 1993,  
1333 Geologic map of the Skykomish 30- by 60-minute quadrangle: U.S. Geological Survey  
1334 Geologic Investigation Series, I-1663, scale 1:100,000.

1335 Tabor, R.W., Frizzell, V.A., Jr., Booth, D.B., and Waitt, R.B., 2000, Geologic map of the  
1336 Snoqualmie Pass 30x60 minute quadrangle, Washington: U.S. Geological Survey Geologic  
1337 Investigations Map, MI-2538, scale 1:100,000, 1 sheet, 57 p. text.

1338 Tabor, R.W., Haugerud, R.A., Hildreth, W., and Brown, E.H., 2003, Geologic map of the Mount  
1339 Baker 30- by 60-minute quadrangle, Washington: U.S. Geological Survey Geologic  
1340 Investigations Series I-2660, scale 1:100,000.

1341 Tepper, J.H., 2016, Eocene breakoff and rollback of the Farallon slab—An explanation for the  
1342 “Challis event”?: Geological Society of America Abstracts with Programs, v. 48, no. 4,  
1343 paper 327-1, <https://doi.org/10.1130/abs/2016CD-274512>.

1344 Tepper, J.H., and Eddy, M.P., 2017, The cause(s) of widespread Eocene magmatism in the  
1345 Pacific Northwest: insights from geochemistry and geochronology of igneous rocks in

1346 Washington, Geological Society of America Abstracts with Programs. V. 49, no. 6, doi:  
1347 10.1130/abs/2017AM-301043

1348 Tepper, J.H., Clark, K.P., Asmerom, Y., and McIntosh, W.C., 2004, Eocene adakites in the  
1349 Cascadia forearc: Implications for the position of the Kula-Farallon ridge: Geological  
1350 Society of America Abstracts with Programs, v. 36, no. 4, p. 69.

1351 Tepper, J.H., Nelson, B.K., Clark, K., and Barnes, R.P., 2008, Heterogeneity in mantle sources for  
1352 Eocene basalts in Washington: Trace element and Sr-Nd isotopic evidence from the  
1353 Crescent and Teanaway Basalts: American Geophysical Union, Fall Meeting 2008,  
1354 abstract id. V41D-2121.

1355 Thorkelson, D.J., and Taylor, R.P., 1989, Cordilleran slab windows: Geology, v. 17, p. 833-836.

1356 Trehu, A.M., Asudeh, I., Brocher, T.M., Luetgert, J.H., Mooney, W.D., Nabelek, J.L., and  
1357 Nakamura, Y., 1994, Crustal architecture of the Cascadia forearc: Science, v. 266, p. 237–  
1358 243, <https://doi.org/10.1126/science.266.5183.237>.

1359 Tikoff, B., Housen, B.A., Maxson, J.A., Nelson, E.M., Trevino, S., and Shipley, T.F., 2023,2, Hit-  
1360 and-run model for Cretaceous–Paleogene tectonism along the western margin of  
1361 Laurentia, *in* Whitmeyer, S.J., Williams, M.L., Kellett, D.A., and Tikoff, B., eds., Laurentia:  
1362 Turning Points in the Evolution of a Continent: Geological Society of America Memoir  
1363 220, [\(in press\)](#), [Geological Society of America Memoir 220, p. 659-705](#),  
1364 doi.org/10.1130/2022.1220(32).

1365 Umhoefer, P.J., and Blakey, R., 2006, Moderate (1600 km) northward translation of Baja British  
1366 Columbia from southern California: An attempt at reconciliation of paleomagnetism and  
1367 geology, *in* Haggart, J.W., Enkin, R.J., and Monger, J.W.H., eds., Paleogeography of the  
1368 North American Cordillera: Evidence for and Against Large-scale Displacements:  
1369 Geological Association of Canada, Special Papers, v. 46, p. 307-329.

1370 Umhoefer, P.J., and Miller, R.B., 1996, Mid-Cretaceous thrusting in the southern Coast Belt,  
1371 British Columbia and Washington, after strike-slip fault reconstruction: Tectonics, v. 15,  
1372 p. 545-565.

1373 Umhoefer, P.J., and Schiarizza, P., 1996, Latest Cretaceous to early Tertiary dextral strike-slip  
1374 faulting on the southeastern Yalakom fault system, southeastern Coast Belt, British  
1375 Columbia: Geological Society of America, v. 108, p. 768-785.

1376 Valley, P.M., Whitney, D.L., Paterson, S.R., Miller, R.B., and Alsleben, H., 2003, Metamorphism  
1377 of the deepest exposed arc rocks in the Cretaceous to Paleogene Cascades belt,  
1378 Washington: evidence for large-scale vertical motion in a continental arc: Journal of  
1379 Metamorphic Geology, v. 21, p. 203-220.

1380 Vanderhaege, O., and Teyssier, C., 2001, Crustal-scale rheological transitions during late-  
1381 orogenic collapse: Tectonophysics, v. 335, p. 211-228.

1382 van Hinsbergen, D.J.J., Steinberger, B., Doubrovine, P.V., and Gassmöller, R., 2011, Acceleration  
1383 and deceleration of India - Asia convergence since the Cretaceous: Roles of mantle

1384 plumes and continental collision: *Journal of Geophysical Research*, v. 116, B06101,  
1385 doi:10.1029/2010JB008051.

1386 Vine, J.D., 1969, Geology and coal resources of the Cumberland, Hobart, and Maple Valley  
1387 quadrangles, King County, Washington: U.S. Geological Survey Professional Paper 624, 67  
1388 p.

1389 Walker, N.W., and Brown, E.H., 1991, Is the southeast Coast Plutonic Complex the consequence  
1390 of accretion of the Insular superterrane? Evidence from U-Pb zircon geochronometry in  
1391 the northern Washington Cascades: *Geology*, v. 19, p. 714-717.

1392 Wallenbrock, C.J., and Tepper, J.H., 2017, Mid-Eocene arc volcanism in the Central Washington  
1393 Cascades: Petrology of the Taneum Formation and its relation to Farallon plate  
1394 subduction and breakoff: *Geological Society of America Abstracts with Programs*, v. 49,  
1395 no. 6, doi: 10.1130/abs/2017AM-301021.

1396 Wells, R.E., and Heller, P.L., 1988, The relative contribution of accretion, shear, and extension to  
1397 Cenozoic tectonic rotation in the Pacific Northwest: *Geological Society of America*  
1398 *Bulletin*, v. 100, p. 325–338.

1399 Wells, R.E., and McCaffrey, R., 2013, Steady rotation of the Cascade Arc: *Geology*, v. 41, p.  
1400 1027–1030, doi:10.1130/G34514.1.

1401 Wells, R.E., Engebretson, D.C., Snavely, P.D., Jr., and Coe, R.S., 1984, Cenozoic plate motions  
1402 and the volcano-tectonic evolution of western Oregon and Washington: *Tectonics*, v. 3,  
1403 275-294.

1404 Wells, R.E., Jayko, A.S., Niem, A.R., Black, G., Wiley, T., Baldwin, E., Molenaar, K.M., Wheeler,  
1405 K.L., DuRoss, C.B., and Givler, R.W., 2000, Geologic map and database of the Roseburg 30  
1406 x 60' Quadrangle, Douglas and Coos Counties, Oregon: U.S. Geological Survey Open-File  
1407 report 00-376, <https://pubs.usgs.gov/of/2000/0376/>.

1408 Wells, R., Bukry, D., Friedman, R., Pyle, D., Duncan, R., Haeussler, P., and Wooden, J., 2014,  
1409 Geologic history of Siletzia, a large igneous province in the Oregon and Washington  
1410 Coast Range: Correlation to the geomagnetic polarity time scale and implications for a  
1411 long-lived Yellowstone hotspot: *Geosphere*, v. 10, p. 692-719, doi: 10.1130/GES01018.1.

1412 Wernicke, B.P., and Getty, S.R., 1997, Intracrustal subduction and gravity currents in the deep  
1413 crust; Sm-Nd, Ar-Ar, and thermobarometric constraints from the Skagit Gneiss Complex,  
1414 Washington: *Geological Society of America Bulletin*, v. 109, p. 1149-1166.

1415 Whalen, J.B., and Hildebrand, R.S., 2019, Trace element discrimination of arc, slab failure, and  
1416 A-type granitic rocks: *Lithos*, v. 348-349, doi.org/10.1016/j.lithos.2019.105179.

1417 White, A., Tepper, J.H., and Dawes, R.L., 2021, Geochemistry and petrology of Eocene to  
1418 Miocene rocks in a rear-arc setting, central Cascades, Washington: *Geological Society of  
1419 America Abstracts with Programs*, v. 53, no. 6. <https://doi.org/10.1130/abs/2021AM-367697>.

1421 White, P.J., 1986, Geology of the Island Mountain area, Okanogan County, Washington  
1422 [M.S. Thesis]: Seattle, Washington, University of Washington, 80 p.

1423 Whitney, D.L., 1992, High-pressure metamorphism in the Western Cordillera of North America:  
1424 an example from the Skagit Gneiss, North Cascades: *Journal of Metamorphic Geology*, v.  
1425 10, p. 71-85.

1426 Whitney, D.L., Paterson, S.R., Schmidt, K.L., Glazner, A.F., and Kopf, C.F., 2004, Growth and  
1427 demise of continental arcs and orogenic plateaux in the North American Cordillera: from  
1428 Baja to British Columbia: *Geological Society, London, Special Publication* 227, p. 167-175.

1429 Whittaker, J.M., Müller, R.D., Leitchenkov, G., Stagg, H., Sdrolias, M., Gaina, C., and Goncharov,  
1430 A., 2007, Major Australian-Antarctic plate reorganization at Hawaiian-Emperor bend time:  
1431 *Science*, v. 318, p. 83–86.

1432 Wintzer, N.E., 2012, Deformational episodes recorded in the Skagit Gneiss Complex, North  
1433 Cascades, Washington, USA: *Journal of Structural Geology*, v. 42, p. 127-139.

1434 Woods, M T., and Davies, G.F., 1982, Late Cretaceous genesis of the Kula plate: Earth and  
1435 Planetary Science Letters, v. 58, p. 161-166.

1436 Wright, N.M., Muller, R.D., Seton, M., and Williams, S.E., 2015, Revision of Paleogene plate  
1437 motions in the Pacific and implications for the Hawaiian-Emperor bend: *Geology*, v. 43,  
1438 p. 455–458.

1439 Wu, J. T-J., and Wu, J., 2019, Izanagi-Pacific ridge subduction revealed by a 56 to 46 Ma  
1440 magmatic gap along the northeast Asian margin: *Geology*, v. 47, 953-957.

1441 Wyld, S.J., Umhoefer, P.J., and Wright, J.E., 2006, Reconstructing northern Cordilleran terranes  
1442 along known Cretaceous and Cenozoic strike-slip faults: Implications for the Baja British

1443 Columbia hypothesis and other models, *in* Haggart, J.W., Enkin, R.J., and Monger, J.W.H.,  
1444 eds., Paleogeography of the North American Cordillera: Evidence for and Against Large-  
1445 scale Displacements: Geological Association of Canada, Special Papers, v. 46, p. 277-298.

1446 Yeats, R.S., and Engels, J.C., 1971, Potassium-argon ages of plutons in the Skykomish-  
1447 Stillaguamish areas, north Cascades, Washington: U.S. Geological Survey Professional  
1448 Paper 750-D, p. D34-D38.

1449

1450 **TABLE**

1451 Table 1. STRIKE-SLIP FAULT OFFSETS ACROSS WASHINGTON CASCADES.

1452

1453 **FIGURE CAPTIONS**

1454 Figure. 1. Simple plate reconstruction models of the NE Pacific at 60 Ma and 52 Ma showing  
1455 locations of triple junctions. A. Kula – Farallon – North America triple junction. Note the  
1456 southward sweep of the Kula – Farallon Ridge from 60 Ma to 52 Ma in this model ([e.g., Bradley](#)  
1457 [et al., 2003](#)). B. Two triple junctions result from the hypothetical Resurrection plate ([e.g.,](#)  
1458 [Hauessler et al., 2003](#)). Note that in either model there is a triple junction near central to  
1459 southern Vancouver Island at ca. 52 Ma ([e.g., Breitsprecher et al., 2003](#)) and that the Kula ridge  
1460 [interacted with the continental margin back to ca. 83 Ma \(e.g., Engebretson et al., 1985;](#)  
1461 [Thorkelson and Taylor \(1989\)](#). The hypothetical Orcas plate model is on a coarser scale and is  
1462 [not shown; it calls for the final consumption of the plate at ~50 Ma \(Clennett et al., 2020\).](#) -

1463 Sanak-Baranof is a belt of near-trench intrusions, which provide part of the evidence of a ridge  
1464 interacting with a trench ([e.g., Bradley et al., 2003](#)).

1465

1466 Figure 2. Generalized tectonic map of Paleogene rock types, structures, and tectonics of the  
1467 greater Pacific Northwest region considered in this study. Note the location of Siletzia (including  
1468 subsurface), near-trench intrusions, major dextral strike-slip faults, basins, magmatic rocks, and  
1469 metamorphic core complexes and bounding normal faults. Western, Central, and Eastern belts  
1470 are subdivisions used in text. An = Anaconda core complex; Br = Bitterroot lobe of Idaho  
1471 batholith; Cb = Chelan block of North Cascades crystalline core; Csz = Coast shear zone; Ef =  
1472 Entiat fault; Ff = Fraser fault; K = Kettle core complex; LCFz = Lewis and Clark fault zone; Ok =  
1473 Okanogan core complex; P = Priest River core complex; Pf = Pasayten fault; RLf = Ross Lake  
1474 fault; SCf = Straight Creek fault; Sh = Shuswap core complex; V = Valhalla complex. VI =  
1475 Vancouver Island; Wb = Wenatchee block of North Cascades crystalline core; Yf = Yalakom fault.  
1476 Box shows location of Fig. 3. States and Provinces: BC = British Columbia; ID = Idaho; MT =  
1477 Montana; OR = Oregon; WA = Washington.

1478

1479 Figure 3. Simplified geologic map of central and northern Washington State, and adjacent  
1480 southern British Columbia (modified from Eddy et al., 2016a). BP=Barlow Pass Formation;  
1481 Ccb=Chilliwack batholith; CHK=Chuckanut Formation; CM=Cooper Mountain pluton; CP=Castle  
1482 Peak stock; CRb=Columbia River Basalt Group; DD=Dinkelman decollement; DH=Duncan Hill  
1483 pluton; Ef=Entiat fault; Epc=Eagle Plutonic Complex; FDfz = Foggy Dew fault zone; FRfz=Frazer

1484 River fault zone; GH=Golden Horn batholith; GPsz=Gabriel Peak shear zone; HZf=Hozameen  
1485 fault; Lfz=Leavenworth fault zone; LP=Lost Peak stock; MO=Mount Outram pluton;  
1486 MP=Monument Peak stock; MPS=Mount Pilchuck stock; N=Naches Formation; NP=Needle Peak  
1487 pluton; NWcts=Northwest Cascades thrust system; OP=Oval Peak pluton; Orb=Okanogan Range  
1488 batholith; PC=Pipestone Canyon Formation; Pf=Pasayten fault; PG=Puget Group; Pv=Princeton  
1489 volcanics; R=Roslyn Formation; RC=Railroad Creek pluton; RLf=Ross Lake fault; SW=Swauk  
1490 Formation; SWG=Swakane Gneiss; T=Teanaway Formation; WEMB=Western and eastern  
1491 mélange belts; Yi=Yale intrusions.

1492

1493 Figure 4. Reconstruction map at ca. 55 Ma based on features in Figures 2 and 3 (see text for  
1494 details). Note that the western belt has been offset 150 km to the south relative to the central  
1495 zone and >300 km to the south relative to the eastern belt. The ridge which Siletzia formed on  
1496 is near central to southern Vancouver Island and the Swauk basin has formed inboard of Siletzia  
1497 in the western belt. There is a lull in magmatism in the southern part of the Coast Mountains  
1498 and North Cascades arc. B. Proposed plate tectonic setting at ca. 55 Ma based on features in  
1499 Figures 2 and 3. Note the position of major faults (both active and non-active) in gray for  
1500 reference. Br = Bitterroot lobe of Idaho batholith; Cb = Chelan block of North Cascades  
1501 crystalline core; Csz = Coast shear zone; Ef = Entiat fault; K = Kettle core complex; Ok =  
1502 Okanogan core complex; P = Priest River core complex; Pf = Pasayten fault; RLf = Ross Lake  
1503 fault; Sh = Shuswap core complex; V = Valhalla complex; VI = Vancouver Island; Wb =  
1504 Wenatchee block of North Cascades crystalline core; Yf = Yalakom fault. States and Provinces:  
1505 BC = British Columbia; MT = Montana; WA = Washington.

1506

1507 | Figure 5. [A.](#) Reconstruction map [and proposed plate tectonic setting](#) at ca. 51 Ma based on  
1508 | features in Figures 2 and 3. By 51 Ma, the ridge has reached Vancouver Island and Siletzia has  
1509 | collided with the continental margin. The Swauk basin has begun to invert and Challis-Kamloops  
1510 | magmatism is active, as are core complexes and extensional basins in the eastern zone. [B.](#)  
1511 | [Proposed plate tectonic setting.](#) An = Anaconda core complex; Br = Bitterroot core complex; Cb  
1512 | = Chelan block of North Cascades crystalline core; Csz = Coast shear zone; Ef = Entiat fault; K =  
1513 | Kettle core complex; Lcfz = Lewis and Clark fault zone; Ok = Okanogan core complex; P = Priest  
1514 | River core complex; Pf = Pasayten fault; Rlf = Ross Lake fault; Sh = Shuswap core complex; V =  
1515 | Valhalla complex; VI = Vancouver Island; Wb = Wenatchee block of North Cascades crystalline  
1516 | core; Yf = Yalakom fault. States and Provinces: BC = British Columbia; CA = California; ID = Idaho;  
1517 | MT = Montana; NV = Nevada; UT = Utah; WA = Washington.

1518

1519 | Figure 6. [A.](#) Reconstruction map [and proposed plate tectonic setting](#) at ca. 48 Ma based on  
1520 | features in Figures 2 and 3. The subduction zone has shifted outboard of Siletzia. Some of the  
1521 | dextral strike-slip faults in the North Cascades have accelerated or initiated, and major dike  
1522 | swarms intruded in the central and northern Washington Cascades coincident with a magmatic  
1523 | flare-up. Challis-Kamloops magmatism continued, but is beginning to wane, as is extension  
1524 | associated with core complexes. [B. Proposed plate tectonic setting. The approximate location of](#)  
1525 | [the idealized slab window assumes that the Farallon plate was moving NE and the Kula-Farallon](#)  
1526 | [ridge intersected the continental margin as shown. In](#) C, [Eocene magmatism across NE to](#)

1527 north-central Washington and the pattern of inferred rollback ~~of~~ magmatism to the southwest  
1528 are shown.a. Filled circles are localities of U-Pb zircon ages of plutonic rocks, as inferred from  
1529 Heavy dashed lines are contours of the U-Pb zircon ages (references cited in text). An =  
1530 Anaconda core complex; Br = Bitterroot core complex; Cb = Chelan block of North Cascades  
1531 crystalline core; Chb = Chumstick basin; Csz = Coast shear zone; Ef = Entiat fault; Fa = Farallon  
1532 plate; Ff = Fraser fault; K = Kettle core complex; LCfz = Lewis and Clark fault zone; Ok =  
1533 Okanogan core complex; P = Priest River core complex; Pab = Pasco basin; Pf = Pasayten fault;  
1534 RLf = Ross Lake fault; SCf = Straight Creek fault; Sh = Shuswap core complex; V = Valhalla  
1535 complex; VI = Vancouver Island; Wb = Wenatchee block of North Cascades crystalline core.  
1536 States and Provinces: BC = British Columbia; ID = Idaho; MT = Montana; NV = Nevada; UT =  
1537 Utah; WA = Washington.

1538

1539 Figure 7. Reconstruction map and proposed plate tectonic setting at ca. 44–40 Ma based on  
1540 features in Figures 2 and 3. The ancestral Cascades arc (“Cascadia”) has initiated, scattered  
1541 basins extend from the western to eastern belts, and magmatism has ended in the North  
1542 Cascades and almost all of the Challis-Kamloops belt. The Farallon – Pacific ridge is migrating to  
1543 the northwest relative to North America. Ff = Fraser River fault; LCfz = Lewis and Clark fault  
1544 zone; PG = Puget Group; Rb = Roslyn basin; SCf = Straight Creek fault. VI = Vancouver Island; Yf  
1545 = Yalakom fault. States and Provinces: BC = British Columbia; ID = Idaho; MT = Montana; OR =  
1546 Oregon; WA = Washington.

1547

1548 Figure 8. Summary of timing of major events described in the text. Within the magmatism,  
1549 sedimentation and deformation panels, features are generally arranged from west (left) to east  
1550 (right). Arrows designate where processes began before 60 Ma or ended after 40 Ma.

1551

1552 Figure 9. Tectonic model for 49.5–45 Ma magmatic flare-up in the Washington Cascades. The  
1553 star schematically shows the location of the northern Washington Cascades where the slab has  
1554 broken, south of the postulated slab window to the north. See text for explanation.